

1983

Free radical reactions of some transition and organotransition metal complexes

Michael Steven McDowell
Iowa State University

Follow this and additional works at: <https://lib.dr.iastate.edu/rtd>

 Part of the [Inorganic Chemistry Commons](#)

Recommended Citation

McDowell, Michael Steven, "Free radical reactions of some transition and organotransition metal complexes " (1983). *Retrospective Theses and Dissertations*. 8939.
<https://lib.dr.iastate.edu/rtd/8939>

This Dissertation is brought to you for free and open access by the Iowa State University Capstones, Theses and Dissertations at Iowa State University Digital Repository. It has been accepted for inclusion in Retrospective Theses and Dissertations by an authorized administrator of Iowa State University Digital Repository. For more information, please contact digirep@iastate.edu.

INFORMATION TO USERS

This reproduction was made from a copy of a document sent to us for microfilming. While the most advanced technology has been used to photograph and reproduce this document, the quality of the reproduction is heavily dependent upon the quality of the material submitted.

The following explanation of techniques is provided to help clarify markings or notations which may appear on this reproduction.

1. The sign or "target" for pages apparently lacking from the document photographed is "Missing Page(s)". If it was possible to obtain the missing page(s) or section, they are spliced into the film along with adjacent pages. This may have necessitated cutting through an image and duplicating adjacent pages to assure complete continuity.
2. When an image on the film is obliterated with a round black mark, it is an indication of either blurred copy because of movement during exposure, duplicate copy, or copyrighted materials that should not have been filmed. For blurred pages, a good image of the page can be found in the adjacent frame. If copyrighted materials were deleted, a target note will appear listing the pages in the adjacent frame.
3. When a map, drawing or chart, etc., is part of the material being photographed, a definite method of "sectioning" the material has been followed. It is customary to begin filming at the upper left hand corner of a large sheet and to continue from left to right in equal sections with small overlaps. If necessary, sectioning is continued again—beginning below the first row and continuing on until complete.
4. For illustrations that cannot be satisfactorily reproduced by xerographic means, photographic prints can be purchased at additional cost and inserted into your xerographic copy. These prints are available upon request from the Dissertations Customer Services Department.
5. Some pages in any document may have indistinct print. In all cases the best available copy has been filmed.

**University
Microfilms
International**

300 N. Zeeb Road
Ann Arbor, MI 48106

8407103

McDowell, Michael Steven

FREE RADICAL REACTIONS OF SOME TRANSITION AND
ORGANOTRANSITION METAL COMPLEXES

Iowa State University

PH.D. 1983

**University
Microfilms
International** 300 N. Zeeb Road, Ann Arbor, MI 48106

PLEASE NOTE:

In all cases this material has been filmed in the best possible way from the available copy. Problems encountered with this document have been identified here with a check mark .

1. Glossy photographs or pages _____
2. Colored illustrations, paper or print _____
3. Photographs with dark background _____
4. Illustrations are poor copy _____
5. Pages with black marks, not original copy _____
6. Print shows through as there is text on both sides of page _____
7. Indistinct, broken or small print on several pages
8. Print exceeds margin requirements _____
9. Tightly bound copy with print lost in spine _____
10. Computer printout pages with indistinct print _____
11. Page(s) _____ lacking when material received, and not available from school or author.
12. Page(s) _____ seem to be missing in numbering only as text follows.
13. Two pages numbered _____. Text follows.
14. Curling and wrinkled pages _____
15. Other _____

University
Microfilms
International

Free radical reactions of some transition and
organotransition metal complexes

by

Michael Steven McDowell

A Dissertation Submitted to the
Graduate Faculty in Partial Fulfillment of the
Requirements for the Degree of
DOCTOR OF PHILOSOPHY

Department: Chemistry
Major: Inorganic Chemistry

Approved:

Signature was redacted for privacy.

In Charge of Major Work

Signature was redacted for privacy.

For the Major Department

Signature was redacted for privacy.

For the Graduate College

Iowa State University
Ames, Iowa

1983

TABLE OF CONTENTS

	Page
DEDICATION	xii
GENERAL INTRODUCTION	1
PART I. A CONVENIENT ROUTE TO SUPEROXIDE ION IN AQUEOUS SOLUTION	2
STATEMENT OF THE PROBLEM	3
INTRODUCTION	4
RESULTS AND DISCUSSION	10
General Comments and Mechanism	10
Identification of Photolysis Product as Superoxide Ion	12
Investigation of Factors Affecting the Yield of Superoxide Ion	18
Flash photolysis studies	18
Steady state photolysis experiments	21
Xe plasma lamp as source	21
Hg lamp as UV source	28
Use of sunlight as UV source	30
Concluding Remarks	30
EXPERIMENTAL	32
Reagents	32
Equipment	32
Solution Preparations	33
Acetone as sensitizer	33
Benzophenone as sensitizer	33
Photolysis Experiments	34
General	34
Flash photolysis experiments	34
Steady state experiments	34
Use of sunlight	35
Kinetics	35

	Page
REFERENCES	37
APPENDIX. SUPPLEMENTAL DATA	40
PART II. SOME ELECTRON TRANSFER REACTIONS OF SUPEROXIDE ION IN AQUEOUS SOLUTIONS	44
STATEMENT OF THE PROBLEM	45
LITERATURE BACKGROUND	47
Superoxide Ion as a Reductant	47
The Marcus Correlation and Its Application	48
RESULTS AND INTERPRETATION	53
Co(III) Reductions	53
Deuterium and Solvent Effects	59
Physical and Chemical Effects	60
Selection of basic (pH 11.3-11.9) media	60
Presence of Complexing Anions	61
Activation parameters	61
Effect of oxygen on the system	61
Mechanism of the reaction	63
Other Co(III) Complexes	66
Ferricinium Ion Reduction	67
DISCUSSION	71
The $O_2(aq)/O_2^-$ Self-Exchange Rate Constant	71
Applications of the $O_2(aq)/O_2^-$ Exchange Rate Constant	75
Conclusion	77
EXPERIMENTAL	78
Reagents--All Experiments	78
Equipment--All Experiments	78

	Page
Reagent Solutions--Co(III) Reactions	79
FeCp ₂ ⁺ Reactions	79
Methods, Procedures, and Data Treatment	80
Co(III) reactions	80
Cp ₂ Fe ⁺ reactions	84
REFERENCES	86
APPENDIX. SUPPLEMENTAL DATA	91
PART III. REACTIONS OF BIS(DIMETHYLGLYOXIMATO)COBALT(II) COMPLEXES WITH POLYHALOMETHANES	97
STATEMENT OF THE PROBLEM	98
HISTORICAL BACKGROUND	100
RESULTS AND DISCUSSION	117
Solvents	117
Stoichiometry and the Products of Reaction	117
Kinetics	121
Reaction in the Presence of Radical Scavenging Agents	122
Mathematical Simulations	130
INTERPRETATION	134
EXPERIMENTAL	140
Materials	140
Solvents	140
Polyhalogenomethanes	141
Cobaloxime(II) reagents	141
Organocobaloxime(III) reagents	143
Inorganic cobaloxime(III) reagents	144
Scavenging agents	146
Stoichiometric Studies	146
Identification of Products from Co(dmgh) ₂ py/CHBr ₃ Reaction	147

	Page
UV-Vis spectra	148
¹ H NMR spectra	149
Thin layer chromatography and column chromatography	149
Identification of Products of Co(dmgh) ₂ py + CHBr ₃ Reaction in C ₆ H ₆	154
Result	155
Unsuccessful Syntheses of Trihalomethylcobaloximes(III)	155
Conversion of XCo(dmgh) ₂ py to charged cobaloxime(III) complex with Ag ⁺	155
Ag ₂ O synthesis	156
Zn reduction method and Schrauzer methods	156
Stoichiometry of the ClCo(dmgh) ₂ PPh ₃ /C ₅ H ₅ N and ClCo(dmgh) ₂ PPh ₃ /4-CH ₃ C ₅ H ₄ N reactions	157
Kinetics	157
Conventional methods	157
Flash photolysis initiated reactions	163
Activation parameters	165
Determination of molar absorptivities for absorbing species in (pyridine)cobaloxime(III) - carbon tetrachloride-4-hydroxy-2,2,6,6-tetramethyl - piperidinoxy - benzene system	165
Mathematical modeling of the reaction sequence represented by equations 30-32	167
REFERENCES	169
APPENDIX. SUPPLEMENTAL DATA	172
GENERAL SUMMARY	182
ACKNOWLEDGMENTS	183

LIST OF TABLES

	Page
Table I-1. Values of the second-order rate constants k for the O_2^- disproportionation reaction	15
Table I-2. Yields of O_2^- from flash photolysis	19
Table I-A-1. Effect of distance from UV source on superoxide ion yield	40
Table I-A-2. Yields of superoxide ion as a function of alcohol and ketone concentrations	41
Table II-1. Summary of the second order rate constants for outer sphere superoxide ion reductions in aqueous solution	49
Table II-2. Summary of the kinetic data on the reactions of superoxide ion in aqueous solution applicable to Marcus theory for estimation of the $O_2(aq)/O_2^-$ electron self exchange rate constant	52
Table II-3. Summary of rate constants for the $Co(III)-O_2^-$ reactions	57
Table II-4. Activation parameters for superoxide ion reductions of $Co(III)$ amine complexes	62
Table II-5. Calculation of the $O_2(aq)/O_2^-$ self exchange rate constant utilizing data for the $Co(III)$ and $Fe(III)$ systems	72
Table II-6. Some superoxide ion reactions involving small molecules and anions and large molecules	76
Table II-A-1. $Co(NH_3)_6^{+3} + O_2^-$	91
Table II-A-2. $Co(en)_3^{+3} + O_2^-$	93
Table II-A-3. $Co(chxn)_3 + O_2^-$	94
Table II-A-4. Data for calibration curve (Figure II-5), $[O_2^-]$ vs. photolysis time	95
Table II-A-5. $FeCp_2^+ + O_2^-$	96
Table III-1. Stoichiometry of the cobaloxime(II)-polygenomethane reaction	119

	Page
Table III-2. Values of the second-order rate constants k_1 for the reaction of $\text{Co}(\text{dmgH})_2\text{L}$ with polyhalomethanes	124
Table III-3. Activation parameters for the reaction of $\text{Co}(\text{dmgH})_2\text{L}$ with polyhalomethanes	124
Table III-4. Comparison between enthalpy of activation for the cobaloxime(II)-polyhalogenomethane reaction and the bond dissociation energy of the C-X bond	136
Table III-5. Analyses of bis(ligand)cobaloxime(II) complexes	143
Table III-6. Analyses of organocobaloxime(III) complexes	145
Table III-7. Cobalt analyses for inorganic cobaloxime(III) complexes	145
Table III-8. ^1H NMR of 4 cobaloximes(III) (CDCl_3 , TMS as reference, 0.0)	149
Table III-A-1. Kinetic data for the reaction of CCl_4 and $\text{Co}(\text{dmgH})_2\text{PPh}_3$ at 25.0°C in acetone	172
Table III-A-2. Kinetic data for the reaction of CCl_4 and $\text{Co}(\text{dmgH})_2\text{PPh}_3$ at $T \neq 25^\circ\text{C}$ in acetone	173
Table III-A-3. Kinetic data for the reaction of CCl_4 with $\text{Co}(\text{dmgH})_2\text{PPh}_3$ in benzene	174
Table III-A-4. Kinetic data for the reaction of CCl_4 with $\text{Co}(\text{dmgH})_2\text{py}$ in benzene	175
Table III-A-5. Kinetic data for the reaction of CCl_4 with $\text{Co}(\text{dmgH})_2\text{L}$ ($\text{L} \neq \text{PPh}_3$) at 25.0°C in acetone and benzene	176
Table III-A-6. Kinetic data for the reaction of CHBr_3 with $\text{Co}(\text{dmgH})_2\text{py}$ in acetone and benzene	177
Table III-A-7. Kinetic data for the reaction of CHBr_3 with $\text{Co}(\text{dmgH})_2\text{PPh}_3$ in acetone and benzene at 25.0°C	178
Table III-A-8. Kinetic data for the reaction of BrCCl_3 with $\text{Co}(\text{dmgH})_2\text{py}$ in benzene	179
Table III-A-9. Kinetic data for the reaction of CBr_4 with $\text{Co}(\text{dmgH})_2\text{py}$ in benzene	180

	Page
Table III-A-10. Kinetic data for the reactions of BrCCl_3 and CCl_4 with $\text{Co}(\text{dmgH})_2\text{py}$ in benzene at 25.0°C in the presence of 4-ATMPO	181

LIST OF FIGURES

	Page
Figure 1-1. UV absorption spectrum of the long-lived metastable species produced by a 6-s photolysis of Ph_2CO ($6.3 \mu\text{M}$) in 5.0 M aqueous 2-propanol at pH 12.5 (the absorbance, D , was measured in a cell of 2.00-cm optical path). The scales of D and of the decadic molar absorptivity, ϵ/M^{-1} , calculated from the values of ϵ given ³⁰ for λ 230-270 nm; the latter are shown as solid points	13
Figure 1-2. Typical kinetic trace (line) for the disproportionation reaction of O_2^- at λ 245 nm. Conditions are 5.0 M 2-propanol, $25 \mu\text{M}$ Na_2EDTA , $6.3 \mu\text{M}$ Ph_2CO , pH 12.2, $T = 24.94^\circ\text{C}$. Darkened circles are calculated absorbance-time values from equation 20. Inset: Second order kinetic plot of $[\text{O}_2^-]_t$ vs. $t[\text{O}_2^-]_t$ for absorbance time curve shown	16
Figure 1-3. Rate constant-pH profile for the decay of the metastable O_2^- prepared with use of a ketone photosensitizer ($6.3 \mu\text{M}$ benzophenone or 8.2 - 41.0 mM acetone) in aqueous alcohol (1 M methanol or 1 - 5 M 2-propanol) after photolysis. The solid point at pH 11.6 is for 12 M ethanol, ³⁸ and the dashed line for aqueous solution ³⁰ at $\sim 24^\circ\text{C}$. Kinetic measurements were made at λ 245-252 nm	17
Figure 1-4. Yields of superoxide ion produced by successive 25 J flashes on (A) air-saturated 1.0 M methanol solution, and (B) air-saturated 1.0 M 2-propanol solution. Open circles are experiments done in 5.0 cm cell, solid circles for 10.0 cm cells. All solutions contain 8.2 mM acetone and $\sim 15 \mu\text{M}$ Na_2EDTA	20
Figure 1-5. Yields of O_2^- at varying distances from photolyzing source (Xe plasma lamp)--1.0 cm (squares) and 3.5 cm (circles). Solution was oxygen-saturated and contained $6.3 \mu\text{M}$ Ph_2CO and 5.0 M 2-propanol, pH = 12.2	22
Figure 1-6. Yields of O_2^- from continuously purged (circles) and pre-saturated (squares) solutions containing 1.0 M 2-propanol, 41 mM acetone at pH 12.2	24

	Page
Figure I- 7. Yields of O_2^- vs. photolysis times at varying 2-propanol concentrations: 1.0 M (○), 3.0 M (□), 7.0 M (■), and 10.0 M (△). Solutions are oxygen-saturated and contain 41 mM acetone, pH 12.2	25
Figure I- 8. Yields of O_2^- for a solution of 5.0 M 2-propanol also containing 41 mM acetone, dioxygen saturated, pH 12.2	26
Figure I- 9. Yields of O_2^- vs. photolysis time for solutions containing 5.0 M 2-propanol and varying amounts of acetone: .041 M (○), .049 M (△), .068 M (□), and .082 M (■), pH = 12.2	27
Figure I-10. Yields of O_2^- vs. photolysis time employing Hg arc lamp chamber as UV source. Solution contains 5.0 M 2-propanol and either 6.3 μ M Ph_2CO (○) or 41.0 mM acetone (●), dioxygen saturated, pH = 12.4	29
Figure II- 1. Plot of the pseudo-first-order rate constants at 25°C vs. $[Co(NH_3)_6^{+3}]$ for its reaction with O_2^- in 1 M 2-propanol, pH 11.3-11.9 under aerobic (●) and anaerobic conditions (○)	54
Figure II- 2. Plot of the pseudo-first-order rate constants at 25.0°C vs. $[Co(en)_3^{+3}]$ for its reaction with O_2^- in 1 M 2-propanol, pH 11.3-11.7 under aerobic (●) and anaerobic conditions (○)	55
Figure II- 3. Plot of pseudo-first-order rate constants given at 25.0°C vs. $[Co(chxn)_3^{+3}]$ for its reaction with O_2^- in 1 M 2-propanol, pH 11.7 under aerobic (●) and anaerobic conditions (○)	56
Figure II- 4. Plot of pseudo-first-order rate constants at 25.0°C vs. $[FeCp_2^+]$ for its reaction with O_2^- in 1 M 2-propanol pH 11.0 under aerobic conditions	70
Figure II- 5. Calibration curve of O_2^- yield vs. photolysis time for 1.0 M 2-propanol solution (pH 11.7) containing 4.6 μ M Ph_2CO and 19.21 μ M Na_2EDTA . Solutions are also saturated with O_2 . Photolyses conducted in 2.0 cm cell at T = 25.0°C. Line is drawn through origin with slope = 3.30. The number above a given data point is the number of individual measurements at that photolysis time	82

	Page
Figure III-1. Molecular structure of an organocobaloxime, where R = alkyl or aryl group	99
Figure III-2. Molecular structure of vitamin B ₁₂ . The positive charges of the cobalt(III) ion are balanced by the negative charges on the corrin ring, the cyanide, and the phosphate	101
Figure III-3. Illustrating the results of spectrophotometric titrations of Co(dmgh) ₂ py by BrCCl ₃ : (a) No added radical scavenger; (b) in the presence of excess 4-HTMPO	118
Figure III-4. Plots of the pseudo-first-order rate constants at 25.0°C vs. [CCl ₄] for its reaction with Co(dmgh) ₂ L in acetone (A, B, E) and Benzene (C, D) for L = 4-picoline (A, C), pyridine (B, D), and triphenylphosphate (E)	123
Figure III-5. Competitive reactivity of 4-HTMPO and Co(dmgh) ₂ py toward ·CCl ₃ , generated from BrCCl ₃ (○) and from CCl ₄ (□) as illustrated by the variation of m (equation 11) with the ratio of initial concentrations. The solid line shows the same quantity using kinetic data simulated by forward integration techniques for the ratio $k_3/k_2 = 1.8$	129
Figure III-6. The enthalpy of activation associated with halogen atom abstraction reaction of equation 1 is linearly correlated with the bond dissociation enthalpy for the given polyhalomethane (○). The correlation does not extend to benzyl bromide, however (□)	137

DEDICATION

I wish to dedicate this dissertation to the memory of my father, Warner S. McDowell, who left this life and entered an eternal one on August 31, 1983. A nonscientific man during his lifetime, his final act was a significant contribution to the study of the treatment of cancer. Let it be known that I love my father very much and will miss him dearly.

GENERAL INTRODUCTION

A photochemical method for the production of superoxide ion in aqueous solution is the subject of Part I. In Part II, this synthetic method is used in the study of $O_2^{\cdot -}$ and its electron transfer reactions with several Co(III) complexes and ferricinium ion.

In Part III, the reactions of several polyhalomethanes with the bis(dimethylglyoximate)cobalt(II) complex are investigated.

PART I. A CONVENIENT ROUTE TO SUPEROXIDE ION IN AQUEOUS SOLUTION

STATEMENT OF THE PROBLEM

The preparation of superoxide ion, O_2^- , in aqueous solution is not a trivial problem. The stringent conditions of the working medium and the need for specialized equipment and techniques prevent superoxide ion from being as common a laboratory reagent as it should be.

It is intended to show that O_2^- can readily be prepared in very good yields ($>300 \mu M$) using conventional light sources such as a Hg arc lamp in a moderately short period of time (30 s) as well as producing somewhat lower yields ($\sim 50 \mu M$) in a very short period of time (several μs) using the flash photolysis technique. This was accomplished by photochemically producing the triplet state of a ketone (acetone or benzophenone) in the presence of an alcohol (methanol or 2-propanol) and oxygen at $pH > 11$.

The photolysis product was verified to be the superoxide ion by comparison of its UV spectrum and rates of disproportionation with those reported for authentic samples of O_2^- . Finally, the yield of superoxide ion was examined as functions of light source, length of photolysis, flash energy, and alcohol and ketone concentrations.

INTRODUCTION

The production of superoxide ion, O_2^- , in solution has been a problem of interest to the chemist and biochemist for many years. The inherent instability of O_2^- , especially in protic media, is but one complication.¹ Another is the frequent need for specialized equipment, such as described in subsequent paragraphs of this section. Yet, in spite of these and other difficulties, several methods have been developed.

For aprotic media, three practical methods for the preparation of a superoxide ion containing solution have evolved.

Tetramethylammonium superoxide, $N(CH_3)_4O_2^-$, was first synthesized in 1964.² This material is readily soluble in aprotic solvents (up to 0.05 M in CH_3CN ³) and provides stable solutions of O_2^- , but there are limitations to this approach. The compound is not commercially available and its synthesis is not trivial. The yields of the high purity product are low. Efforts to increase the yield result in a loss of purity.

Potassium superoxide, KO_2 , on the other hand, is a material that is commercially available. Its use as a source of O_2^- suffers as it is only slightly soluble in aprotic solvents.^{4,5} Despite this, it has been used successfully as a superoxide source in DMSO.⁶

Through the use of crown ethers as either solubilizing or phase transfer agents, KO_2 has become a powerful source of O_2^- in solvents such as DMSO,^{7,8} benzene,⁹ and toluene.¹⁰ Unfortunately, this method is not without limitations also. The purity of KO_2 available is low

(96%) with KOH, K_2O_2 , and K_2CO_3 as the major contaminants. No method of purification is presently known. The slow decomposition of the crown ethers in these solutions is also of concern.⁹

A third method for aprotic media, and the cleanest, is the electrochemical reduction of dioxygen in the presence of a supporting electrolyte. First successful in DMSO,¹¹ this method has been extended for use in solvents such as DMF,^{12,13} CH_3CN ,^{13,14} and pyridine.¹⁵ Electrochemical generation of O_2^- allows for its in situ preparation in the presence of substrate. This has proven most successful.¹⁶⁻²¹ There are also some disadvantages with this technique. It requires electrochemical apparatus, the fluxes of O_2^- produced are low, and possible interferences from reactions with the electrolyte and the electrode exist.

Several chemical and biochemical reactions have been demonstrated to produce superoxide ion in both protic and aprotic media. In many instances, the superoxide ion is a transient intermediate in the system, reacting further. There are a few, though, where O_2^- is the final and persisting product.

A number of enzymatic reactions have been used to generate O_2^- in solution. The xanthine/xanthine oxidase system has been used successfully in aqueous media.²² A number of biochemical reagents have also been used. A series of reduced flavins, including riboflavin, FMN, and FAD, when reacted with dioxygen, produce superoxide ion efficiently.^{12,23}

In aprotic media, significant amounts of O_2^- have been produced

from the reaction of hydrogen peroxide and tetra-n-propyl-ammonium hydroxide. This has been done in pyridine,²⁴ DMA,¹⁵ and DMF.¹⁵ Another source of O_2^- is the reaction of dioxygen with the dianions of p-hydroquinone or ascorbic acid.²⁵

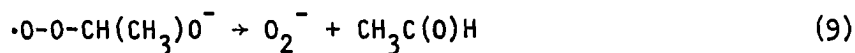
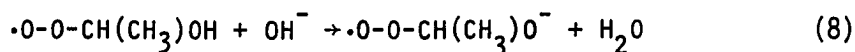
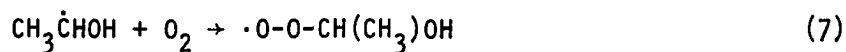
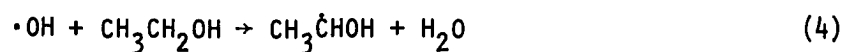
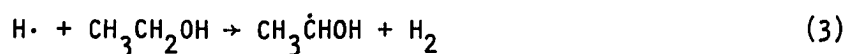
The biochemical reactions aside, the above methods are not applicable to aqueous media. Electrochemical reduction of dioxygen in aqueous media results in complete reduction to H_2O_2 (or HO_2^-). The process can be stopped after the first reduction step to O_2^- by addition of a surfactant such as triphenylphosphine oxide. This method has been limited to the assaying of biological fluids and crude homogenates.²⁶ The slow infusion of aprotic solutions of O_2^- into alkaline protic media has also been done but this is also a little used method.²⁷

For protic media, only two methods have proven highly successful in the production of O_2^- in such media. Pulse radiolysis techniques are well documented and will not be discussed here.^{1,28-33} Photochemical methods are the other source of O_2^- and will be examined in some detail as they bear directly on the studies here.

A number of photochemical systems have been shown to produce O_2^- in aqueous media. Flash photolysis of formate-oxygen solutions³⁴ and of H_2O_2 solutions³⁵ have yielded superoxide ion. The continuous photolysis of water in the vacuum-UV at $\lambda 184.9$ nm was demonstrated to produce O_2^- by its reaction with a superoxide dismutase.³⁶ Recently, the photolysis of aqueous formate³⁷ and aqueous alcoholic³⁸ solutions containing dioxygen have been used as sources of O_2^- .

The method of most interest to the study here is the photolysis

of aqueous alcoholic solutions containing O_2 .³⁸ This is the technique of Bielski³⁹ et al. and is highly successful in generating significant fluxes of O_2^- in short periods of time. Vacuum-UV photolysis of aqueous solutions containing varying amounts of ethanol produces the superoxide ion. The proposed mechanism leading to O_2^- is given below in equations 1-9.



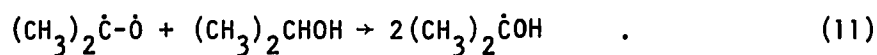
The superoxide ion results from the reaction of dioxygen with the α -hydroxyethyl radical (a reducing radical) and those that follow. It certainly also does arise from the reaction of dioxygen with hydrogen atom (equation 5), but this is the minor pathway.

This method bases itself on the reaction of dioxygen with the

reducing radical species. In addition to the reactions given above leading to the α -hydroxyethyl radical, there are other ways of generating it. Additionally, it need not be the radical derived from ethanol but it can be any α -hydroxyalkyl or aryl radical. This is the basic improvement to the method of Bielski et al. that is made.

The triplet state of a ketone such as acetone or benzophenone can be produced by UV irradiation of the stable singlet state.⁴⁰ Since most ketones absorb in the wavelength region of λ 200-300 nm, normal UV sources rather than special sources and glassware for vacuum-UV work can be used. This eliminates from Bielski's method the need for a more costly and much less convenient vacuum-UV apparatus and greatly simplifies the photolyses.

The reason for excitation of a ketone to its triplet state is that these species have been demonstrated to be very efficient hydrogen atom abstractors.⁴⁰ So-called "activated" hydrogens, such as the α -hydrogens of primary and secondary alcohols, are readily removed by the triplet state. As an illustration, excitation of acetone to its triplet state in the presence of 2-propanol results in the formation of two α -hydroxyisopropyl radicals, as shown in equations 10 and 11:



The replacement of equations 10 and 11 for equations 1 through 6 in Bielski's mechanism presents the alternative mechanism and method

for superoxide ion production.

A second feature of this mechanism is that the reaction is catalytic. In equation 9, the final products from the internal electron transfer are O_2^- and a ketone or aldehyde depending upon the starting alcohol. Therefore, the ketone consumed in reaction 10 is recovered in equation 9. Moreover, for every 1 ketone consumed, 2 are returned. This allows the system presented here to remain essentially unchanged from Bielski's as a high concentration of ketone is not necessary.

It is now the intention to show that UV-irradiation of a solution containing alcohol, ketone, and dioxygen will result in a good yield of superoxide ion. Additionally, the effect of such parameters as concentration of ketone and alcohol and the source of UV-radiation will be examined.

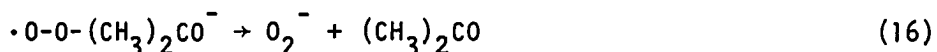
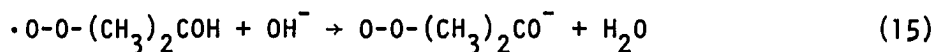
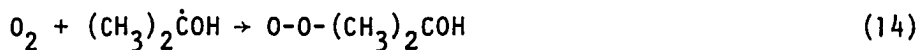
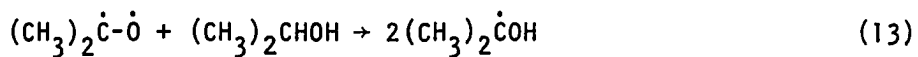
RESULTS AND DISCUSSION

General Comments and Mechanism

The use of acetone as the ketone sensitizer presents a possible complication. Ketones containing α -hydrogens will undergo self-reaction in the presence of strong base. This is the well-known aldol condensation. Since the majority of the experiments were conducted at pH greater than 11, the potential for complication exists. Fortunately, this was not the case. No change was observed in the UV spectrum of acetone during a 2-hour period when the ketone was subjected to the experimental pH conditions. Benzophenone does not present this problem either as it contains no α -hydrogens.

A second concern about the presence of ketone is that superoxide ion may possibly react with it. Although only an average nucleophile in aqueous solution,⁴¹ O_2^- does attack the carbonyl carbon of organic esters in aprotic media.⁴²⁻⁴⁴ There is also a report of the slow degradation of acetone in the presence of superoxide ion but no specific details were given.³ This also proved to be unimportant as the kinetic behavior exhibited by superoxide ion in its disproportionation reaction followed very clean second order kinetics (see below). This was found in the pH range 11.0-12.5. At higher pH, the decay of O_2^- was faster than expected and not as well-behaved as in the lower pH work. This may be due to superoxide ion reacting with acetone and/or an impurity. Studies using benzophenone were not extended to above pH 12.5.

Equations 12-16 present again the mechanism in operation here. Acetone and 2-propanol are also again used for illustrative purposes.



The catalytic nature of this process is demonstrated by complete recovery of the starting ketone. The UV spectrum of the superoxide ion generating solution before photolysis and after photolysis followed by complete decay of O_2^- to dioxygen and hydrogen peroxide are virtually identical. The entire procedure can be repeated again on the same solution because the starting ketone is recovered. Eventually, ketone will begin to increase in concentration as one alcohol is converted to one ketone in addition to recovering the original ketone. A second indication of the catalytic nature of the sensitization is in the benzophenone studies. Solutions containing $6 \mu\text{M}$ benzophenone routinely produced several hundred micromolar of O_2^- .

Another point to consider in this mechanism is in reaction 15. The presence of hydroxide ion is critical for two reasons. The first is that it retards O_2^- self-reaction as equation 17 has a rate $< 6 \text{ M}^{-1} \text{ s}^{-1}$ ^{30,45} and



is thermodynamically unfavored while equation 18 occurs



very quickly ($k_{18} = 1.5 \times 10^7 \text{ M}^{-1} \text{ s}^{-1}$).^{28,29,30,46} Because it is consumed in equation 15, pH constraints must be very exact. The pH range of 11 to 12.5 was selected as changes in hydroxide ion would be minimal and the use of buffers would not be necessary. A second requirement for the presence of OH^- is the rate of equation 15. α -hydroxyalkylperoxy radicals decay by internal electron transfer at much less than diffusion controlled rates (10 s^{-1} for the methanol derived species to 665 s^{-1} for the 2-propanol derived species).⁴⁷⁻⁵⁰ Their conjugate bases, though, decay at very high rates. This complication may hinder the use of this method here to study HO_2 reactions as (1) the substrate may react with the peroxy radical first as it is long lived enough under acidic conditions, and (2) the only rate observed may simply be the rate of electron transfer within the peroxy radical, the substrate acting only as an indicator of this process.

Identification of Photolysis Product as Superoxide Ion

O_2^- has been well-characterized by numerous methods and consequently, a limited number of identification studies were done to prove the photolysis product to be superoxide ion. The two methods of identification selected were UV spectroscopy and measurement of the rate of loss of the photolysis product.

Figure 1-1 compares the UV spectrum of the species generated during photolysis (line) with that taken from the literature as reported for

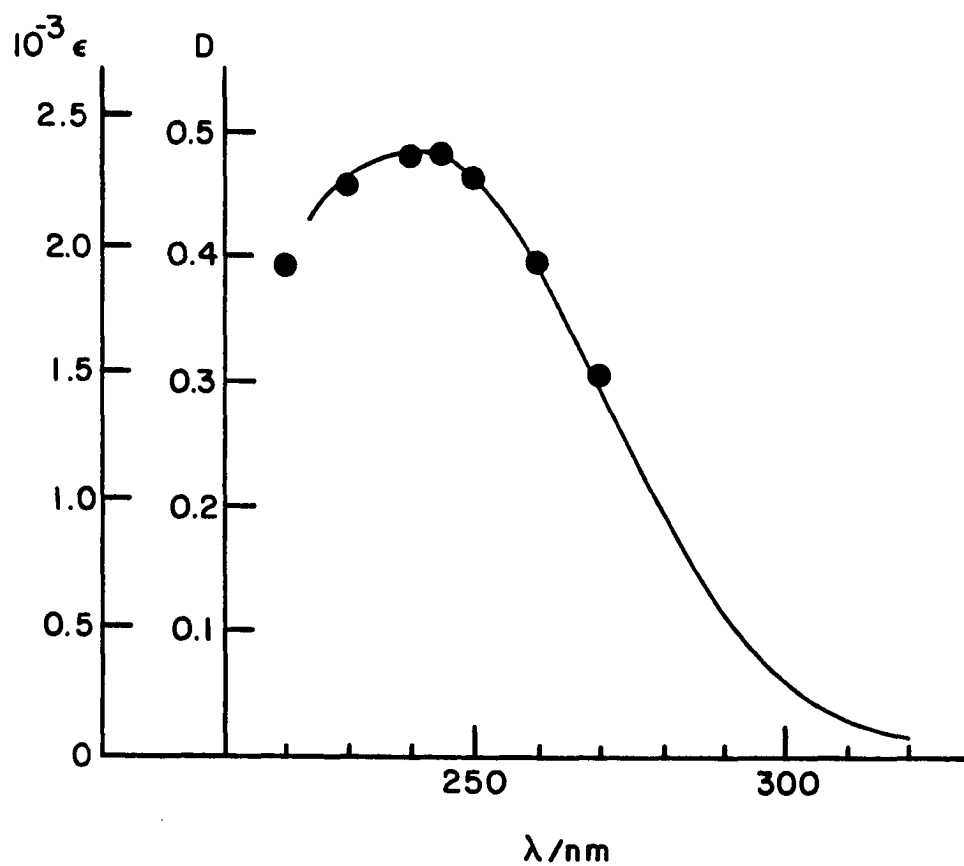


Figure 1-1. UV absorption spectrum of the long-lived metastable species produced by a 6-s photolysis of Ph_2CO ($6.3 \mu\text{M}$) in 5.0 M aqueous 2-propanol at pH 12.5 (the absorbance, D , was measured in a cell of 2.00-cm optical path). The scales of D and of the decadic molar absorptivity, $\epsilon/\text{M}^{-1} \text{ cm}^{-1}$, were matched by using $[\text{O}_2^-] = 1.02 \times 10^{-4} \text{ M}$, calculated from the values of ϵ given³⁰ for λ 230-270 nm; the latter are shown as solid points

an authentic sample of superoxide ion (blackened circles).³⁰ The spectrum here was obtained by difference (making allowance for ketone) of a photolyzed and an unphotolyzed solution. The excellent agreement seen between the spectra in Figure 1-1 is one indication that the photolysis product is superoxide ion.

Further support of the supposition that O_2^- is the photolysis product was obtained by measuring the rate of disproportionation of the product and comparing it with literature precedent for O_2^- . Table 1-1 contains the rate constants measured in this study. They were obtained by monitoring the loss of O_2^- at $\lambda 245$ nm and then fitting the absorbance-time data to an integrated second order rate equation. Figure 1-2 presents a typical kinetic trace (line) along with the fitted data (darkened circles). The rate of disproportionation proved to show a second order dependence on superoxide ion concentration; it also proved to be independent of alcohol and ketone concentration. The same rate constant was found regardless of the method used to generate it-- steady state or flash photolysis.

Figure 1-3 presents the pH profile of the disproportionation rate in the pH range 11.0-12.5. The rate constant k comes from the rate law given in equation 19. Consistent with earlier reports,³⁰ the plot

$$\frac{-d[O_2^-]}{dt} = k [O_2^-]^2 \quad (19)$$

is linear in this pH range. Also given in Figure 1-3 are rate constants measured in other studies of superoxide ion disproportionation. The dashed line is for aqueous solution³⁰ while the blackened circle

Table 1-1. Values of the second-order rate constants k for the O_2^- disproportionation reaction^{a,b}

Alcohol/ concentration	Sensitizer/ concentration	Photolysis method	pH	$k(M^{-1} s^{-1})$
CH ₃ OH/1.0 <u>M</u>	(CH ₃) ₂ CO/0.0082 <u>M</u>	Flash ^c	11.1 (11.5) ^d	113.1±2.5 ^e
2-PrOH/1.0 <u>M</u>	(CH ₃) ₂ CO/0.0082 <u>M</u>	Flash	11.1 (11.3)	72.6±0.9
CH ₃ OH/1.0 <u>M</u>	(CH ₃) ₂ CO/0.0082 <u>M</u>	Flash	11.2 (11.5)	80.9±4.3 ^e
2-PrOH/1.0 <u>M</u>	(CH ₃) ₂ CO/0.0082 <u>M</u>	Flash	11.2 (11.6)	47.9±0.7 ^e
2-PrOH/1.0 <u>M</u>	(CH ₃) ₂ CO/0.0082 <u>M</u>	Flash	11.3 (11.4)	53.8±0.6
2-PrOH/1.0 <u>M</u>	(CH ₃) ₂ CO/0.0082 <u>M</u>	Flash	11.35 (11.5)	53.0±0.5 ^e
CH ₃ OH/1.0 <u>M</u>	(CH ₃) ₂ CO/0.0082 <u>M</u>	Flash	11.6 (11.9)	28.2±0.5 ^e
2-PrOH/1.0 <u>M</u>	(CH ₃) ₂ CO/0.0082 <u>M</u>	Flash	11.65 (11.8)	22.2±0.9
2-PrOH/1.0 <u>M</u>	(CH ₃) ₂ CO/0.041 <u>M</u>	Flash	11.8 (11.9)	19.7±0.6 ^e
2-PrOH/1.0 <u>M</u>	(CH ₃) ₂ CO/0.041 <u>M</u>	Flash	11.8 (11.9)	23.0±0.4
2-PrOH/1.0 <u>M</u>	(CH ₃) ₂ CO/0.0082 <u>M</u>	Flash	11.9 (12.0)	10.8±0.2 ^e
2-PrOH/1.0 <u>M</u>	(CH ₃) ₂ CO/0.041 <u>M</u>	Flash	12.0 (12.1)	11.2±0.6
2-PrOH/1.0 <u>M</u>	(CH ₃) ₂ CO/0.041 <u>M</u>	Steady state ^f	12.0 (12.1)	11.8±0.4
2-PrOH/5.0 <u>M</u>	(CH ₃) ₂ CO/0.041 <u>M</u>	Steady state	12.2 (12.4)	5.9±0.1
2-PrOH/5.0 <u>M</u>	Ph ₂ CO/6.3 <u>μM</u>	Steady state	12.2 (12.4)	5.9±0.2
2-PrOH/5.0 <u>M</u>	Ph ₂ CO/6.3 <u>μM</u>	Steady state	12.3 (12.5)	7.5±0.1

^aλ245 nm, T = 25.0±0.1°C, O₂ saturated unless otherwise noted.

^bIn addition to alcohol and sensitizer, solutions also contain ~25 μM Na₂EDTA.

^cSee Experimental Section.

^dValue in parentheses is calculated pH and nonenclosed value is measured pH.

^eAir saturated.

^fSee Experimental Section on photolyses employing Xe Plasma lamp.

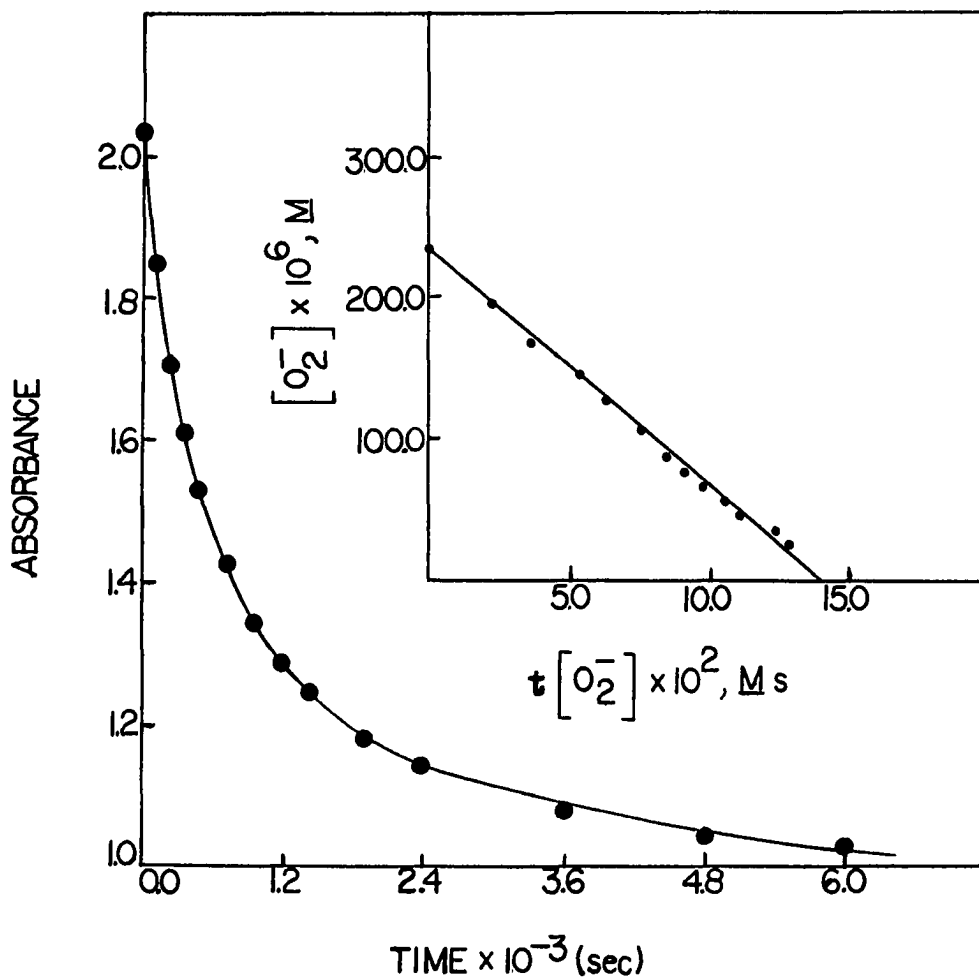


Figure 1-2. Typical kinetic trace (line) for the disproportionation reaction of O_2^- at $\lambda 245$ nm. Conditions are 5.0 M 2-propanol, 25 μM Na_2EDTA , 6.3 μM Ph_2CO , pH 12.2, $\bar{T} = 24.94^\circ C$. Darkened circles are calculated absorbance-time values from equation 20. Inset: Second-order kinetic plot of $[O_2^-]_t$ vs. $t[O_2^-]_t$ for absorbance time curve shown

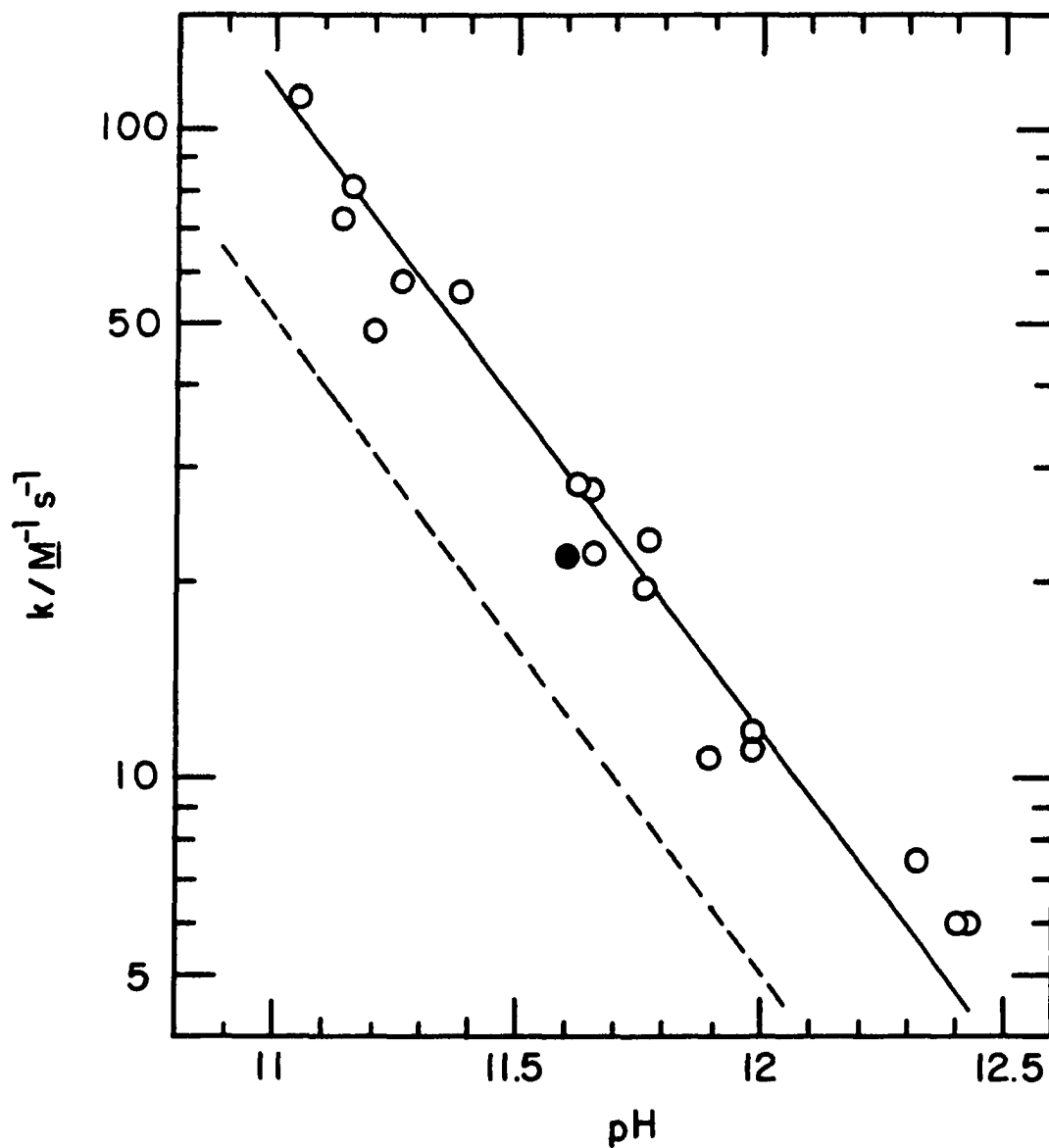


Figure 1-3. Rate constant-pH profile for the decay of the metastable O_2^- prepared with use of a ketone photosensitizer ($6.3 \mu\text{M}$ benzophenone or $8.2\text{-}41.0 \text{ mM}$ acetone) in aqueous alcohol (1 M methanol or $1\text{-}5 \text{ M}$ 2-propanol) after photolysis. The solid point at pH 11.6 is for 12 M ethanol,³⁸ and the dashed line for aqueous solution³⁰ at -24°C . Kinetic measurements were made at $\lambda 245\text{-}252 \text{ nm}$

at pH 11.6 ($k = 22 \text{ M}^{-1} \text{ s}^{-1}$) is for 12 M ethanolic solution. The results here are approximately 20% higher than this latter value. This may be a solvent effect as a factor of approximately 2 is noted in the disproportionation rate in aqueous formate solution as opposed to aqueous ethanolic solution.³⁸

These results substantiate that the species produced here is the superoxide ion. The modification of the Bielski method has succeeded in providing a convenient method for producing O_2^- .

Investigation of Factors Affecting the Yield of Superoxide Ion

Studies involving the use of flash photolysis to generate the superoxide ion species were kept to a minimum. This technique is considered a specialized one and the intention here is to provide a general and very accessible method. The majority of the studies in this section will involve the use of common laboratory UV sources.

Flash photolysis studies

In Table 1-2, the results of the experiments using the flash photolysis unit are given. Figure 1-4 presents a plot of the yield of O_2^- with successive flashes.

The studies were conducted on air-saturated 1.0 M methanol or 2-propanol solution containing 8.2 mM acetone and ~15 μM Na_2EDTA . The flash energy was 25 J and all measurements were made at pH 12.5 to minimize loss of O_2^- by disproportionation.

Nearly identical yields are found whether a 5.0 or a 10.0 cm cell is used. This is because photolysis occurs across the cell for its

Table 1-2. Yields of O_2^- from flash photolysis^a

Flash number	Yield O_2^- , μM^b	
	5.0 cm cell	10.0 cm cell
1. 1.0 M MeOH/0.0082 M Me ₂ CO/pH = 12.5		
0	0.0	0.0
1	50.8 ± 2.4	36.0 ± 0.25
2	73.5 ± 1.9	61.6 ± 3.4
3	76.1 ± 2.3	69.7 ± 1.9
4	57.7 ± 3.3	65.9 ± 2.1
2. 1.0 M Me ₂ CHOH/0.0082 M Me ₂ CO/pH = 12.5		
0	0.0	0.0
1	46.6 ± 2.2	41.6 ± 1.9
2	64.5 ± 1.3	61.2 ± 1.7
3	64.4 ± 1.3	65.5 ± 2.4
4	41.9 ± 3.5	51.1 ± 3.4

^aSee Experimental.

^bSee Experimental Section.

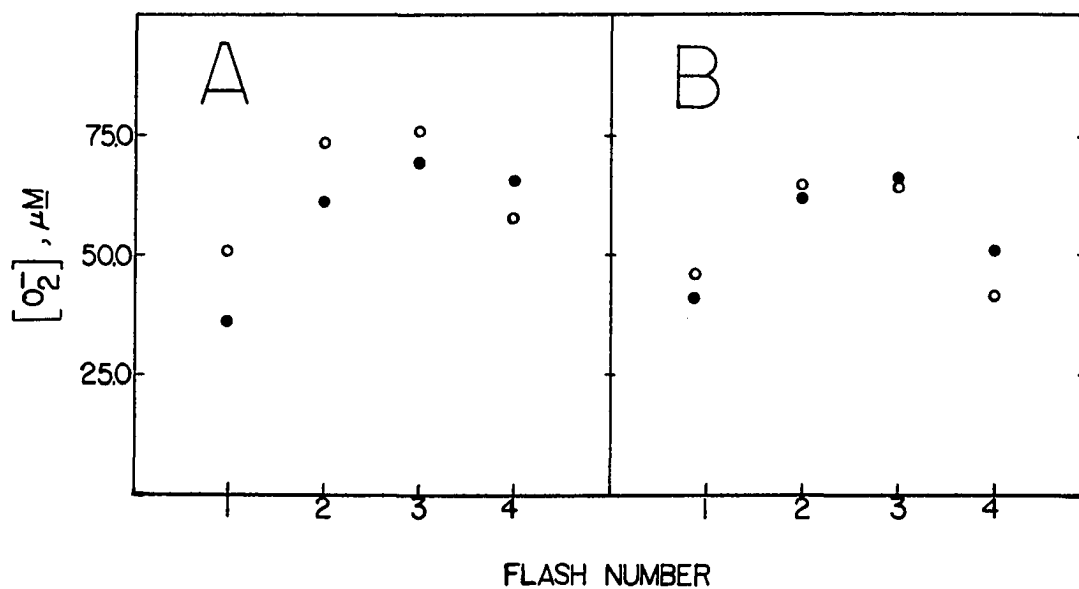


Figure 1-4. Yields of superoxide ion produced by successive 25 J flashes on (A) air-saturated 1.0 M methanol solution, and (B) air-saturated 1.0 M 2-propanol solution. Open circles are experiments done in 5.0 cm cell, solid circles for 10.0 cm cells. All solutions contain 8.2 mM acetone and $\sim 15 \mu M Na_2EDTA$

entire length as opposed to photolysis down the center of the cell. Use of either methanol or 2-propanol also produces similar yields. Use of dioxygen saturated solutions should produce higher yields at each flash.

The drop-off in yield at the fourth flash is a consequence of less and less dioxygen being available for reaction with the reducing radical (equation 14). The radical has opportunity now to react with O_2^- (producing HO_2^- most likely) and subsequently the yield falls off. This also occurs in the steady state photolysis experiments with prolonged irradiation for the same reason as above.

Steady state photolysis experiments

Three UV sources were examined--a Xe plasma lamp, a Rayonet photo-chamber containing medium pressure Hg lamps, and sunlight. Additionally, the use of benzophenone as the ketone sensitizer was examined.

Xe plasma lamp as source

Several parameters were varied and their effect on the yield of O_2^- was investigated using the Xe plasma lamp source.

The distance at which the cell was placed from the Xe lamp has a marked effect upon the yield of O_2^- . Figure 1-5 contains two curves for photolysis at a distance of 1 cm from the lamp (circles) and at a distance of 3.5 cm (squares). The closer the lamp, the more efficient the photolysis as less excitation radiation is lost. There is a trade-off, though, in moving the cell close to this source. A large IR component also is present in the Xe lamp and the reaction cell has a

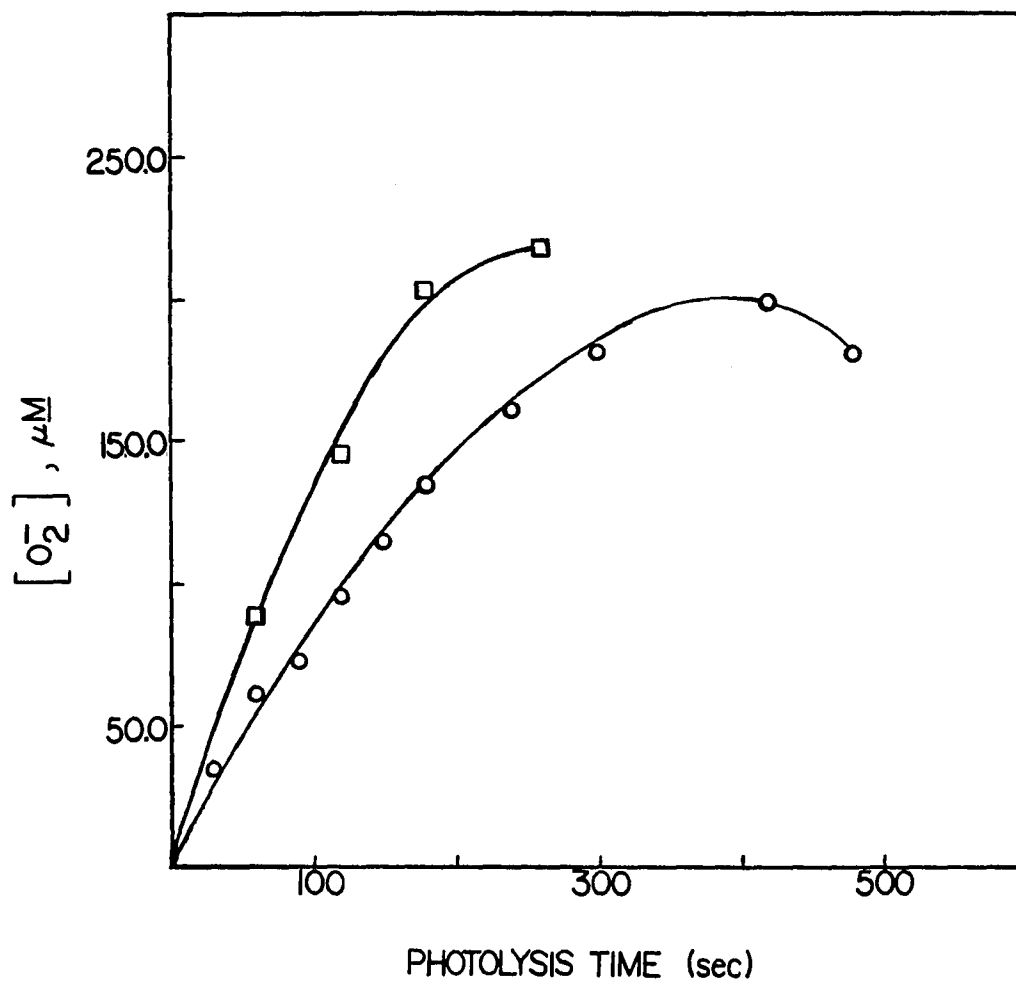


Figure 1-5. Yields of O_2^- at varying distances from photolyzing source (Xe plasma lamp)--1.0 cm (squares) and 3.5 cm (circles). Solution was oxygen-saturated and contained $6.3 \mu M$ Ph_2CO and $5.0 M$ 2-propanol, pH = 12.2

tendency to heat up, especially since several minute photolysis periods are required with this lamp for good yields. Note that these long photolysis periods are required even with the more efficient photosensitizer benzophenone (see below).

Experiments were tried where the solution was continuously purged with dioxygen during the photolysis in the attempt to gain higher yields of O_2^- . Very curiously, the yields were much lower in the purged system rather than in the pre-saturated system. Figure 1-6 presents a plot of these data obtained on a 1.0 M 2-propanol solution containing 41 mM acetone at pH 12.2.

The effect the concentrations of alcohol and ketone have on the yields of O_2^- was also examined.

In a system where the acetone concentration was held fixed at 0.041 M, the effect of the concentration of 2-propanol on the yield of superoxide ion was studied. The yield increased with increasing alcohol concentration up to 5.0 M and then began to fall off. Figures 1-7 and 1-8 give plots showing how the concentration of 2-propanol affects the O_2^- yield. As can be seen, 3.0 M and 7.0 M give almost identical yields while 1.0 M and 10.0 M give far less. Figure 1-8 gives the results for 5.0 M only, which is considered as the optimum alcohol concentration in this system.

The same variation was done with acetone concentration. Figure 1-9 shows that increasing acetone concentration above 0.068 M nets little or no increase in superoxide ion yield. This is most likely because these experiments were conducted in 2.0 cm cells and an acetone concentration

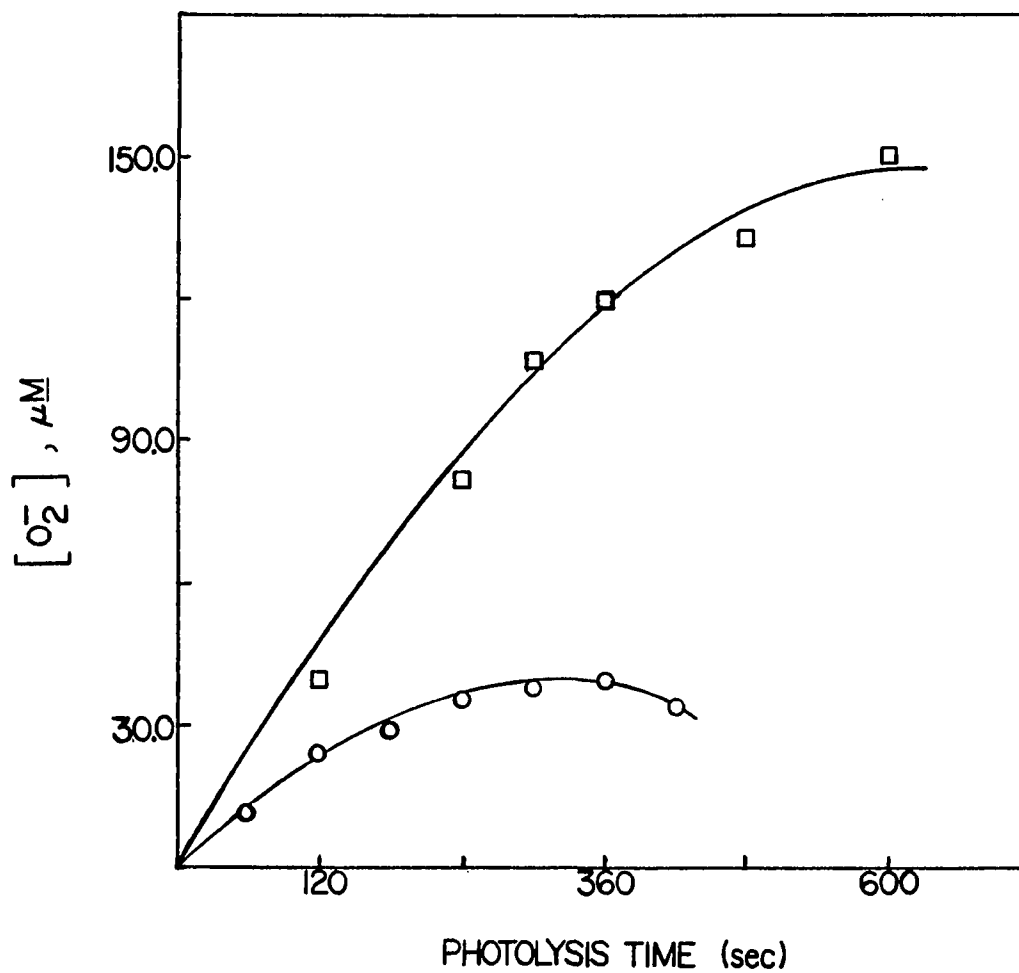


Figure 1-6. Yields of O_2^- from continuously purged (circles) and pre-saturated (squares) solutions containing 1.0 M 2-propanol, 41 mM acetone at pH 12.2

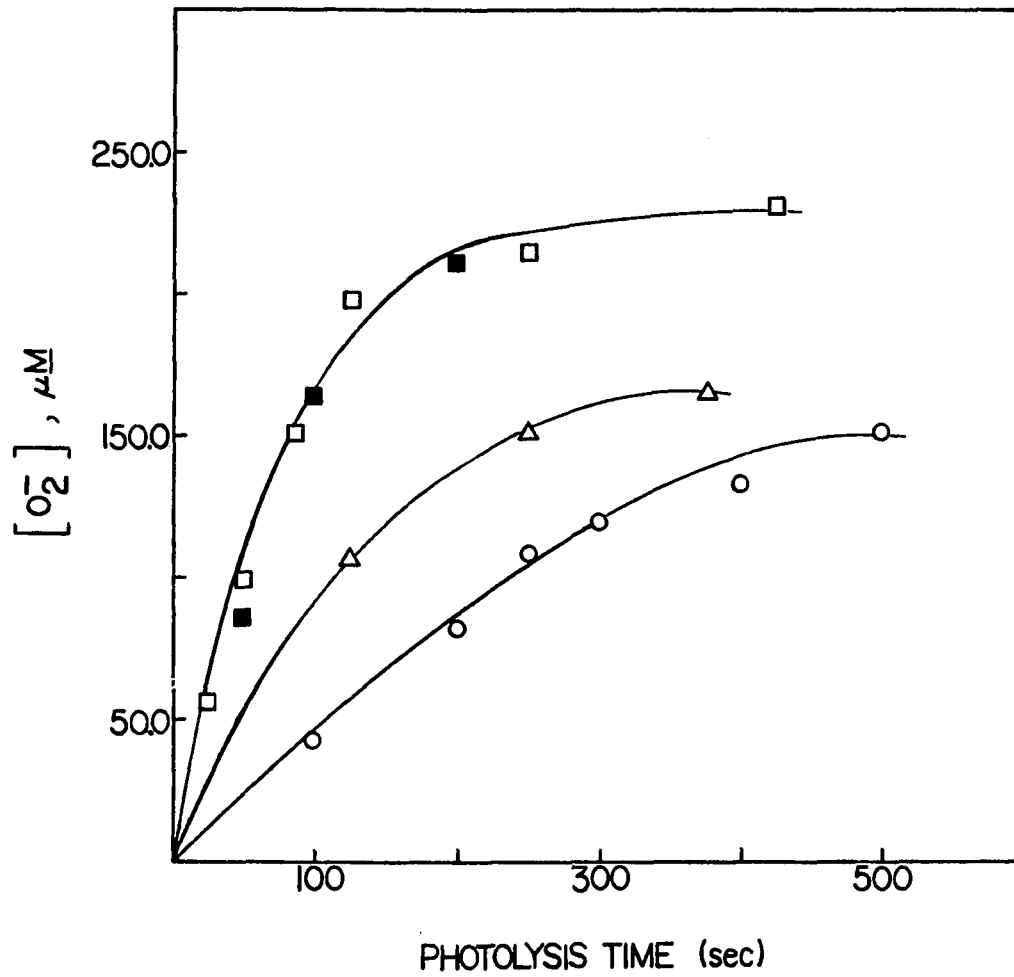


Figure 1-7. Yields of O_2^- vs. photolysis times at varying 2-propanol concentrations: 1.0 M (O), 3.0 M (\square), 7.0 M (\blacksquare), and 10.0 M (\triangle). Solutions are oxygen-saturated and contain 41 mM acetone, pH 12.2

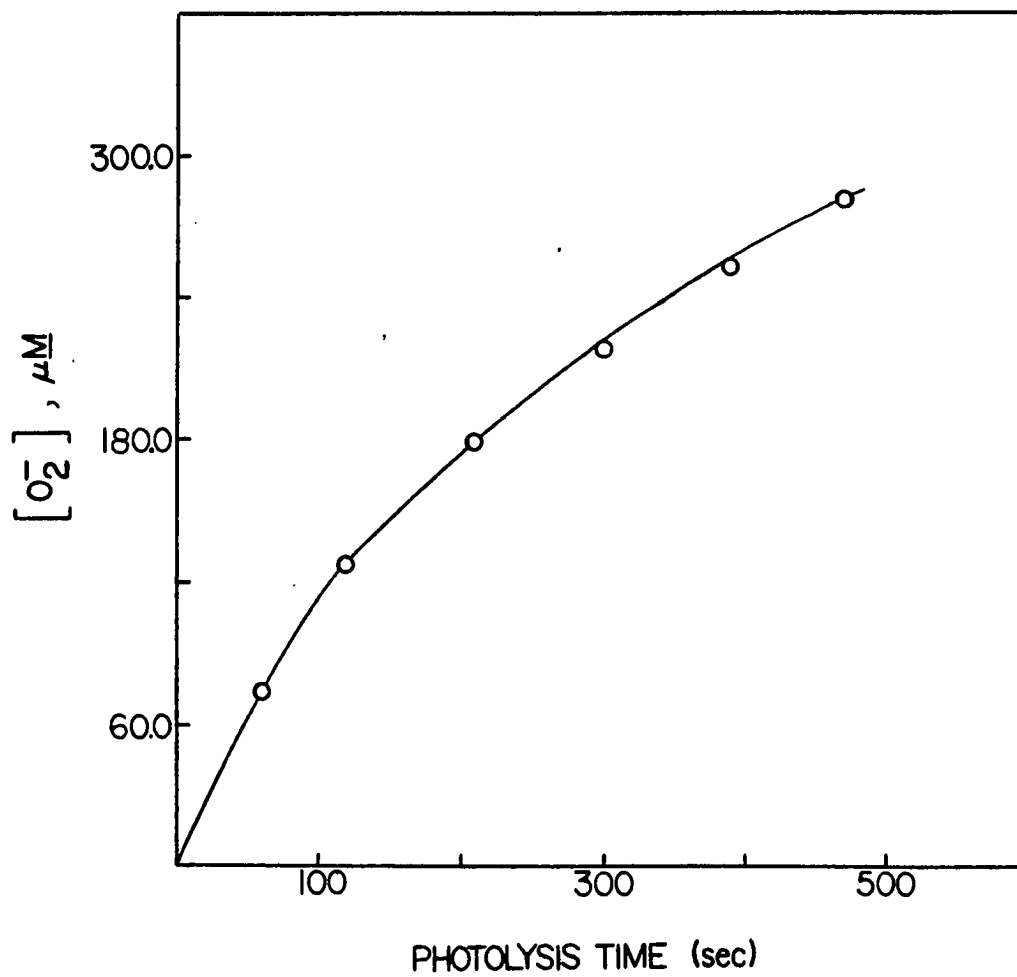


Figure 1-8. Yields of O_2^- for a solution of 5.0 M 2-propanol also containing 41 mM acetone, dioxxygen saturated, pH 12.2

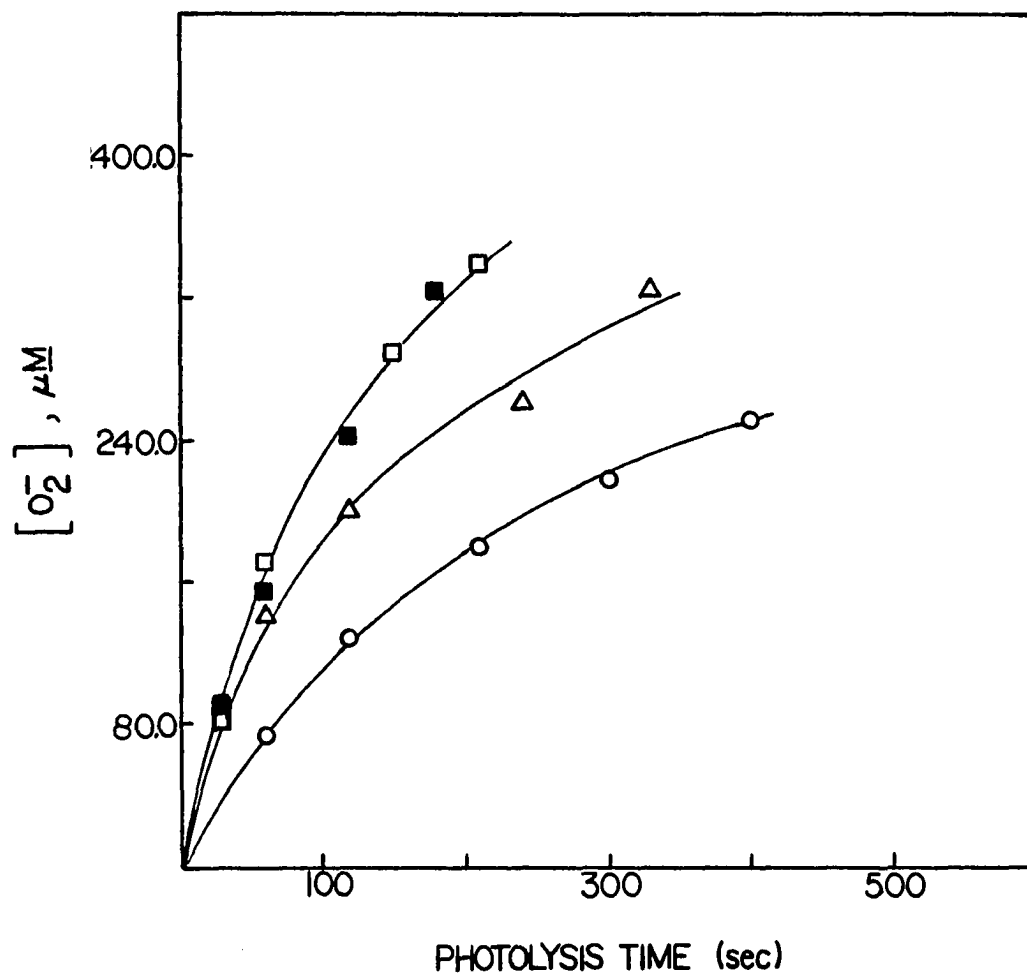


Figure 1-9. Yields of O_2^- vs. photolysis time for solutions containing 5.0 M 2-propanol and varying amounts of acetone: .041 M (O), .049 M (Δ), .068 M (\square), and .082 M (\blacksquare), pH = 12.2

of 0.068 M results in an absorbance in the UV of over 2.0 at its maximum wavelength. An absorbance of 2.0 corresponds to 99% light absorption, so more acetone in the system will result in no further photosensitization. Therefore, 0.068 M acetone is considered the optimal working concentration for a 2.0 cm cell.

The final result then is a solution containing 5.0 M alcohol and 0.068 M acetone for best results when using the Xe lamp. Perhaps misleading are the graphs. It should be noted that the maximum yields are given in the Figures 1-4 to 1-9. Photolyses at greater times than those plotted sometimes resulted in very minor increases in O_2^- yields but usually resulted in a substantial loss of O_2^- .

Hg lamp as UV source

Very little work was done on this UV source although it proved highly efficient. Only two sets of experiments were tried, one employing benzophenone as sensitizer, the other employing acetone. Identical results were obtained.

A standard Rayonet photoreactor was used. Figure 1-10 shows the results found using this UV source. The immediate feature to notice is the significant shortening in the required photolysis time, 30 s producing almost 400 μM O_2^- . This work was done using the optimal 2-propanol concentration of 5.0 M (see above).

The result that shorter photolysis times are required is probably a consequence that irradiation occurs from all directions (the cell being suspended by a wire or placed upon a reflective platform) and hence the

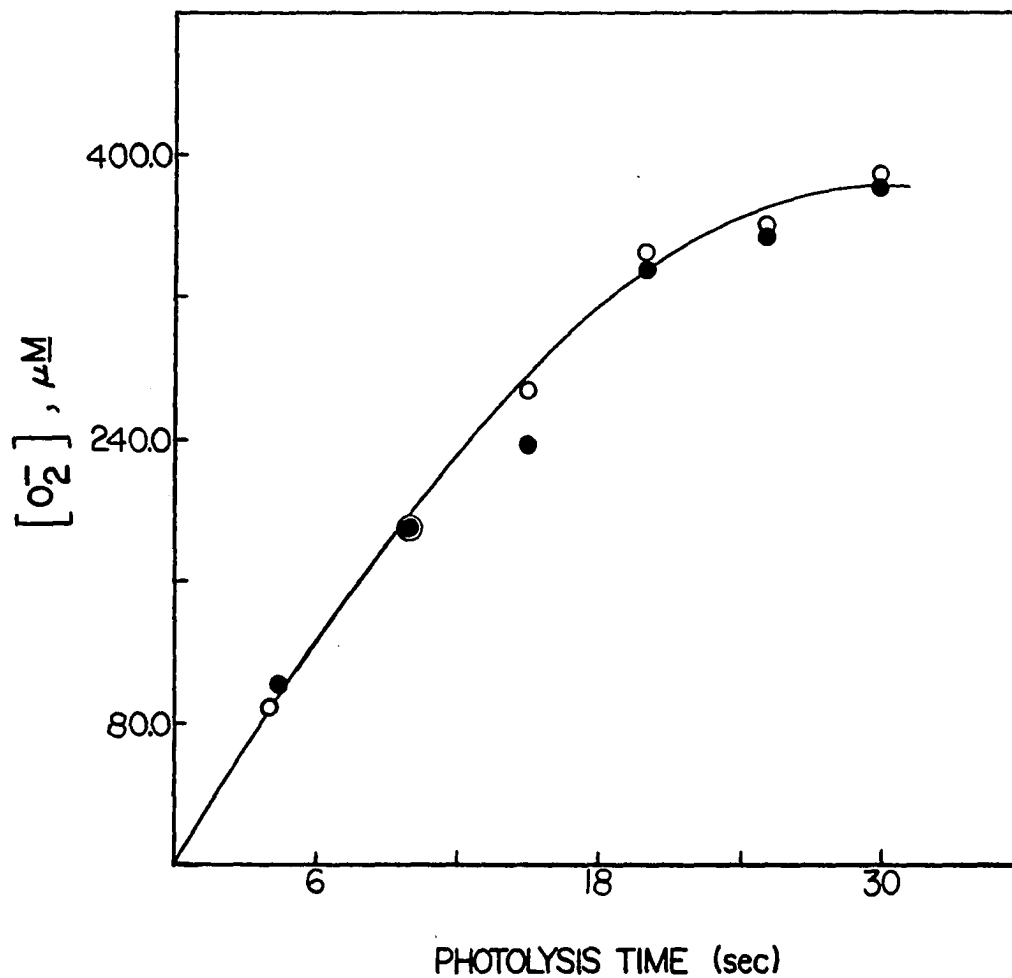


Figure I-10. Yields of O_2^- vs. photolysis time employing Hg arc lamp chamber as UV source. Solution contains 5.0 M 2-propanol and either 6.3 μM Ph_2CO (O) or 41.0 mM acetone (●), dioxygen saturated, pH = 12.4

photolysis becomes more efficient. As happened with the Xe lamp, yields fell off sharply beyond 30 s.

The Hg lamp system is a much more efficient system and is preferred over the Xe plasma lamp. Several reasons exist for this. First, shorter photolysis times allow for a better control of temperature as the cell need not be out of its thermostating bath very long. Second, the IR component is much smaller in the Hg lamps and the chance of heating the cell is lessened greatly. Third, since irradiation is omnidirectional and not unidirectional, cell placement is not a critical concern.

Use of sunlight as UV source

Eighty-five μM of superoxide ion was produced in a cylindrical quartz spectrophotometer cell (2-cm optical path, 6-cm^3 volume) held for ~5 min in direct sunlight when the cell was partially surrounded by shiny aluminum foil to act as a reflector. The solution contained $6.3 \mu\text{M}$ Ph_2CO and 5.0 M 2-propanol at pH 12.1.

Concluding Remarks

A very efficient method of producing superoxide ion has been found employing a number of commonly used UV sources. An additional feature of this method is the little modification done to the previous working solution. Small amounts of acetone and minute amounts of benzophenone are the only change made.

The method is also very flexible in that there is a choice in the alcohols that may be used as well as the variability in their concentrations (the same is true for the ketone sensitizer). Also, the method

is mobile in that the O_2^- may be generated in situ in the presence of substrate by flash photolysis for fast reactions or it can generate O_2^- with the substrate to be added later as in the case of slower reactions. In Part II of this thesis, both instances will be demonstrated.

EXPERIMENTAL

Reagents

All water used throughout these experiments was distilled water further purified by either passage through a Millipore-Q filtering system, passage through a Barnstead PCS filtering system, or by triple distillation.

Acetone (Aldrich Gold Label), methanol (Aldrich Gold Label), 2-propanol (Aldrich Gold Label), KOH (Fischer Scientific), Na₂EDTA (Mallinckrodt), and Ph₂CO (Eastman Kodak) were all used without further purification. Oxygen (Air Products, 99.7%) was further purified by passage through a Koby Junior gas filter.

Equipment

All glassware, including spectrophotometric cells, were carefully and thoroughly cleaned. The normal routine included chromic acid bathing followed by at least 7 distilled water washings and 3 isopropanol washings. Drying was achieved by placing in an oven at 120°C. Spectrophotometric cells and syringes were allowed to air dry.

Rubber septa were prepared for use by soaking overnight in either methanol or isopropanol, then washed thoroughly with distilled water and allowed to air dry. Syringe needles were readied in a similar fashion.

All UV spectral measurements were conducted on a Cary 219 spectrophotometer. Kinetic measurements were also made on this instrument. The pH of the solutions was measured using a Beckman pH meter equipped

with a glass electrode. Steady state photolyses were performed using a Sorenson Supply XL51 Xe lamp or a Rayonet Photochemical Reactor equipped with medium pressure Hg lamps. Flash photolyses were done on a Xenon Corp. flash photolysis unit.

Solution Preparations

Acetone as sensitizer

Approximately one-half the volume of the desired volumetric flask was filled with water containing $\sim 30 \mu\text{M Na}_2\text{EDTA}$. The pH was then adjusted by either addition of the solid KOH reagent or addition of a standardized (by KHP or standardized HClO_4) KOH solution. This was followed by addition of the alcohol and then water until approximately a 2 mL volume remained. Acetone was then added, the flask brought to the mark with water, and the solution thoroughly mixed. All volumes above were delivered either by syringe or buret.

The solution was used as is for air-saturated experiments. For oxygen-saturated experiments, a gentle flow of the gas was passed through the solution for 15 minutes. Care was taken to not apply too vigorous a purge as some acetone may then be lost.

Benzophenone as sensitizer

The above method was followed with one exception. The benzophenone was introduced in the form of a solution in the desired alcohol rather than adding the solid reagent.

Photolysis Experiments

General

All yields were calculated by recording the absorbance prior to photolysis at $\lambda 245$ nm and immediately after. Beer's Law, using $\epsilon_{0_2}^{\lambda 245 \text{ nm}} = 2350 \text{ M}^{-1} \text{ cm}^{-1}$,³⁰ was used to calculate the concentration.

Cells were prepared by rinsing and filling with the desired solution. Thermostatting was done in a few instances, but the majority of the experiments were conducted at room temperature (23-27°C).

Flash photolysis experiments

The flash photolysis was conducted with unfiltered UV-visible radiation from fast-extinguishing Xenon flash lamps in the Xenon Corporation's Model 710 system.⁵¹ Flash energies were normally 25-50 J.

Steady state experiments

Two sources were used. The first was a Sorenson Supply XL51 Xe lamp. The photolyzing radiation was passed through the cell lengthwise at a distance of 2-3 cm. Because of the time required in these experiments, the cell was rotated end for end every 30 seconds to prevent overheating of the solution and cell. When this method was used for a kinetic trace, the cell was rethermostatted 5 minutes after photolysis.

The second source was a standard Rayonet Photoreactor equipped with medium pressure Hg lamps. An aluminum foil covered stage was placed at the bottom of the reactor. The cell was placed upon this stage.

Photolyses were then conducted.

Use of sunlight

Experiments were done by holding the cell by its neck in the sunlight on a bright sunny day. Crumpled aluminum foil was held behind the cell to act as a reflector.

Kinetics

A 2.0 cm cell was rinsed and filled with the reagent solution and thermostatted for 25 minutes at $25.0 \pm 0.1^\circ\text{C}$. Superoxide ion was then generated photochemically by removing the cell from the water bath, wiping dry, and placing in the desired photoreactor. After photolysis was complete, the cell was returned to the water bath and then the decay of the superoxide ion was followed at $\lambda 245$ nm.

The yield of O_2^- was calculated by recording the absorbance at $\lambda 245$ nm before and immediately after photolysis. Beer's Law, using $\epsilon_{\text{O}_2^-}^{245 \text{ nm}} = 2350 \text{ M}^{-1} \text{ cm}^{-1}$,³⁰ was used to determine the concentration of O_2^- .

The pH of the solution was measured before photolysis and at the completion of the kinetic trace. In all cases, pH recorded was lower than the expected pH. This was probably due to the alcohol present. The differences were not serious enough to generate any concern.

The data were analyzed by nonlinear least squares analysis. Fits were made to two equations. The first was to the integrated standard second order equation 20 requiring the knowledge of the starting concentration of the superoxide ion, $[\text{O}_2^-]_0$.

$$D_t = (D_0 + D_\infty [\text{O}_2^-]_0 kt) / (1 + [\text{O}_2^-]_0 kt) \quad (20)$$

The second was to the integrated second-order equation given in equation 21, where the need to know $[O_2^-]_0$ is eliminated. Both equations give equally good fits.

$$D_t = D_\infty + (D_0 - D_\infty) / [1 + k/\epsilon] (D_0 - D_\infty) t] \quad . \quad (21)$$

The values of k/ϵ at each wavelength were within 5% of the first fit's results.

REFERENCES

1. Allen, O. A.; Bielski, B. H. J. in "Superoxide Dismutase"; Oberley, L. W., Ed.; CRC Press; Boca Raton, FL, 1982, 1, 125-141
2. McElroy, A. D.; Hashman, J. S. *Inorg. Chem.* 1964, 3, 1798
3. Peters, J. W.; Foote, C. S. *J. Am. Chem. Soc.* 1976, 98, 873
4. Johnson, E. L.; Pool, K. H.; Hamm, R. E. *Anal. Chem.* 1966, 38, 183
5. Khan, A. U. *Science* 1970, 168, 476
6. Top, S.; Jaouen, G.; McGlinchey, M. *J. C. S. Chem. Comm.* 1980, 643
7. Valentine, J. S.; Curtis, A. B. *J. Am. Chem. Soc.* 1975, 97, 224
8. Matsushita, T.; Shono, T. *Bull. Chem. Soc. Jpn.* 1981, 54, 3743
9. Rosenthal, I.; Frimer, A. *Tetrahedron Lett.* 1976, 2805
10. McCandlish, E.; Miksztal, A. R.; Nappa, M.; Sprenger, A. Q.; Valentine, J. S.; Strong, J. D.; Spiro, T. G. *J. Am. Chem. Soc.* 1980, 102, 4268
11. Sawyer, D. T.; Roberts, J. L., Jr. *J. Electroanal. Chem.* 1966, 12, 90
12. McCord, J. M.; Fridovich, I. *J. Biol. Chem.* 1969, 244, 6049
13. Fee, J. A.; Hildebrand, P. G. *FEBS Letters* 1974, 39, 79
14. Ozawa, T.; Hanaki, A.; Yamamoto, M. *FEBS Letters* 1977, 74, 99
15. Morrison, M. M.; Roberts, J. L., Jr.; Sawyer, D. T. *Inorg. Chem.* 1979, 18, 1971
16. Merritt, M. V.; Sawyer, D. T. *J. Org. Chem.* 1970, 35, 2157
17. Sagae, H.; Fujihara, M.; Lund, H.; Osa, T. *Heterocycles* 1979, 13, 321
18. Sagae, H.; Fujihara, M.; Lund, H.; Osa, T. *Bull. Chem. Soc. Jpn.* 1980, 53, 1537
19. Hussey, C. L.; Laher, T. M.; Achord, J. M. *J. Electrochem. Soc.* 1980, 127, 1484

20. Nanni, E. J., Jr.; Stallings, M. D.; Sawyer, D. T. J. Am. Chem. Soc. 1980, 102, 4481
21. Roberts, J. L., Jr.; Sawyer, D. T. J. Am. Chem. Soc. 1981, 103, 712
22. Bray, R. C. Biochem. J. 1961, 81, 189
23. Michelson, A. M.; McCord, J. M.; Fridovich, I. "Superoxide and Superoxide Dismutases"; Academic Press: New York, 1977
24. Roberts, J. L., Jr.; Morrison, M. M.; Sawyer, D. T. J. Am. Chem. Soc. 1978, 100, 329
25. Sawyer, D. T.; Richens, D. T.; Nanni, E. J., Jr.; Stallings, M. D. Dev. Biochem. 1980, 11A, 1
26. Rigo, A.; Viglino, P.; Rotilio, G. Anal. Biochem. 1975, 68, 1
27. McCord, J.; Fridovich, I. J. Biol. Chem. 1968, 243, 5753
28. Bielski, B. H. J.; Gebicki, J. M. Adv. Radiat. Chem. 1970, 2, 177
29. Czapski, G. Annu. Rev. Phys. Chem. 1971, 22, 171
30. Bielski, B. H. J. Photochem. Photobiol. 1978, 28, 645
31. Ilan, Y. A.; Meisel, D.; Czapski, G. Israel J. Chem. 1974, 12, 891
32. Behar, D.; Czapski, G.; Rabani, J.; Dorfman, L. M.; Schwartz, H. A. J. Phys. Chem. 1970, 74, 3209
33. Bielski, B. H. J.; Richter, H. W. J. Am. Chem. Soc. 1977, 99, 3019
34. Baxendale, J. H. Radiat. Res. 1962, 17, 312
35. Ghormley, J. A.; Hochandal, C. H.; Riley, J. F.; Boyle, J. W. ORNL-3994, Oak Ridge National Laboratory, 1966
36. McCord, J. M.; Fridovich, I. Photochem. Photobiol. 1973, 117, 115
37. Holroyd, R. A.; Bielski, B. H. J. J. Am. Chem. Soc. 1978, 100, 5796
38. Gebicki, J. M.; Bielski, B. H. J. J. Am. Chem. Soc. 1982, 104, 796
39. This method (and those similar) shall be referred to as the Bielski method in subsequent paragraphs. The senior author of this series of papers is B. H. J. Bielski and due credit is given.

40. Turro, N. J. "Modern Molecular Photochemistry"; The Benjamin/Cummings Publishing Co., Inc.: Menlo Park, California, 1978; Chapters 9, 10, pp. 365-366
41. Sawyer, D. T.; Valentine, J. S. *Acc. Chem. Res.* 1981, 14, 393
42. San Filippo, J., Jr.; Romano, L. J.; Chern, C.-I.; Valentine, J. S. *J. Org. Chem.* 1976, 41, 586
43. Magno, F.; Bontempelli, G. *J. Electroanal. Chem.* 1976, 68, 337
44. Gibian, M. J.; Sawyer, D. T.; Ungermann, T.; Tangpoonpholvivat, R.; Morrison, M. M. *J. Am. Chem. Soc.* 1979, 101, 640
45. Divisek, J.; Kastening, B. *J. Electroanal. Chem.* 1975, 65, 603
46. Bielski, B. H. J.; Schwarz, H. A. *J. Phys. Chem.* 1968, 72, 3836
47. Bothe, E.; Behreus, G.; Schulte-Frohlinde, D. *Z. Naturforsch* 1977, 32b, 886
48. Ilan, Y.; Rabani, J.; Henglein, A. *J. Phys. Chem.* 1976, 84, 1558
49. Rabani, J.; Klug-Roth, D.; Henglein, A. *J. Phys. Chem.* 1974, 78, 2089
50. Bothe, E.; Schuchmann, M. N.; Schulte-Frohlinde, D.; von Sonntag, C. *Photochem. Photobiol.* 1978, 28, 639
51. Ryan, D. A. Ph.D. thesis, Iowa State University, 1981

APPENDIX. SUPPLEMENTAL DATA

Table 1-A-1. Effect of distance from UV source^a on superoxide ion yield^{b,c}

Distance ^d (cm)	Photolysis time ^e (sec)	Yield O_2^- ^f (μM)
3.5	30	35.1
3.5	60	61.9
3.5	90	72.6
3.5	120	95.1
3.5	150	120.0
3.5	180	135.0
3.5	240	160.0
3.5	300	180.0
3.5	420	199.0
3.5	480	180.0
1.0	60	89.2
1.0	120	145.0
1.0	180	205.0
1.0	260	218.0

^aXe plasma lamp.

^bSolutions contain 6.3 μM Ph_2CO , 16 μM Na_2EDTA , 5.0 M 2-propanol, oxygen saturated, pH = 12.2.

^cData plotted in Figure 1-4.

^dAs measured from cell face to photolysis source.

^e ± 1 sec.

^fAs determined from absorbance at $\lambda 245$ nm (see Experimental).

Table 1-A-2. Yields of superoxide ion as a function of alcohol and ketone concentrations^a

[2-Propanol] (M)	[Acetone] (M)	Photolysis time (s)	Yield O ₂ ^{-b} (μM) ²
<u>1. Acetone as Sensitizer</u>			
1.05	.041	60	11.7 ^c
		120	24.5 ^c
		180	29.4 ^c
		240	35.7 ^c
		300	38.3 ^c
		360	39.8 ^c
		420	34.3 ^c
1.05	.041	480	35.1 ^c
		120	42.8
		240	81.5
		300	109.0
		360	120.0
		480	133.0
		600	150.0
3.01	.041	900	145.0
		30	56.6
		60	99.6
		105	150.0
		150	198.0
		300	214.0
5.0	.041	450	231.0
		60	73.4
		120	128.0
		210	180.0
		300	190.0
		300	192.0
		300	218.0
		360	153.0 ^d
390	253.0		

^aAll solutions are oxygen saturated, contain 16 μM Na₂EDTA, pH is between 12.0 and 12.4. UV source is Xe plasma lamp unless otherwise noted.

^bAs determined from absorbance at λ245 nm (see Experimental).

^cContinuous purge of O₂ during photolysis.

^dCell out of light path.

Table 1-A-2. Continued.

[2-Propanol] (M)	[Acetone] (M)	Photolysis time (s)	Yield O ₂ ⁻ (μM)
5.0	.041	450	253.0 ^e
		450	278.0
		450	284.0
		480	183.0 ^e
5.0	.041	4	88.5 ^f
		10	190.0 ^f
		15	267.0 ^f
		20	344.0 ^f
		25	359.0 ^f
		30	390.0 ^f
5.0	.049	60	134.0
		120	201.0
		240	262.0
		330	325.0
		420	198.0
5.0	.068	30	82.6
		60	172.0
		150	289.0
		210	342.0
		240	287.0
		240	193.0 ^e
5.0	.082	30	91.5
		60	155.0
		120	243.0
		180	325.0
7.0	.041	60	86.0
		120	164.0
		240	210.0
		360	186.0
		480	191.0
10.0	.041	150	106.0
		300	150.0
		450	164.0

^eCell extremely hot (overheated during photolysis).

^fHg arc lamp chamber as UV source.

Table 1-A-2. Continued.

[2-Propanol] (<u>M</u>)	[Ph ₂ CO] (<u>μM</u>)	Photolysis time (sec)	Yield O ₂ ⁻ (<u>μM</u>)
5.0	6.3	5	103.0 ^f
		10	190.0 ^f
		15	238.0 ^f
		20	329.0 ^f
		25	356.0 ^f
		30	383.0 ^f

PART II. SOME ELECTRON TRANSFER REACTIONS OF SUPEROXIDE
ION IN AQUEOUS SOLUTIONS

STATEMENT OF THE PROBLEM

The superoxide ion, O_2^- , is an important species in many chemical, biochemical, and biological systems¹⁻⁸ and has therefore received great attention. Numerous reviews^{4,9-13} of its properties and reactivity have been made. The reading of such reviews reveals an area of superoxide ion chemistry that is limited in detailed information. Data concerning the redox chemistry of O_2^- in aqueous solution appears rather scarce. Among the reasons for this are the inherent instability of superoxide ion in aqueous and/or protic media and the difficulty of its preparation in such media.

Recently, a very clean and convenient method of producing superoxide ion in aqueous solution has been developed in this laboratory.¹⁴ This presents then the opportunity to investigate O_2^- and its redox chemistry, particularly its behavior as an outer sphere reductant. This will be examined through its reactions with a series of Co(III) amine complexes and ferricinium ion.

Through such studies, it is also hoped to gain further understanding about the electron exchange process between dioxygen and superoxide ion in aqueous solution (equation 1):



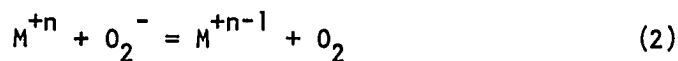
In particular, it is desired to evaluate the electron self-exchange rate constant k_{11} for this process. This is of interest because (1) no direct measurement of this value has been accomplished, (2) there exists a very large discrepancy in the values obtained by indirect means, and

(3) once determined, such a value can find utility in the evaluation of other self-exchange rate constants, such as those of metalloproteins and related species and of other small molecules such as O_3 .

LITERATURE BACKGROUND

Superoxide Ion as a Reductant

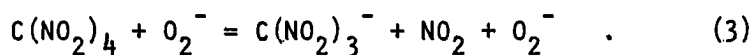
The ability of superoxide ion to react as a one-electron reductant as shown in equation 2 has been demonstrated in both aqueous and non-aqueous media. Among the examples in aqueous solution are Cu^{+2} hydrate



and a variety of Cu(II) complexes,^{15,16} the EDTA complexes of Fe(III) ^{17,18} and Mn(III) ,¹⁹ and ferricytochrome C.²⁰ These reactions are believed to proceed via a nonouter sphere pathway involving interaction of the metal center with superoxide ion prior to electron transfer.

More relevant to the present studies are reductions following an outer sphere mechanism. Although rarer in occurrence than the nonouter sphere type, they are known and well-documented. Examples include both organic and inorganic substrates.

Tetranitromethane, $\text{C(NO}_2)_4$, is readily reduced by O_2^- in aqueous solution as shown in equation 3.²¹



Quinones²²⁻²⁴ constitute a class of organic compounds also reduced by superoxide ion. Benzoquinone,²² duroquinone,²³ and 2,3-dimethyl-1,4-naphthoquinone²³ are three of the many quinones that have been investigated. These reactions are very rapid and yield the corresponding semiquinone and dioxygen. Inorganic complexes that undergo one-electron

reduction are $\text{Fe}(\text{CN})_6^{-3}$,²⁵ $\text{Mo}(\text{CN})_8^{-3}$,²⁶ and $\text{Ru}(\text{NH}_3)_5 \text{ isn}^{+3}$.²⁷ Table II-1 summarizes the kinetic data for these reactions.

Additional information about outer sphere reductions by superoxide ion can be obtained indirectly. Kinetic measurements on the reverse of equation 2, i.e., outer sphere oxidation by dioxygen resulting in superoxide ion production, have been made on a series of Ru(II) amine complexes^{28,29} and the $\text{Co}(\text{sep})^{+2}$ ³⁰ complex. These data, coupled with the equilibrium constant for equation 2 (determined from the standard reduction potentials with the E° for the $\text{O}_2(\text{aq})/\text{O}_2^-$ couple taken as -0.16 V ^{4,31}), allows the calculation of the rate constant for the forward reduction process. These calculated values are also given in Table II-1.

It is evident that there are relatively few known reactions involving superoxide ion as an outer sphere reductant. The importance of such data is that they can be employed in the calculation of the $\text{O}_2(\text{aq})/\text{O}_2^-$ electron self exchange rate constant. This is accomplished through the Marcus correlation.

The Marcus Correlation and Its Application

The Marcus correlation^{32,33} for outer sphere electron transfer reactions predicts the relationship given in equation 4:

$$k_{12} = (k_{11}k_{22}K_{12}f)^{1/2} \quad (4)$$

$$\log_{10} f = \frac{(\log_{10} K_{12})^2}{4 \log_{10} \left(\frac{k_{11}k_{22}}{Z^2} \right)}$$

The terms k_{11} and k_{22} are the reactant electron self-exchange rate

Table 11-1. Summary of the second order rate constants for outer sphere superoxide ion reductions in aqueous solution

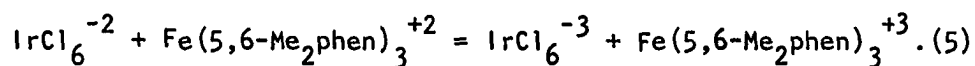
Oxidant	$k_{12} (\text{M}^{-1} \text{s}^{-1})^a$	Reference
$\text{C}(\text{NO}_2)_4$	1.9×10^9	21
Quinones	$10^6 - 10^9$	22-24
$\text{Fe}(\text{CN})_6^{-3}$	2.70×10^2	25
$\text{Mo}(\text{CN})_8^{-3}$	3.0×10^5	26
$\text{Ru}(\text{NH}_3)_5 \text{isn}^{+3}$	2.18×10^8	27
	(1.57×10^8)	29
$\text{Ru}(\text{NH}_3)_6^{+3}$	(2.0×10^5)	28,29
$\text{Ru}(\text{en})_3^{+3}$	(1.3×10^7)	28,29
$\text{Ru}(\text{NH}_3)_4 \text{phen}^{+3}$	(3.5×10^9)	29
$\text{trans-}[\text{Ru}(\text{NH}_3)_4 \text{isn}(\text{H}_2\text{O})]^{+3}$	(3.3×10^8)	29
$\text{cis-}[\text{Ru}(\text{NH}_3)_4 \text{isn}(\text{H}_2\text{O})]^{+3}$	(3.4×10^7)	29
$\text{trans-}[\text{Ru}(\text{NH}_3)_4 \text{isn}(\text{Cl})]^{+2}$	(1.8×10^7)	29
$\text{Ru}(\text{NH}_3)_5(4\text{-vinyl-py})^{+3}$	(3.2×10^7)	29
$\text{Co}(\text{sep})^{+3}$	(0.87)	30

^aValues in parentheses are calculated from the equilibrium constant K_{12} of equation 2 and the second order rate constant for the reverse of equation 2, $K_{12} = k_f/k_r$.

constants, K_{12} is the one electron equilibrium constant, and Z is the collision frequency ($10^{11} \text{ M}^{-1} \text{ s}^{-1}$).

One of the utilities of the Marcus correlation is its employment as a tool in the estimation of electron self-exchange rate constants that are difficult to obtain by direct methods. This is done by determining the rate constant k_{12} of a cross reaction where one redox partner has a known self-exchange rate constant. These data are then applied to equation 4, solving for f and k_{11} (or k_{22}) simultaneously.

To illustrate this, the $\text{IrCl}_6^{-2}/\text{IrCl}_6^{-3}$ system will be used. The electron self exchange rate constant for this system was estimated in 1963 by applying the Marcus equation to data obtained for the cross reaction given in equation 5.³⁴



A value of $2.5 \times 10^4 \text{ M}^{-1} \text{ s}^{-1}$ was calculated. In 1966, the exchange rate constant was determined by a direct measurement. The actual value proved to be $2.3 \times 10^5 \text{ M}^{-1} \text{ s}^{-1}$.³⁵ This example points out an important consideration when using the Marcus correlation. Predicted values are very often in fair agreement with experimental values but should not be taken as exact. This is because equation 4 is not an exact formulation as a number of approximations are built into it.

The Marcus correlation is not restricted to systems involving only transition metal complexes. A number of studies have been made involving redox partners such as small molecules, inorganic radical anions, and organic radical cations. The Marcus correlation has successfully

been used in evaluating the electron self-exchange rate constants for the following systems: $\text{ClO}_2(\text{aq})/\text{ClO}_2^-$; ³⁶ $\text{NO}_2(\text{aq})/\text{NO}_2^-$; ³⁶ I_2^-/I^- ; ³⁷ $(\text{SCN})_2^-/2\text{SCN}^-$; ³⁷ $\text{I}_2(\text{aq})/\text{I}_2^-$; ³⁸ $\text{Br}_2(\text{aq})/\text{Br}_2^-$; ^{38,39} $(\text{SO}_3)_2\text{NO}^-/(\text{SO}_3)_2\text{NO}^-$; ⁴⁰ and the N-alkylphenathiazine radical cations/N-alkylphenathiazines. ⁴¹

The dioxygen-superoxide ion system has also been investigated in similar fashion. Table II-2 summarizes the kinetic data for the $\text{O}_2(\text{aq})/\text{O}_2^-$ system.

In examining the column headed k_{11} , the calculated electron self-exchange rate constant for $\text{O}_2(\text{aq})/\text{O}_2^-$, it is noted that these values are very far from being a constant one. This is one of the anomalies of superoxide ion chemistry. The failure of Marcus theory to predict a constant value for the $\text{O}_2(\text{aq})/\text{O}_2^-$ exchange rate constant is a question not easily answered.

A second feature to notice is that within a given series of reactants (the Ru(III) amine complexes and the quinones), a fairly constant value for k_{11} is found. Between the two series, though, there is a 3-4 order of magnitude difference. This is a question that is also not readily explained.

At present, the number of data points is rather limited. The extension of Table II-2 to other oxidants is required before any reasonable explanation can be made. The studies presented here take the first step in such an undertaking.

Table 11-2. Summary of the kinetic data on the reactions of superoxide ion in aqueous solution applicable to Marcus theory for estimation of the $O_2(aq)/O_2^-$ electron self exchange rate constant^a

Oxidant	k_{12}^b	k_{22}^c	$E^{\circ d}$	K_{12}^e	k_{11}^f	f^g	References
Quinones	10^6-10^9	10^7-10^8	-0.24 to +0.10	10^{-2} to 10^{+4}	10^6-10^7	≤ 0.75	22,23,24
$Fe(CN)_6^{-3}$	2.70×10^2	5×10^3	0.37	9.6×10^8	5.7×10^{-7}	0.02	25
$Mo(CN)_8^{-3}$	3.0×10^5	3.0×10^4	0.75	2.7×10^{15}	2.3×10^{-4}	4.0×10^{-6}	26
$Ru(NH_3)_5isn^{+3}$	2.18×10^8	4.7×10^5	0.387	1.9×10^9	4.1×10^3	0.01	27,29
$Ru(NH_3)_6^{+3}$	2.0×10^5	4.0×10^3	0.051	3.8×10^3	4.3×10^3	0.60	29
$Ru(NH_3)_4phen^{+3}$	3.5×10^9	1.2×10^7	0.533	5.6×10^{11}	1.6×10^3	1.1×10^{-3}	29
$Co(sep)^{+3}$	0.87	5.1	-0.26	2.0×10^{-2}	11.8	0.92	30

^aReactions are written as $Ox + O_2^- = Red + O_2$. In cases where the actual data were published for the reverse reaction, the forward rate constant was calculated from the equilibrium constant $K_{12} = k_f/k_r$.

^bRate constant in $M^{-1} s^{-1}$ for the cross reaction.

^cExchange rate constant for the oxidant in $M^{-1} s^{-1}$.

^dStandard reduction potential in V vs. NHE for oxidant.

^eEquilibrium constant for the cross reaction calculated from the standard reduction potentials.

^fExchange rate constant for $O_2(aq)/O_2^-$ couple calculated from Marcus correlation.

^g f value obtained from Marcus correlation in the simultaneous solution of equation 4.

RESULTS AND INTERPRETATION

Co(III) Reductions

The reduction of several Co(III) complexes by superoxide ion was examined in aqueous 1.0 M 2-propanol solution, pH 11.3-11.9. The experiments were conducted under pseudo-first-order conditions with the Co(III) reactant in excess. The superoxide ion was photochemically generated in the reaction cell¹⁴ (a 2.0-cm cylindrical quartz spectrophotometric cell) and reaction was initiated by the injection of the Co(III) complex into the cell. Loss of O_2^- in the UV (λ 245-270 nm) was used to monitor the reaction. The rate of superoxide ion disappearance was independent of wavelength and was complete within several minutes. Figures 11-1, 11-2, and 11-3 show the dependence of k_{obs} , the pseudo-first-order rate constant on $[Co(III)]$. In all studies, a linear relationship is observed.

A rate law consistent with such results is given in equation 6.

$$\frac{-d[O_2^-]}{dt} = k_{12} [Co(III)][O_2^-] \quad (6)$$

Table 11-3 gives the second-order rate constants k_{12} for the reactions of $Co(NH_3)_6^{+3}$, $Co(ND_3)_6^{+3}$, $Co(en)_3^{+3}$, and $Co(chxn)_3^{+3}$ (chxn = trans-1,2-diaminocyclohexane) with superoxide ion. Also included are the complexes $Co(phen)_3^{+3}$ and $Co(CN)_6^{-3}$. In the latter two cases, reactions proved to be either too rapid or too slow for accurate measurements and only upper or lower limits of the second-order rate constants are presented. For the complexes $Co(NH_3)_6^{+3}$, $Co(en)_3^{+3}$, and $Co(chxn)_3^{+3}$, two

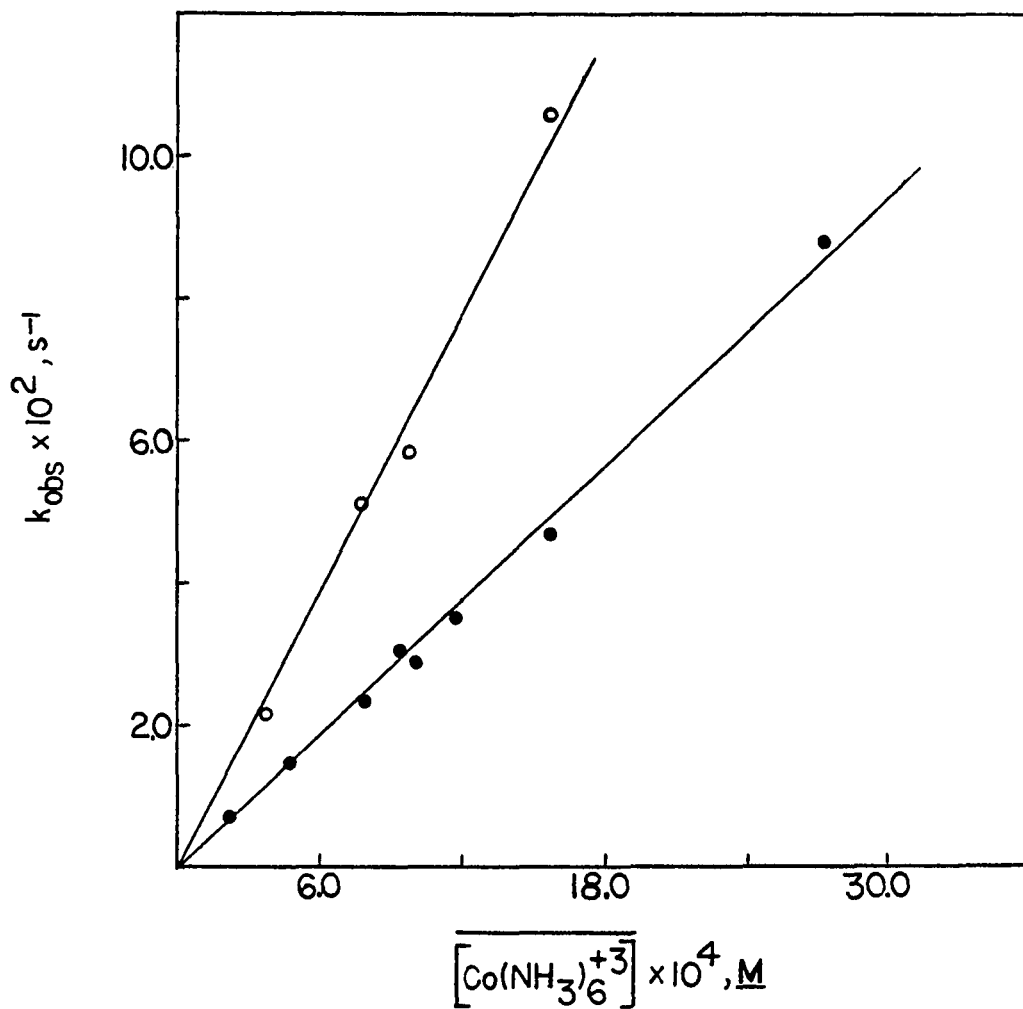


Figure 11-1. Plot of the pseudo-first-order rate constants at 25.0°C vs. $[\text{Co}(\text{NH}_3)_6^{+3}]$ for its reaction with O_2^- in 1 M 2-propanol, pH 11.3-11.9 under aerobic (●) and anaerobic (○) conditions

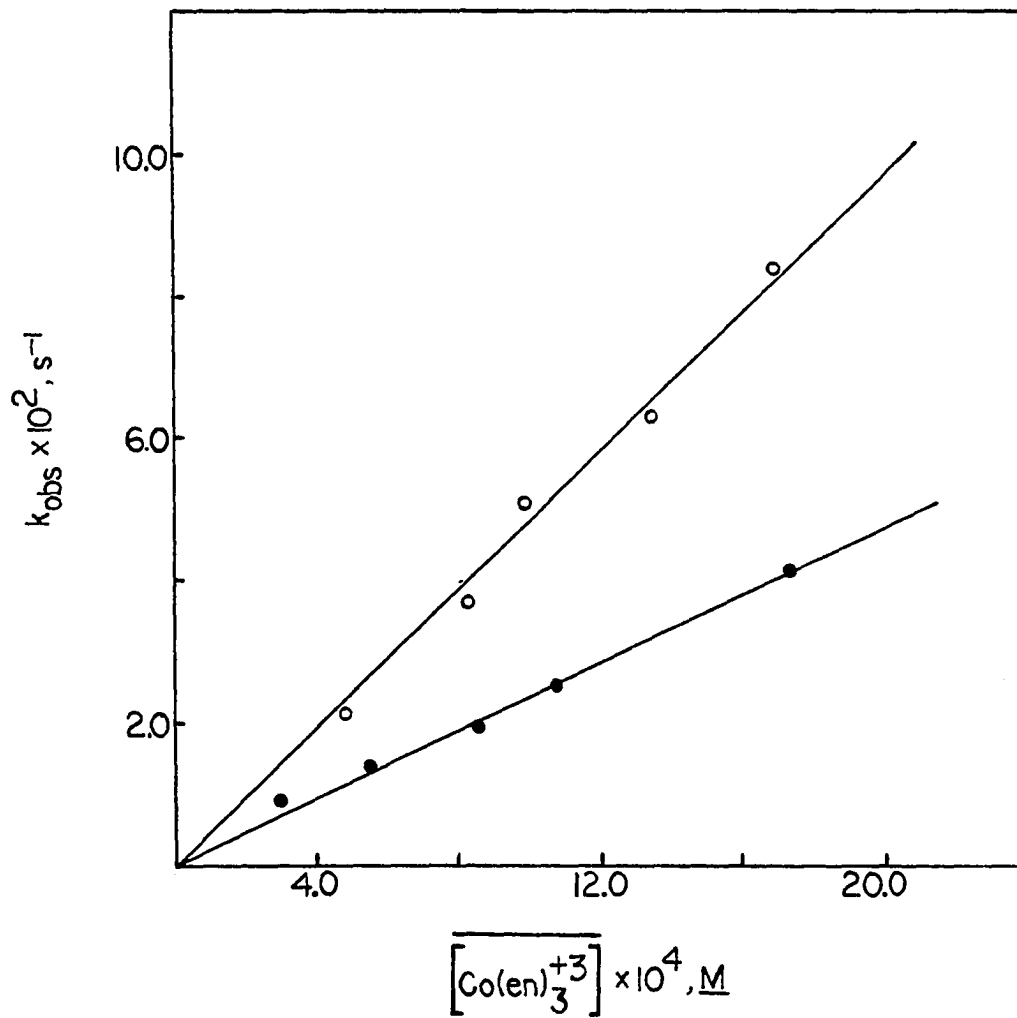


Figure 11-2. Plot of the pseudo-first-order rate constants at 25.0°C vs. $[\text{Co(en)}_3^{+3}]$ for its reaction with O_2^- in 1 M 2-propanol, pH 11.3-11.7 under aerobic (●) and anaerobic conditions (○)

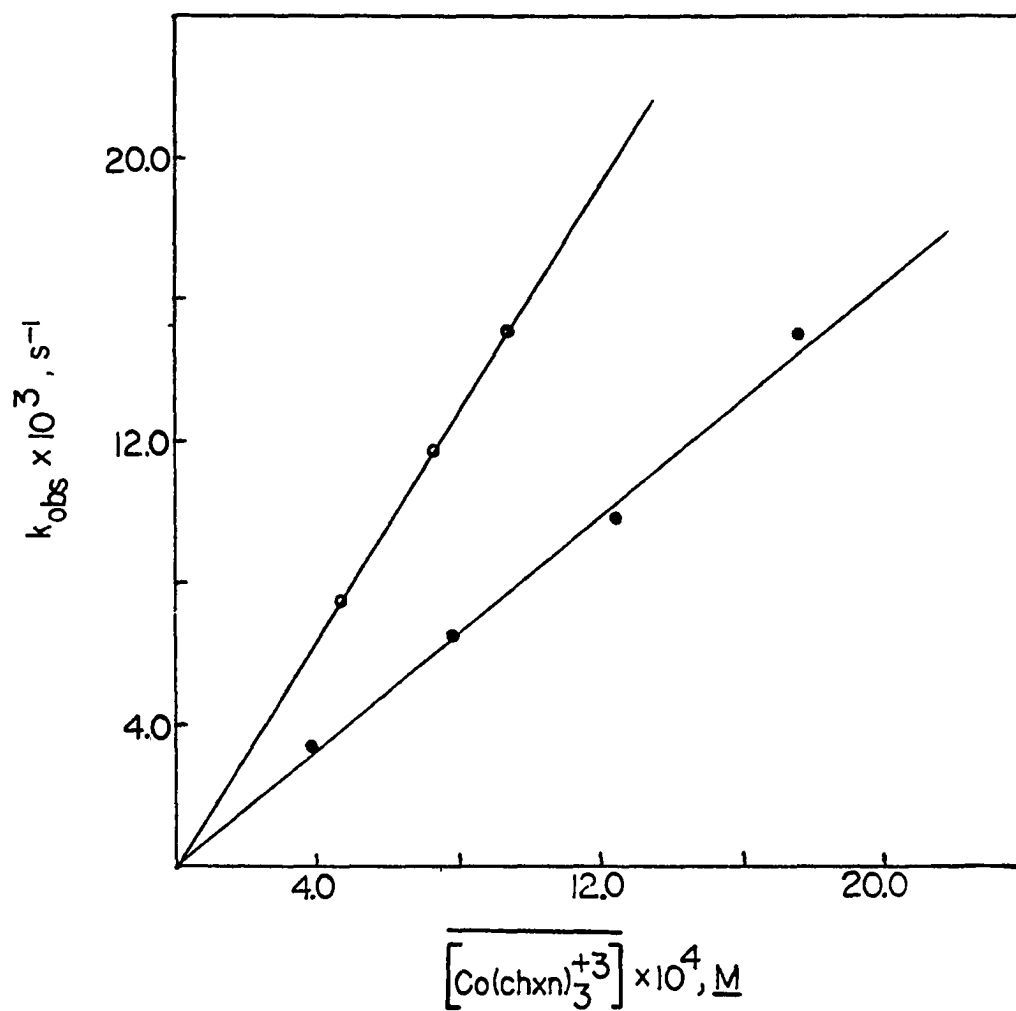


Figure 11-3. Plot of pseudo-first-order rate constants at 25.0°C vs. $[\text{Co}(\text{chxn})_3^{+3}]$ for its reaction with O_2^- in 1 M 2-propanol, pH 11.7 under aerobic (●) and anaerobic conditions (O)

Table 11-3. Summary of rate constants for the $\text{Co(III)}-\text{O}_2^-$ reactions^a

Complex	T(°C)	$k_{12}^{\text{O}_2}$ ($\text{M}^{-1} \text{s}^{-1}$)	$k_{12}^{\text{N}_2}$ ($\text{M}^{-1} \text{s}^{-1}$)	$\frac{k(\text{N}_2)}{k(\text{O}_2)}$
$\text{Co}(\text{NH}_3)_6^{+3\text{b}}$	34.39	61.5 ± 4.9 (2) ^c	--	
	25.00	31.3 ± 0.5 (16)	63.9 ± 1.7 (4)	2.04 ± 0.09
	10.89	11.7	--	
	9.80	12.1	--	
	2.14	6.2	--	
$\text{Co}(\text{ND}_3)_6^{+3\text{d,e}}$	25.00	28.4 ± 2.0 (2)	--	
$\text{Co}(\text{en})_3^{+3\text{b}}$	25.00	23.8 ± 0.4 (5)	47.5 ± 1.1 (6)	2.00 ± 0.08
	16.81	14.8	--	
	5.40	6.5 ± 0.6 (2)	--	
$\text{Co}(\text{chxn})_3^{+3\text{f}}$	25.00	16.4 ± 0.3 (6)	31.2 ± 0.4 (3)	1.90 ± 0.06
	15.22	8.84	--	
	9.01	5.66	--	
	6.16	4.78	--	
$\text{Co}(\text{phen})_3^{+3}$	25.00	$>10^{4\text{g}}$	--	
$\text{Co}(\text{CN})_6^{-3}$	25.00	$<3^{\text{g}}$		

^aIn aqueous 1 M 2-propanol, pH 11.3-11.9.

^bIncludes experiments with both chloride and perchlorate complexes.

^cValue in parentheses is number of individual experiments.

^dPrepared in situ from $\text{Co}(\text{NH}_3)_6^{+3}$ (see text).

^eExperiment in >90% D_2O .

^fChloride complex used.

^gUncertainties are 1 standard deviation.

values are reported at 25.0°C, $k_{12}^{O_2}$ and $k_{12}^{N_2}$. The former refers to the reaction under aerobic conditions, while the latter refers to the reaction under anaerobic conditions. The last column in Table 11-3 shows that $k_{12}^{N_2}$ and $k_{12}^{O_2}$ are related by a factor of 2.

The respective rate constants k_{12} for $Co(NH_3)_6^{+3}$, $Co(en)_3^{+3}$, and $Co(chxn)_3^{+3}$ are 31.3, 23.8, and 16.4 $M^{-1} s^{-1}$ at 25.0°C. These results are surprising in view of the differences in standard reduction potential of the oxidants. $Co(en)_3^{+3}$ and $Co(chxn)_3^{+3}$ are very comparable in E° , -0.24 V⁴² and -0.26 V⁴³ (vs. NHE), respectively. It would be expected that they react at comparable rates and this is observed.

$Co(NH_3)_6^{+3}$ has an E° value of 0.0 to +0.10 V^{44,45} (some uncertainty in the E° value is due to the instability of the $Co(NH_3)_6^{+2}$ species, see Discussion) and would therefore be expected to react at a greater rate than either of the two chelate complexes. The explanation for superoxide ion's insensitivity to the nature of the oxidant is found in the electron self-exchange rate constants of the Co(III) complexes.

$Co(NH_3)_6^{+3}$ has an exchange rate constant of approximately $10^{-7} M^{-1} s^{-1}$.⁴⁶ $Co(en)_3^{+3}$ is a faster exchanging complex with $k_{22} = 2.4 \times 10^{-5} M^{-1} s^{-1}$.⁴⁷ Although not measured, $Co(chxn)_3^{+3}$ probably exchanges similarly to $Co(en)_3^{+3}$ and its electron exchange rate constant can be estimated at $\sim 10^{-5} M^{-1} s^{-1}$ also. This difference in exchange rate constants compensates for the difference in standard reduction potentials and the net result is the indifference displayed by O_2^- with respect to the nature of the oxidants.

Deuterium and Solvent Effects

As a probe of the outer sphere nature of these electron transfer reactions, studies were done in both H_2O and $>90\% \text{D}_2\text{O}$ as well as examining the rates of reduction of $\text{Co}(\text{NH}_3)_6^{+3}$ and $\text{Co}(\text{ND}_3)_6^{+3}$. Within experimental error, the $\text{Co}(\text{NH}_3)_6^{+3}$ reduction in H_2O and the $\text{Co}(\text{ND}_3)_6^{+3}$ reduction in $>90\% \text{D}_2\text{O}$ gave identical results-- $k_{12} = 31.3$ and $28.4 \text{ M}^{-1} \text{ s}^{-1}$, respectively. This is the expected result if an outer sphere mechanism were in operation and therefore confirms this suspicion. The cross experiments of $\text{Co}(\text{NH}_3)_6^{+3}$ in D_2O and $\text{Co}(\text{ND}_3)_6^{+3}$ in H_2O could not be performed because of the rapid exchange of hydrogen and deuterium in the ammonia ligand at these pHs (11.3-11.9).⁴⁸ They would be expected to give similar results as above.

Some comment is necessary on the $\text{Co}(\text{ND}_3)_6^{+3}$ in $>90\% \text{D}_2\text{O}$ experiment. The perdeuterio complex was prepared in situ by allowing the normal complex to stand several minutes in $>90\% \text{D}_2\text{O}$ at pH 11.7. This is more than adequate time to insure total exchange of the ligand hydrogens.⁴⁸ This was the preferred source of $\text{Co}(\text{ND}_3)_6^{+3}$ as experiments employing $\text{Co}(\text{ND}_3)_6(\text{ClO}_4)_3$ lead to extraneous results. Rate constants 25-30% higher than anticipated were obtained when the solid complex was used as a source of either $\text{Co}(\text{ND}_3)_6^{+3}$ or $\text{Co}(\text{NH}_3)_6^{+3}$. It is believed this compound introduced some impurity into the system resulting in the faster than expected rates. These results are rejected.

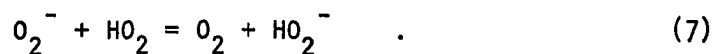
Physical and Chemical Effects

Selection of basic (pH 11.3-11.9) media

The criteria for this lie in the fact that the lifetime of O_2^- in aqueous/protic media is highly pH dependent, decreasing with lower pH.¹³ At the chosen pH values, O_2^- is sufficiently long-lived (on the order of several minutes to an hour for the first half-life) to be conveniently worked with. The decay rate is so sensitive to pH that the measured second order rate of decay was used in many instances as a "pH meter" to indicate the reaction medium's pH level.

Because of the need for basic media, the choice of the Co(III) complexes was restricted. The complexes studied undergo base hydrolysis very slowly at these pHs, and therefore provide no side reactions as would occur if $Co(NH_3)_5Br^{+2}$ were chosen. Additionally, the pKa values of the selected complexes are several units greater than the solution's pH and only one reactive species was therefore present in solution.

It is not surprising to find no pH effect on the rate constants. It is difficult to envision any acid-base equilibria in this system, particularly at the pH levels employed here. At very high pH, conjugate base possibilities could arise. At lower pH, equation 7 could become competitive with the reduction process.



Neither of these situations is expected to occur in these studies.

Presence of Complexing Anions

Because of the design of the experiment, highly concentrated (>0.1 M) stock solutions of the Co(III) reagent were sometimes needed. This required the use of the chloride salt of $\text{Co(NH}_3)_6^{+3}$ as the perchlorate salt proved too insoluble. Free Cl^- had no effect upon the rates of reduction as identical values were obtained when using $\text{Co(NH}_3)_6(\text{ClO}_4)_3$ or $\text{Co(NH}_3)_6\text{Cl}_3$. The same holds true in the Co(en)_3^{+3} system. The only noticeable effect the presence of Cl^- had upon the system was the background absorbance was higher than when ClO_4^- was present. This is attributed to the formation of weak ion pairs and their absorbance contribution in the UV. This does not occur with perchlorate present as it is a poor complexing anion.

Activation parameters

As shown in Table II-3, these reductions were also studied as a function of temperature. In Table II-4 are given the enthalpy and entropy of activation for these reactions as calculated from the Eyring equation (see Experimental).

The close similarities in the values of ΔH^\ddagger and ΔS^\ddagger for the three Co(III) complexes is a further indication of a common mechanism shared by all three. With regard to the magnitude of the values, there are no surprises. The values are typical of bimolecular reactions.

Effect of oxygen on the system

The presence and/or absence of dioxygen in the system has no direct effect upon the rate determining step of electron transfer

Table 11-4. Activation parameters for superoxide ion reductions of Co(III) amine complexes^{a,b}

Complex	ΔH^\ddagger		ΔS^\ddagger	
	kcal/mole	kJ/mole	cal/mole K	J/mole K
Co(NH ₃) ₆ ⁺³	11.3±0.4	47.2±1.5	-13.8±1.2	-57.8± 5.1
Co(en) ₃ ⁺³	10.5±0.7	44.1±3.0	-16.9±2.5	-70.7±10.5
Co(chxn) ₃ ⁺³	10.4±0.2	43.4±0.8	-18.2±0.7	-76.2± 2.7

^aAs calculated from the Eyring equation using $k_{12}^{O_2}$.

^bFor reaction in aqueous 1 M 2-propanol, pH 11.3-11.9.

although it does have an effect upon the rate constant. This is because the presence of dioxygen dictates the course of the subsequent reactions.

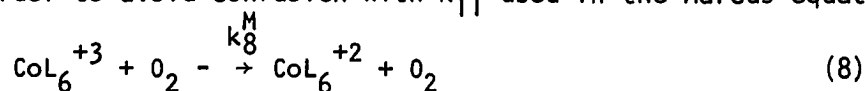
As is evident in Figures 11-1, 11-2, and 11-3, the loss of O_2^- is faster in the anaerobic systems. Comparison of the slopes of the lines in these figures (see Table 11-3) indicates that superoxide ion is lost twice as fast when dioxygen is absent. The relationship, then, between $k_{12}^{O_2}$ and $k_{12}^{N_2}$ is $k_{12}^{N_2} = 2 k_{12}^{O_2}$.

Both superoxide ion and dioxygen are capable of reoxidizing the Co(II) product of electron transfer. Under aerobic conditions, dioxygen was initially present in an ~10 fold excess over superoxide ion (~1 mM vs. ~100 μM). This excess is sufficiently great enough to scavenge (reoxidize) the Co(II) species. When the level of dioxygen is very close to zero (anaerobic conditions), the Co(II) species is reoxidized by superoxide ion. This brings about the situation where

one or two superoxide ions is consumed per electron transfer step. The presence of dioxygen oversees this.

Mechanism of the reaction

Equations 8-11 outline a plausible reaction sequence for the superoxide ion reductions investigated. The superscript M refers to "mechanism" in order to avoid confusion with k_{11} used in the Marcus equation.



The first step is outer sphere electron transfer between Co(III) and O_2^- . This step is essentially irreversible although in the Marcus correlation consideration, it is assumed to be reversible. The irreversible nature of the electron transfer stems from the fact that outer sphere oxidation of Co(II) complexes is much slower than inner sphere oxidation. The sequence of equation 9 followed by either 10 or 11 will occur at a rate faster than the reverse of 8. As an example, for the $\text{Co(NH}_3)_6^{+2}$ oxidation by O_2 , the rate constant is calculated to be $1.2 \times 10^{-3} \text{ M}^{-1} \text{ s}^{-1}$. This is significantly smaller than values expected for k_9^M , k_{10}^M , and k_{11}^M .

The second step, equation 9, is expected to be very rapid. The loss of ligands upon reduction of various Co(III) amine complexes has been studied and in acidic solution, this process has been found to be

very fast.^{49,50} The studies were not extended to the basic pH range, but it is still reasonable to expect that one or more of the coordination sites on the Co(II) species is replaced by a solvent molecule. Complete decomposition of the Co(II) complex to Co(II) hydroxo species is not anticipated because of the dioxygen studies (see above). If reaction 9 were complete to Co^{+2} hydrate, then no effect due to dioxygen would be expected as Co^{+2} hydrate is not oxidized by either dioxygen or superoxide ion and the rate of O_2^- loss should be the same under both anaerobic and aerobic conditions. In acidic solution, three ammonias are immediately lost upon reduction ($t_{1/2} < 1 \mu\text{sec}$) of $\text{Co}(\text{NH}_3)_6^{+3}$. In basic solution, it is uncertain whether or not three are also lost as the driving force of protonation of the ammonias is now absent. The loss of one ammonia or opening of one coordination site is definite as outer sphere oxidations are too slow for CoL_6^{+2} complexes (see above). Replacement of two coordination sites by solvent is also a definite consideration. Loss of three nitrogens about the Co(II) center would probably not lead to stable Co(III) products after reoxidation; therefore, n is most likely 1 or 2 in equation 9.

Reactions 10 and 11 are substitution of solvent by O_2 or O_2^- followed by inner sphere oxidation. The products P_1 and P_2 are unidentified but are believed to be Co(III) complexes containing either bound superoxide or peroxide ions. They most likely undergo further reaction to more stable products.

Some comment can be made on the relative values of k_{10} and k_{11} from the oxygen experiments. The observation that a 10-fold excess of

dioxygen can completely overcome reaction 11 indicates that k_{11}^M can be no greater than k_{10} but could be significantly smaller, i.e., $k_{11}^M \leq k_{10}^M$. A second observation is that in both anaerobic and aerobic systems, clean pseudo-first-order kinetics were seen through three half-lives. This is of importance because at the first half-life's end, the concentrations of O_2^- and O_2 should be very close to one another, and if $k_{10}^M \approx k_{11}^M$, then deviations in the kinetic traces should be observed as the rate of the loss of O_2^- would be changing from $2 k_{obs}$ to k_{obs} . Since this is not seen, the conclusion is $k_{11}^M > k_{10}^M$. These two statements are in obvious contradiction to one another.

The explanation for all of this is the statement $k_{11}^M \approx 3 k_{10}^M$. This satisfies all the observations above. The 10-fold excess of dioxygen would still effectively scavenge the Co(II) species if the ratio of rate constants is three or possibly four. The expected competition between dioxygen and superoxide may not be observed because of this ratio and also because many of the reactions followed produced small absorbance changes (<.2). Consequently, the competition may be too small to detect and the floating of the D-infinity value during analysis may further hide it. In any event, k_{11}^M is most likely on the order of 3 (or 4) times that of k_{10}^M .

To quantify reactions 10 and 11, there are several literature precedents. Oxygen uptake studies and oxidations by dioxygen involving Co(II) amine complexes have been investigated. Second order rate constants for these reactions were found to be in the range 10^3 - 10^5 $M^{-1} s^{-1}$.^{51,52} It is reasonable, then, to assign k_{10}^M a similar value.

This, in turn, assigns k_{11}^M a value also in the range 10^3 - $10^5 \text{ M}^{-1} \text{ s}^{-1}$. Very few Co(II)-superoxide ion reactions have been studied. Those that have been involve Co(II) complexes containing macrocyclic ligands and rate constants have been reported between 10^7 - $10^8 \text{ M}^{-1} \text{ s}^{-1}$.⁵³ This is obviously too high for the prediction here. This is not serious, though, as the macrocyclic nature of the complex may lead to enhanced reactivity and as a consequence, higher rate constants for its reaction with O_2^- . It is then with good confidence that the above assignment of rate constants is made.

Other Co(III) Complexes

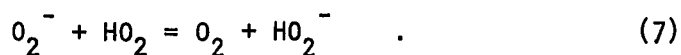
Two other Co(III) complexes were briefly examined. $\text{Co}(\text{phen})_3^{+3}$ was found to react very rapidly with O_2^- , the reaction essentially being complete within the mixing time (~5 s). A lower limit of $1.0 \times 10^4 \text{ M}^{-1} \text{ s}^{-1}$ is assigned this reaction based on a 1 second half-life and $[\text{Co(III)}]_0 = [\text{O}_2^-]_0 = 1.1 \times 10^{-4} \text{ M}$. On the other hand, $\text{Co}(\text{CN})_6^{-3}$ reacted very slowly with O_2^- . A 13-fold excess of Co(III) (sufficient enough in the earlier studies to easily overcome the disproportionation reaction of O_2^-) had no effect on the system, O_2^- decaying by self-reaction at its expected rate. A 40-fold excess led to slight perturbation in the second order decay kinetics of O_2^- and first order behavior was far from being evident. An upper limit of $3 \text{ M}^{-1} \text{ s}^{-1}$ is assigned this reaction based on the assumption of greater than a 100-fold excess of $\text{Co}(\text{CN})_6^{-3}$ is required to overcome O_2^- self-decay and that $\text{Co}(\text{NH}_3)_6^{+3}$, with $k_{12} = 31.3 \text{ M}^{-1} \text{ s}^{-1}$, overcomes O_2^- self-decay at a 10-fold excess.

These results are in accord with the expected behavior of these complexes-- Co(phen)_3^{+3} is an excellent oxidant while Co(CN)_6^{-3} is a rather poor one.

Ferricinium Ion Reduction

The reaction between superoxide ion and ferricinium ion, Cp_2Fe^+ or Fc^+ , is a more complicated system than the $\text{Co(III)}-\text{O}_2^-$ system discussed previously. This is because the pH constraints are more rigid, the reaction is several orders of magnitude faster, and side reactions now exist that must be compensated for.

The pH level of these experiments is the most critical aspect in the Cp_2Fe^+ studies. The pH must be in the basic range for two reasons. The first is to enhance the lifetime of O_2^- by preventing reaction 7.¹³



The second and more important reason is that if the pH level is too low, formation of superoxide ion from the α -hydroxyisopropyl- and α -hydroxydiphenylmethyl-peroxy radicals may be too slow to prevent reaction with FeCp_2^+ . These processes are base catalyzed⁵⁴⁻⁵⁷ and if insufficient base is present, the peroxy radicals may be long-lived enough to react with substrates present in the system. This was not a problem in the Co(III) systems as the O_2^- was generated prior to the addition of the Co(III) complex. In the FeCp_2^+ studies, it is a concern as the O_2^- is generated in the presence of the ferricinium ion (see below).

Another consideration in the selection of pH was ferricinium ion's instability at high pH. Cp_2Fe^+ is stable only in acidic solution and

undergoes a complicated decomposition to several products in the presence of OH^- .^{58,59} The rate of decomposition increases with increasing pH. This works against the above arguments in pH selection. Fortunately, the decomposition is not very rapid until very high pH is reached. It was found that pH 11 is a very good pH to conduct these experiments. At this pH, O_2^- is very rapidly produced from the precursor peroxy radicals and Cp_2Fe^+ is decaying at such a slow rate that 1 or 2% of the starting ferricinium ion is lost.

The experiment was studied using the flash photolysis technique. In addition to being an easy approach to the studies, it is one of the few viable methods with which the studies could be made. This is because of the very rapid reaction between O_2^- and Cp_2Fe^+ ($k_{12} = 8.2 \times 10^6 \text{ M}^{-1} \text{ s}^{-1}$). Flash photolysis is ideally suited for reactions such as these.

The experiment consisted of adding a known amount of OH^- to a solution of Cp_2Fe^+ in acid such that the final pH = 11. The reaction cell was then transferred to the flash photolysis instrument and reaction initiated by photochemically producing O_2^- . The loss of Cp_2Fe^+ at $\lambda 617 \text{ nm}$ was followed although this was the excess reagent. This was done because UV monitoring of O_2^- was not possible. Between 5-6 μM O_2^- was produced.

The working concentration range of Cp_2Fe^+ was limited to a maximum concentration of $\sim 100 \mu\text{M}$. This is because Cp_2Fe^+ reacts at diffusion controlled rates with the α -hydroxyalkyl radicals⁶⁰ used to generate O_2^- from O_2 . By keeping Cp_2Fe^+ at these concentrations, it ensures that

the majority of the radicals will react with dioxygen. This is because in dioxygen-saturated solution, the concentration of O_2 is ~ 1 mM. Since it, too, reacts at diffusion controlled rates,^{61,62} this ~ 10 -fold excess makes certain that the radicals will react with O_2 and not Cp_2Fe^+ .

The data (see Appendix) obtained in these studies are plotted in Figure 11-4. The slope of the line is $(8.6 \pm 0.3) \times 10^6 \text{ M}^{-1} \text{ s}^{-1}$. These results were obtained at $T = 25.0^\circ\text{C}$ in 1.0 M 2-propanol.

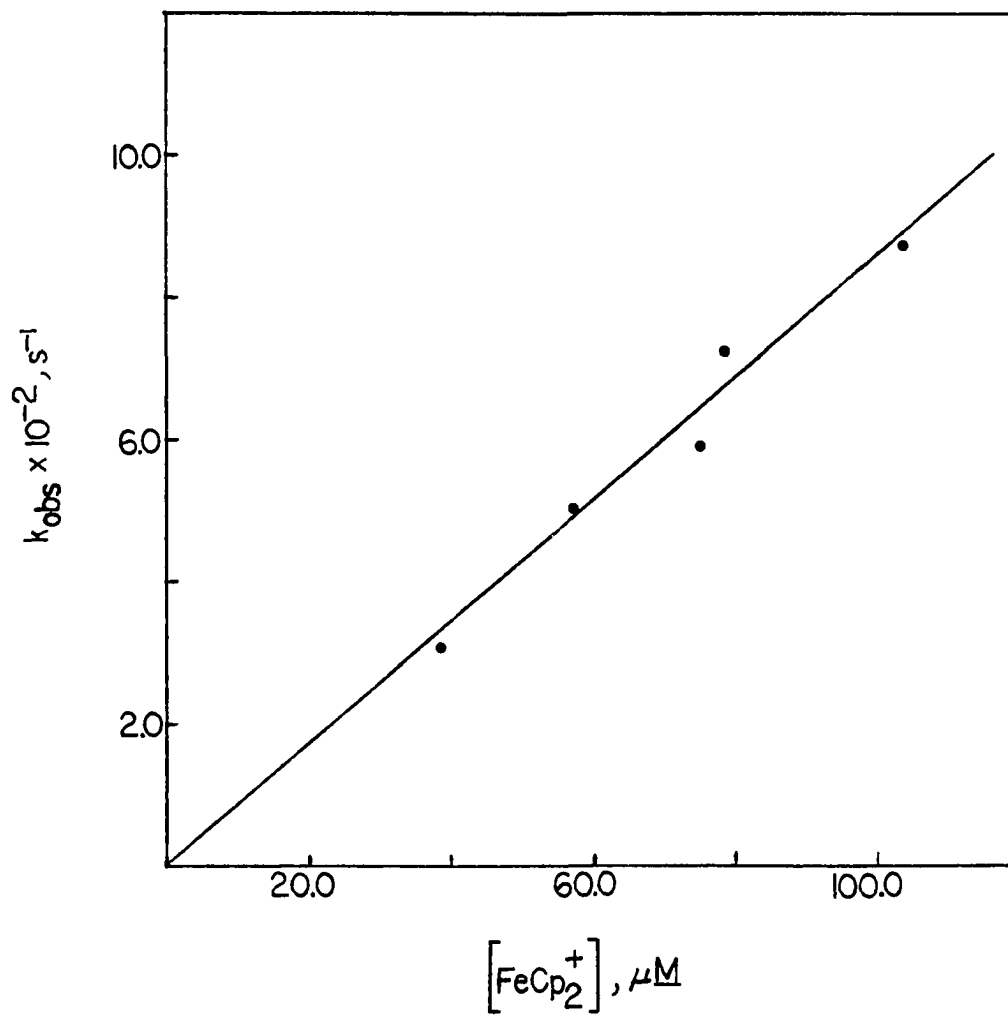


Figure 11-4. Plot of pseudo-first-order rate constants at 25.0°C vs. $[\text{FeCp}_2^+]$ for its reaction with O_2^- in 1 M 2-propanol, pH 11.0 under aerobic conditions

DISCUSSION

The $O_2(aq)/O_2^-$ Self-Exchange Rate Constant

Among the primary reasons for the undertaking of the studies presented here was to add further data to Table 11-2 which summarizes the known reactions involving O_2^- as an outer sphere reductant that have applicability to the Marcus correlation. Table 11-5 is such an extension using the information obtained here.

The calculated k_{11} values are typical of values obtained in other studies, i.e., the expected constancy in k_{11} is absent. It is less than satisfying to see that 13 orders of magnitude are covered. Even less desirable is the three order of magnitude spread between two very closely related complexes-- $Co(NH_3)_6^{+3}$ and $Co(en)_3^{+3}$. With the studies accomplished here, the problem of the inconstancy of k_{11} for the $O_2(aq)/O_2^-$ exchange rate constant appears even less resolved. Before discussing possible explanations for this anomaly, some comment on the data in Table 11-5 is necessary.

The E° value given for $Co(NH_3)_6^{+3}$ is an accepted and commonly used standard reduction potential. Values as low as $E^\circ=0.00\text{ V}$ ⁴⁴ have also been reported for this potential. Reasons for the question surrounding the $Co(NH_3)_6^{+3/+2}$ couple's potential lie in the fact that the $Co(II)$ complex is labile and unstable. This does not allow measurement of its potential without complication. If the lower value of 0.00 V is used in conjunction with the data in Table 11-5, the k_{11} from the $Co(NH_3)_6^{+3}$ experiment is $2.3 \times 10^7 \text{ M}^{-1} \text{ s}^{-1}$ ($f=0.82$). This value is closer to the

Table 11-5. Calculation of the $O_2(aq)/O_2^-$ self exchange rate constant utilizing data for the Co(III) and Fe(III) systems^{a,b}

Oxidant	k_{12}^c	k_{22}^d	$E^\circ{}^e$	K_{12}^f	k_{11}^g	f^h
$Co(NH_3)_6^{+3}$	31.3	$10^{-7}{}^i$	$0.10{}^j$	2.55×10^4	6.2×10^5	.62
$Co(en)_3^{+3}$	23.8	$2.4 \times 10^{-5}{}^k$	$-0.24{}^l$	4.4×10^{-2}	5.7×10^8	.94
$Co(chxn)_3^{+3}$	16.4	--	$-0.26{}^m$.020	--	--
$FeCp_2^+$	8.6×10^6	$5.7 \times 10^6{}^n$	$0.55{}^n$	1.08×10^{12}	1.2×10^{-3}	.01

^aAqueous 1.0 M 2-propanol solution.

^bReactions are written as $Ox + O_2^- = Red + O_2$.

^cRate constant for cross reaction in $M^{-1} s^{-1}$.

^dExchange rate constant for the oxidant in $M^{-1} s^{-1}$.

^eStandard reduction potential in V vs. NHE of oxidant.

^fEquilibrium constant for the cross reaction calculated from standard reduction potentials ($E^\circ O_2(aq)/O_2^- = -.16V$).

^gExchange rate constant for $O_2(aq)/O_2^-$ couple in $M^{-1} s^{-1}$ calculated from Marcus correlation.

^h f value corresponding to k_{11} in solution of Marcus correlation.

ⁱReference 46.

^jReference 45.

^kReference 47.

^lReference 42.

^mReference 43.

ⁿReference 63.

Co(en)_3^{+3} value and is more in line with the observation that a related series of complexes (quinones and Ru(III) amines) generate a constant k_{11} value within themselves. Therefore, because of the uncertainty in E° value, k_{11} from $\text{Co}(\text{NH}_3)_6^{+3}$ data lies in the range $6.2 \times 10^{+5}$ to $2.3 \times 10^7 \text{ M}^{-1} \text{ s}^{-1}$.

The reason no k_{11} value is given for the $\text{Co}(\text{chxn})_3^{+3}$ complex is that its electron exchange rate constant is not known. The assumption of a similar k_{22} value to $\text{Co}(\text{en})_3^{+3}$ results in a k_{11} for $\text{O}_2(\text{aq})/\text{O}_2^-$ of $6.15 \times 10^8 \text{ M}^{-1} \text{ s}^{-1}$ ($f = .91$). This is not surprising in view of the fact that for all columns in Table II-5, $\text{Co}(\text{en})_3^{+3}$ and $\text{Co}(\text{chxn})_3^{+3}$ have very similar values.

Now, to turn to the problem of why Marcus theory fails in its application to the $\text{O}_2(\text{aq})/\text{O}_2^-$ system. The first point to address is the reaction itself, given again in equation 12.



It has been demonstrated that in certain reactions of superoxide ion, the product is singlet oxygen rather than the more stable triplet oxygen.⁶⁴⁻⁶⁶ If this were the situation in the studies given in Tables II-2 and II-4, then the k_{11} results are erroneous as the incorrect E° values were applied. This is not the situation though. From thermodynamic arguments, it can be shown that the oxidant must have a standard reduction potential of greater than 0.78 V, the E° for reaction 13.



Since only $\text{Mo}(\text{CN})_8^{-3}$ has a potential this great, this argument cannot account for the very large spread in the k_{11} values.

The possibility that some of the complexes in Tables 11-2 and 11-4 do not react in an outer sphere fashion is another valid argument. The majority of them do, though, so this does not completely solve the problem. There is some reason to believe that the quinones may react through superoxide ion directly attacking the ring structure of the compounds. Ferricinium ion may also be questionable as the complex is not "closed shell", i.e., there is an available coordination site on the metal center. Nucleophiles have been shown to attack the iron center in Cp_2Fe^+ . In any event, elimination of these complexes from consideration in evaluating the $\text{O}_2(\text{aq})/\text{O}_2^-$ exchange rate constant does little to improve the situation.

A standard explanation when the Marcus correlation behaves poorly is the question of adiabaticity in the system. Adiabaticity is defined as the probability that the electron transfer within the activated complex for both the cross reaction and the exchange reactions is equal to unity. Values less than unity can arise because of poor orbital overlap and/or a mismatch in the overlap. This is a possibility in the $\text{O}_2(\text{aq})/\text{O}_2^-$ system because of dioxygen's unique electronic structure.

Another point to consider is the change in solvation upon electron transfer. Regardless of the direction of reaction 12, a large change

in solvation occurs about the O_2 or O_2^- species. This goes against one of the assumptions in the derivation of the Marcus correlation.^{32,33}

It is assumed that both species remain essentially unchanged after the electron transfer with respect to coordination and solvation spheres.

The results and arguments above can have two final interpretations. The first, and more negative view, is that the anomalous behavior observed for the k_{11} value for the $O_2(aq)/O_2^-$ exchange rate constant has not been resolved and only further complicated. A more positive view is that the evidence is indicating a failure on the part of the Marcus correlation. It is unfortunate that the Marcus correlation has proven so successful in the past. If success with the Marcus correlation had been a more rare event, the concern over the $O_2(aq)/O_2^-$ exchange rate constant problem might not be as great.

It is possible that the Marcus correlation is not well-suited for reactions where one or both redox partners are small molecules or involve small molecules as products. As mentioned in the Introduction, a number of small molecules other than O_2 have been involved in Marcus theory applications with success. The success factor here though is an area that requires further investigation. None of these other small molecules have been subjected to as wide or varied a study as O_2 . Extension of these studies may lead to similar anomalies as in the $O_2(aq)/O_2^-$ case.

Applications of the $O_2(aq)/O_2^-$ Exchange Rate Constant

Applications of the $O_2(aq)/O_2^-$ exchange rate constant have a two-fold purpose. The first is to allow calculation of other unknown

electron self-exchange rate constants. The second is a further test of the Marcus theory in applications involving small molecules and very large molecules, such as metalloproteins.

In Table 11-6 are given some known electron transfer reactions of O_2^- with other small molecules or anions and one bioinorganic species. At present, it is not certain if all of the reactions follow outer sphere pathways. For the sake of argument, it shall be assumed they do.

Table 11-6. Some superoxide ion reactions involving small molecules and anions and large molecules

Reaction	k_{12} ($M^{-1} s^{-1}$)	References
$Br_2 + O_2^- = Br_2^- + O_2$	5.6×10^8	67
$O_3 + O_2^- = O_3^- + O_2$	1.52×10^9	68
$CO_3^- + O_2^- = CO_3^{-2} + O_2$	1.5×10^9	69
$ClO_2 + O_2^- = ClO_2^- + O_2$	2.5×10^7	70
$\epsilon \cdot Cu^{+2} + O_2^- = \epsilon \cdot Cu^+ + O_2$ (bovine copper-zinc superoxide dismutase)	--	71

Br_2 and O_3 most likely follow an outer sphere mechanism. It is difficult to imagine the benefits (thermodynamic or energetic) the reaction would gain by going inner sphere. CO_3^- and ClO_2 can quite easily proceed through inner sphere pathways although this has not been definitely proven.

The last consideration, that of bovine copper-zinc superoxide dismutase, is an interesting example, mostly from the point of view that it is quite large in size. Study⁷¹⁻⁷⁶ has been done on the mechanism of its reaction with O_2^- and arguments supporting both inner and outer sphere pathways can be presented. Application of it to Marcus theory may help resolve the matter.

Conclusion

As a final comment on the studies here, the need for more reactions involving O_2^- as an outer sphere reductant is needed. Questions still exist concerning Marcus theory and small molecules, not only O_2 but many others. Significant study has been done and is a contribution to the solution. Further evidence has been added to eventually help arrive at a logical conclusion on this point. Secondly, it is also meant to demonstrate the ease and accessibility of this laboratory's method of superoxide ion production. It has successfully been used in the study of reactions that would have, in the past, required sophisticated instrumentation. It is hoped that such a demonstration will allow others to study similar reactions and/or to find utility in this laboratory's method of O_2^- generation.

EXPERIMENTAL

Reagents--All Experiments

The complexes $\text{Co}(\text{NH}_3)_6\text{Cl}_3$,⁷⁷ $\text{Co}(\text{NH}_3)_6(\text{ClO}_4)_3$,⁷⁷ $\text{Co}(\text{ND}_3)_6\text{Cl}_3$,⁷⁸ $\text{Co}(\text{en})_3\text{Cl}_3$,⁷⁹ $\text{Co}(\text{en})_3(\text{ClO}_4)_3$,⁷⁹ $\text{Co}(\text{chxn})_3\text{Cl}_3 \cdot \text{H}_2\text{O}$,⁸⁰ $\text{Co}(\text{phen})_3(\text{ClO}_4)_3$,⁸¹ $\text{K}_3\text{Co}(\text{CN})_6$,⁸² and Cp_2FePF_6 ⁸³ were prepared according to literature procedures. $(\text{C}_6\text{H}_5)_2\text{CO}$ (Eastman Organic), 2-propanol (Aldrich Gold Label), KOH (Fisher Scientific) and Na_2EDTA (Mallinckrodt) were used without further purification.

All water used in these studies was distilled water followed by passage through a Millipore Q filtering system. All gases used were passed through 5 M KOH to remove trace CO_2 impurities and then through H_2O , followed by passage through two U-shaped drying tubes containing Drierite.

The superoxide ion used in these studies was generated in situ by photochemical means.¹⁴

Equipment--All Experiments

All glassware, including spectrophotometric cells, were carefully and thoroughly cleaned. The normal routine included chromic acid bathing followed by at least 7 distilled water washings and 3 2-propanol washings. Drying was achieved by placing in oven at 150°C . Spectrophotometric cells and syringes were allowed to air dry.

Rubber septa were prepared for use by soaking overnight in either methanol or isopropanol and then thoroughly washed with distilled water and allowed to air dry. Syringe needles were readied in a

similar fashion.

All UV-visible spectral measurements were made on a Cary 219 spectrophotometer. Kinetic measurements were also made on this instrument as well as a Xenon Corp flash photolysis instrument.⁸⁴ When the latter was employed, data were collected and stored on a Nicolet digitalizing oscilloscope.

Reagent Solutions--Co(III) Reactions

The superoxide ion generating solution was prepared in the following manner. A 2.0 L stock solution of 2-propanol (1.1 M), benzophenone (6-10 μM), and Na₂EDTA (25-50 μM) in distilled water was prepared and used for several weeks. To 9 parts this solution was added 1 part standardized KOH to produce a 1.0 M 2-propanol solution, pH 11.3-11.9 dependent upon the concentration of the KOH stock solution. This solution was then saturated with dioxygen by passing of a vigorous flow of the gas through it for at least 20 minutes.

The Co(III) reagent solutions were prepared by dissolving the solid in a 1.0 M 2-propanol solution at the desired pH. (pH was identical for the two stock solutions within a given set of runs.) It was oxygen saturated. Solutions over three hours old were discarded.

Fresh reagent solutions were prepared daily.

FeCp₂⁺ Reactions

A reagent solution of Cp₂Fe⁺ in perchloric acid/2-propanol was prepared by dissolving the solid Cp₂FePF₆ reagent in 0.02 M perchloric

acid in H₂O. 10.0 mL of this solution was added to a stock solution similar to that used for the Co(III) reactions such that the final concentration of all components were as follows: Cp₂Fe⁺ (27-110 μM), 2-propanol (1.0 M), H⁺ (.002 M), Ph₂CO (15-20 μM), and Na₂EDTA (25-50 μM). Solution was oxygen saturated in the same fashion for the Co(III) experiments. These solutions were prepared fresh just prior to immediate use.

Methods, Procedures, and Data Treatment

Co(III) reactions

To a 2.0 cm quartz spectrophotometric cell (thoroughly purged with O₂) was added 5.4-6.0 mL of the superoxide ion generating solution, the exact volume being determined by the amount of Co(III) reagent solution to be added. The final volume after mixing was 6.0 mL. In some cases, a 1.0 cm cell was employed. Volumes used then were 2.8-3.0, final volume being 3.0 mL.

The cell was thermostatted 25 minutes at 25.0°C and 45 minutes for all other temperatures. It was removed from the bath, wiped dry, and placed on an aluminum covered stage in a standard Rayonet chamber. The cell was irradiated for no more than 35 seconds (exact length of time photolyzed being noted) by light emitted from the medium pressure Hg lamps. Cell was then returned to bath.

The amount of O₂⁻ produced was determined in two manners. The first was a direct method. Absorbance before and after irradiation was recorded. The concentration was then calculated from Beer's Law using the following epsilons: λ245 nm, ε^{O₂⁻} = 2350 M⁻¹ cm⁻¹; λ260 nm,

$\epsilon^{O_2^-} = 1990 \text{ M}^{-1} \text{ cm}^{-1}$; and $\lambda 270 \text{ nm}$, $\epsilon^{O_2^-} = 1480 \text{ M}^{-1} \text{ cm}^{-1}$. The second method utilized the calibration curve given in Figure 11-5. Nonlinear least squares analysis produced the relationship $[O_2^-]_0 = 3.30 t$.

Prior to every set of experiments, a check run was performed. This simply consisted of measuring the rate of superoxide ion disproportionation and comparing it to the expected value. Solutions were accepted as good if the calculated second order rate constant from equation 14 was in the range $32.0\text{-}40.0 \text{ M}^{-1} \text{ s}^{-1}$, pH 11.7.

$$D_t = (D_0 + D_\infty [O_2^-]_0 kt) / (1 + [O_2^-]_0 kt) \quad (14)$$

In fact, the calculated rate constant was then used as the measurement of pH of the solution. Rate constants outside this range resulted in the preparation of new stock solutions.

Those experiments requiring an anaerobic atmosphere were purged at this point. While still located in the constant temperature water bath, the cell and solution were purged with a strong and steady flow of dinitrogen for several minutes. After purging, the concentration of O_2^- was determined spectrophotometrically as detailed above.

Reaction was initiated by injection of the Co(III) reagent solution using either standard syringes or microsyringes. The loss of O_2^- was followed at $\lambda 245 \text{ nm}$, $\lambda 260 \text{ nm}$, or $\lambda 270 \text{ nm}$, depending upon the background absorbance. Identical rates were observed regardless of monitoring wavelength.

The reactions were followed until 90% or more of the reaction was complete. Whenever possible, the reactions were followed to completion.

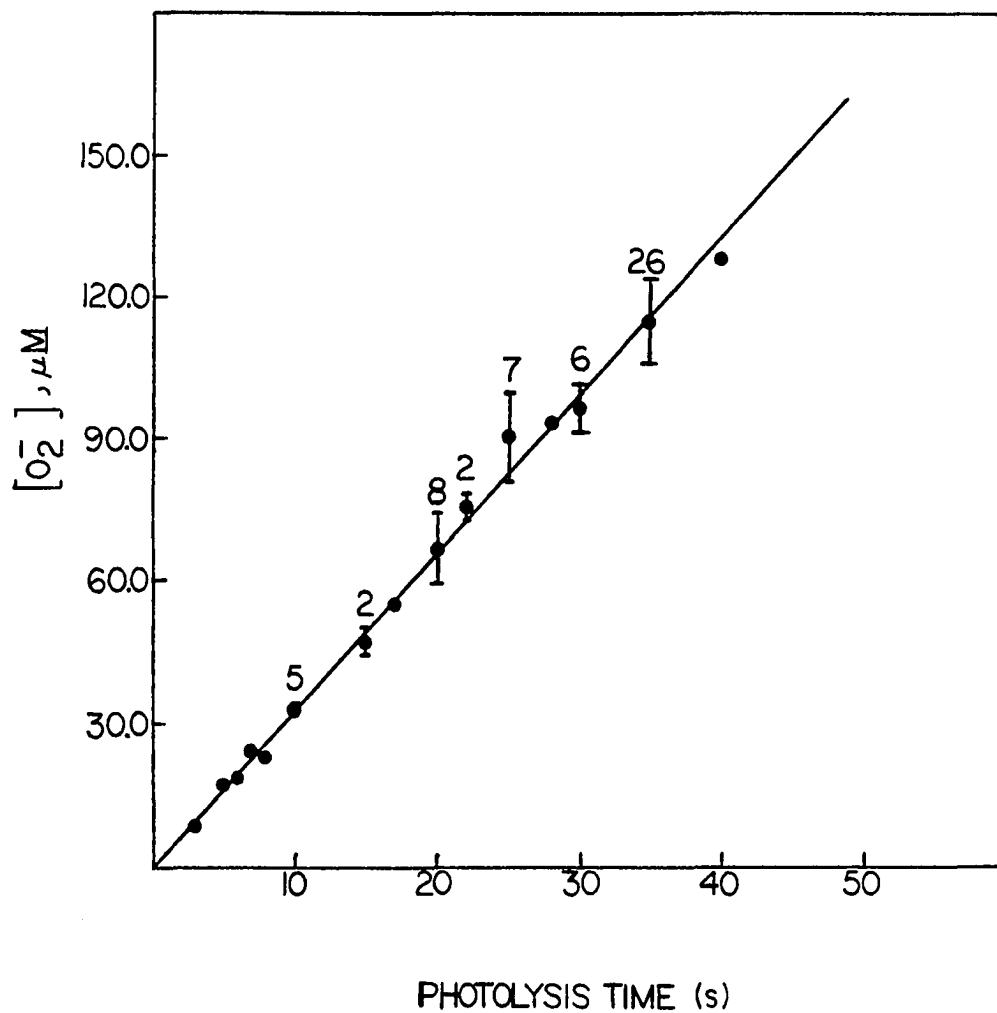


Figure 11-5. Calibration curve of O_2^- yield vs. photolysis time for 1.0 M 2-propanol solution (pH 11.7) containing 4.6 μM Ph_2CO and 19.21 μM Na_2EDTA . Solutions are also saturated with O_2 . Photolyses conducted in 2.0 cm cell at $T = 25.0^\circ\text{C}$. Line is drawn through origin with slope = 3.30. The number above a given data point is the number of individual measurements at that photolysis time

In some instances, most notably in the $\text{Co}(\text{NH}_3)_6^{+3}$ reactions, the final absorbance reading was impossible to attain due to a slow secondary reaction that set in near the end of the first reaction. When this occurred, final absorbance reading was estimated by eye.

The data for these reactions were analyzed by subjecting them to nonlinear least squares analysis. The check runs were fit to a second order expression (equation 14) while the $\text{Co}(\text{III})$ reactions were fit to a first order expression (equation 15).

$$D_t = D_\infty + (D_0 - D_\infty) \exp(-k_{\text{obs}}t) \quad (15)$$

Good to excellent fits of the data to these expressions were noted in all cases through at least the first three half-lives. Whenever the comparison was possible, calculated and experimental final absorbance readings agreed very well.

The second order rate constants for the $\text{Co}(\text{III})$ reactions were obtained also by nonlinear least squares analysis. Data of the sort k_{obs} vs. the average $\text{Co}(\text{III})$ concentration were fit to the equation $y = mx + b$. The intercept b of this expression proved to pass through the origin within experimental error. Consequently, the data were re-analyzed with the expression being fixed through the origin.

Activation parameters were also obtained similarly to the above analyses by fitting to the Eyring equation (equation 16).

$$k/T = R/Nh \exp\left(\frac{-\Delta H^\ddagger}{RT} + \frac{\Delta S^\ddagger}{R}\right) \quad (16)$$

Cp₂Fe⁺ reactions

Two routines were followed in the preparation of the reaction cell. The first involved reaction in 2.0 cm cells. Equal volumes (3.0 mL) of the Cp₂Fe⁺ reagent solution in .002 M H⁺ and 1.0 M 2-propanol and .004 M OH⁻ in 1.0 M 2-propanol were added to the quartz spectrophotometric cell (both solutions already thermostatted). This produced a final pH level of 11.0. Mixing took no more than 10 seconds and within the next 10 seconds, the cell was placed in the flash chamber and reaction initiated.

The second and more accessible routine consisted of filling a 5.0-cm quartz cell with the FeCp₂⁺ solution and then thermostating. A small volume (.625 mL) of a concentrated OH⁻ solution was added such that the solution's final pH was also 11. The cell was then photolyzed. This routine was slightly faster than the first method.

The flash photolysis was conducted with unfiltered UV-visible radiation from fast-extinguishing xenon flash lamps in the Xenon Corporation's Model 710 system.⁸² Flash energies ranged from 25 J to 100 J. Typically 25 J were used. No effect due to the flash energy was noted except for slightly higher transmittance changes with higher energies. A Nicolet digitalizing oscilloscope was used to record and hold the transmittance change, recorded at λ617 nm (Cp₂Fe⁺ = 256 M⁻¹ cm⁻¹).⁶³ The loss of FeCp₂⁺ was followed even though this was the excess reagent. This is because of the flash photolysis instrument's inability to monitor UV bands. The amount of O₂⁻ produced ranged from 4 to 6 μM, as calculated from the transmittance change.

The data were transferred to and stored on magnetic disc. Analysis consisted of taking the voltage vs. time readings and submitting them to nonlinear least squares fitting of a first order expression. Conversion to absorbance was not performed as the voltage changes proved small enough. The second order rate constant was determined by fitting the k_{obs} values vs. the ferricinium ion concentration with the line fixed through the origin.

REFERENCES

1. McCord, J. M.; Fridovich, I. J. Biol. Chem. 1969, 244, 6049
2. (a) McCord, J. M.; Fridovich, I. J. Biol. Chem. 1968, 243, 5753
(b) Knowles, P. F.; Gibson, J. F.; Pick, F. M.; Brick, F.; Bray, R. C. Biochem. J. 1969, 111, 53
3. Michelson, A. M.; McCord, J. M.; Fridovich, I. "Superoxide and Superoxide Dismutases"; Academic Press: New York, 1977
4. Sawyer, D. T.; Valentine, J. S. Acc. Chem. Res. 1981, 14, 393
5. Lee-Ruff, E. Chem. Soc. Rev. 1977, 6, 195
6. Greenstock, C. L.; Wiebe, R. H. in "Oxygen and Oxy-Radicals in Chemistry and Biology"; Rodgers, M. A. J. and Powers, E. L., Eds.; Academic Press: New York, 1981; pp. 119-131
7. Valentine, J. S. in "Biochemical and Clinical Aspects of Oxygen", Caughey, W. S., Ed.; Academic Press: New York, 1979; pp. 659-677
8. Oberley, L. W. "Superoxide Dismutase"; CRC Press: Boca Raton, FL, 1982
9. Fee, J. A.; Valentine, J. S. in Reference 3, pp. 19-60
10. Sawyer, D. T.; Wilshire, J. Acc. Chem. Res. 1979, 12, 105
11. Sawyer, D. T.; Richens, D. T.; Nanni, E. J., Jr.; Stallings, M. D. Dev. Biochem. 1980, 11A, 1
12. Sawyer, D. T.; Nanni, E. J., Jr. in "Oxygen and Oxy-Radicals in Chemistry and Biology"; Rodgers, M. A. J. and Powers, E. L., Eds.; Academic Press: New York, 1981; pp. 15-44
13. Allen, O. A.; Bielski, B. H. J. in Reference 8, pp. 125-141
14. (a) Part I, this thesis
(b) McDowell, M. S.; Bakac, A.; Espenson, J. H. Inorg. Chem. 1983, 22, 847
15. Klug-Roth, D.; Rabani, J. J. Phys. Chem. 1976, 80, 588
16. Brigelius, R.; Spottl, R.; Bors, W.; Lengfelder, E.; Saran, M.; Weser, U. FEBS Lett. 1974, 47, 72

17. McClune, G. J.; Fee, J. A.; McCluskey, G. A.; Groves, J. T. J. Am. Chem. Soc. 1977, 99, 5220
18. Ilan, Y. A.; Czapski, G. Biochim. Biophys. Acta 1977, 498, 386
19. Stein, J.; Fackler, J. P., Jr.; McClune, G. J.; Fee, J. A.; Chan, L. T. Inorg. Chem. 1979, 18, 3511
20. Land, E. J.; Swallow, A. J. Arch. Biochem. Biophys. 1971, 145, 365
21. Rabani, J.; Mulac, W. A.; Matheson, M. S. J. Phys. Chem. 1965, 69, 53
22. Willson, R. L. Trans. Faraday Soc. 1971, 67, 3020
23. Patel, K. B.; Willson, R. J. J. Chem. Soc. Faraday Trans. I 1973, 69, 814
24. Meisel, D. Chem. Phys. Lett. 1975, 34, 263
25. Zehavi, D.; Rabani, J. J. Phys. Chem. 1972, 76, 3703
26. Faraggi, M. J. Phys. Chem. 1976, 80, 2316
27. Stanbury, D. M.; Mulac, W. A.; Sullivan, J. C.; Taube, H. Inorg. Chem. 1980, 19, 3735
28. Pladziewicz, J. R.; Meyer, T. J.; Broomhead, J. A.; Taube, H. Inorg. Chem. 1973, 12, 639
29. Stanbury, D. M.; Haas, O.; Taube, H. Inorg. Chem. 1980, 19, 518
30. Creaser, I. I.; Geue, R. J.; Harrowfield, J. MacB.; Herlt, A. J.; Sargeson, A. M.; Snow, M. R.; Springborg, J. J. Am. Chem. Soc. 1982, 104, 6016
31. Ilan, Y. A.; Meisel, D.; Czapski, G. Israel J. Chem. 1974, 12, 891
32. Marcus, R. A. Annu. Rev. Phys. Chem. 1964, 15, 155
33. Marcus, R. A. Discuss. Faraday Soc. 1960, 29, 21
34. Nurwitz, P.; Kustin, K. Inorg. Chem. 1963, 3, 823
35. Nurwitz, P.; Kustin, K. Trans. Faraday Soc. 1966, 62, 427
36. Lednický, L. A.; Stanbury, D. M. J. Am. Chem. Soc. 1983, 105, 3098

37. Nord, G.; Pederson, B.; Floryan-Løvborg, E.; Pagsberg, P. *Inorg. Chem.* 1982, 21, 2327
38. Woodruff, W. H.; Margerum, D. W. *Inorg. Chem.* 1974, 13, 2578
39. Ige, J.; Ojo, J. F.; Oloboyide, O. *Can. J. Chem.* 1979, 57, 2065
40. Balasobramanian, P. N.; Gould, E. S. *Inorg. Chem.* 1983, 22, 1100
41. Pelizzetti, E.; Mentasti, E. *Inorg. Chem.* 1979, 18, 583
42. (a) Bartelt, H.; Skilandat, H. *J. Electroanal. Chem. Interfacial Electrochem.* 1969, 23, 207
(b) Bjerrum, J. "Metal Ammine Formation in Aqueous Solution"; Haase: Copenhagen, 1941; p. 227
43. Bartelt, H. *J. Electroanal. Chem.* 1970, 25, 79
44. Laitineu, H. A.; Kivalo, P. *J. Am. Chem. Soc.* 1953, 75, 2198
45. Przystao, T. J.; Sutin, N. *J. Am. Chem. Soc.* 1973, 95, 5545
46. Geselowitz, D.; Taube, H. in "Advances in Inorganic and Bioinorganic Mechanisms", Sykes, A. G., Ed.; Academic Press: New York, 1982; pp. 391-407
47. Dwyer, F. P.; Sargeson, A. M. *J. Phys. Chem.* 1961, 65, 1892
48. Basolo, F.; Palmer, J. W.; Pearson, R. G. *J. Am. Chem. Soc.* 1960, 82, 1073
49. Simic, M.; Lilie, J. *J. Am. Chem. Soc.* 1974, 96, 291
50. Lilie, J.; Shinohara, N.; Simic, M. G. *J. Am. Chem. Soc.* 1976, 98, 6516
51. Wilkins, R. G. in "Advances in Chemistry Series" #100; Gould, R. F., Ed.; ACS Press: Washington, D.C., 1971, p. 111-134
52. Wong, C.-L.; Switzer, J. A.; Balakrishna, K. P.; Endicott, J. F. *J. Am. Chem. Soc.* 1980, 102, 5511
53. Simic, M. G.; Hoffman, M. Z. *J. Am. Chem. Soc.* 1977, 99, 2370
54. Bothe, E.; Behreus, G.; Schulte-Frohlinde, D. *Z. Naturforsch.* 1977, 326, 886
55. Ilan, Y.; Rabani, J.; Henglein, A. *J. Phys. Chem.* 1976, 84, 1558

56. Rabani, J.; Klug-Roth, D.; Henglein, A. J. Phys. Chem. 1974, 78, 2089
57. Bothe, E.; Schuchmann, M. N.; Schulte-Frohlinde, D.; von Sonntag, C. Photochem. Photobiol. 1978, 28, 639
58. Pendin, A. A.; Leont'evskaya, P. K. Kinet. Katal. 1976, 17, 341
59. Holeček, J.; Handlír, K.; Klikorka, J.; Dinh Bang, N. Collection Czechoslov. Chem. Commun. 1979, 44, 1379
60. Teitelbaum, Z.; Meyerstein, D. Proc. Int. Conf. Coord. Chem., 16th, 1974, R56
61. Willson, R. L. Trans. Faraday Soc. 1971, 67, 3008
62. Butler, J.; Jayson, G. G.; Swallow, A. J. J. Chem. Soc. Faraday I 1974, 70, 1394
63. Espenson, J. H.; Pladziewicz, J. R. J. Am. Chem. Soc. 1973, 95, 56
64. Mayeda, E. A.; Bard, A. J. J. Am. Chem. Soc. 1973, 95, 6223
65. Danen, W. C.; Arudi, R. C. J. Am. Chem. Soc. 1978, 100, 3944
66. Nanni, E. J., Jr.; Birge, R. R.; Hubbard, L. M.; Morrison, M. M.; Sawyer, D. T. Inorg. Chem. 1981, 20, 737
67. Sutton, H. C.; Downes, M. T. J. Chem. Soc. Faraday Trans. I 1972, 68, 1498
68. Sehested, K.; Holcman, J.; Hart, E. J. J. Phys. Chem. 1983, 87, 1951
69. Adams, G. E.; Boag, J. W.; Michael, B. D. Proc. Roy. Soc. (London) Ser. A 1966, 289, 321
70. Bugaenko, L. T.; Roshektaev, B. M. Russ. J. Phys. Chem. 1967, 41, 1529
71. Fee, J. A. in Reference 3, pp. 173-192
72. Fielden, E. M.; Roberts, P. B.; Bray, R. C.; Lowe, D. J.; Mantner, G. N.; Rotilio, G.; Calalrese, L. Biochem. J. 1974, 139, 49
73. Klug-Roth, D.; Fridovich, I.; Rabani, J. J. Am. Chem. Soc. 1973, 95, 2786

74. Gaber, B. P.; Brown, R. D.; Koenig, S. H.; Fee, J. A. *Biochim. Biophys. Acta* 1972, 271, 1
75. Fee, J. A.; Ward, R. L. *Biochem. Biophys. Res. Comm.* 1976, 71, 427
76. Fee, J. A.; Gaber, B. P. in "Oxidases and Related Redox Systems", King, T. E.; Mason, H. S.; and Morrison, M., Eds.; University Park Press, 1973; pp. 77-82
77. Bjerrum, J.; McReynolds, J. P. *Inorg. Synth.* 1946, 2, 216
78. Anderson, J. S.; Briscoe, H. V. A.; Spoor, N. J. *Chem. Soc.* 1943, 361
79. Work, J. B. *Inorg. Synth.* 1946, 2, 221
80. Beattie, J. K.; Binstead, R. A.; Broccardo, M. *Inorg. Chem.* 1978, 17, 1822
81. Pfeiffer, P.; Werdelmann, B. *Z. Anorg. Chem.* 1950, 263, 36
82. Bigelow, J. H. *Inorg. Synth.* 1946, 2, 225
83. Yang, E. S.; Chan, M. S.; Wahl, A. C. *J. Phys. Chem.* 1975, 79, 2049
84. Ryan, D. A. Ph.D. thesis, Iowa State University, 1981

APPENDIX. SUPPLEMENTAL DATA

Table II-A-1. $\text{Co}(\text{NH}_3)_6^{+3} + \text{O}_2^-$

T(°C)	Compound ^a	[Co(III)] x10 ⁴ , <u>M</u>	[O ₂ ⁻], <u>μM</u>	[Co(III)] x10 ⁴ , <u>M</u>	k _{obs} x10 ³ , s ⁻¹ ^b
(a) Under O ₂ ^c					
25.02	C1	2.53	33.0	2.36	(4.67±.40)
25.01	C1	2.53	33.0	2.36	(5.50±.52)
24.98	C1	2.53	33.0	2.36	6.97±.32
24.96	C1	2.53	33.0	2.36	6.82±.24
25.00	C1	5.03	49.5	4.78	(11.0±.4)
25.02	C1	5.03	49.5	4.78	13.4±.4
24.99	C1	5.03	49.5	4.78	15.2±.7
24.96	C1	5.03	49.5	4.78	15.6±.8
25.02	C1	8.26	66.0	7.93	25.4±.7
25.04	C1	8.26	66.0	7.93	21.6±.3
25.04	C10 ₄	9.96	115.5	9.38	(26.0±1.0)
25.04	C10 ₄	9.96	115.5	9.38	30.4±1.6
25.04	C10 ₄	9.96	115.5	9.38	30.4±2.2
25.00	C10 ₄ ^d	10.7	115.4	10.1	30.1±.2
25.01	C10 ₄ ^d	11.0	115.4	10.4	28.0±.1
25.02	C1	16.2	82.5	15.8	(35.0±1.6)
25.03	C1	16.2	82.5	15.8	(36.2±1.4)
25.04	C1	16.2	82.5	15.8	43.4±1.8
25.05	C1	16.2	82.5	15.8	46.9±2.8
25.04	C1	16.2	82.5	15.8	48.7±3.1
24.98	C1	22.3	99.0	21.8	(47.4±2.9)
24.98	C1	27.9	115.0	27.3	86.8±3.1
24.98	C1	27.9	115.0	27.3	90.7±3.3
24.95	C1	27.9	115.0	27.3	(118.0±20.0)
34.39	C1	8.35	71.3	79.9	46.3±3.4
34.39	C1	8.35	86.6	79.2	51.5±3.5
10.89	C1	8.35	84.1	79.3	9.26±.44

^aC1 = $\text{Co}(\text{NH}_3)_6\text{Cl}_3$; C10₄ = $\text{Co}(\text{NH}_3)_6(\text{C10}_4)_3$.

^bLess reliable values in parentheses.

^cpH 11.3-11.9.

^dSolvent is >90% D₂O.

Table II-A-1. Continued

T(°C)	Compound ^a	[Co(III)] x10 ⁴ , M	[O ₂ ⁻], μM	[Co(III)] x10 ⁴ , M	k _{obs} x10 ³ , s ⁻¹ ^b
9.80	Cl	10.3	99.2	9.80	11.9±.34
2.14	Cl	8.35	67.0	8.01	4.93±.27
(b) Under N ₂ ^c					
25.05	ClO ₄	4.03	68.1	3.69	21.8±1.3
24.99	ClO ₄	8.07	52.6	7.81	50.9±2.6
25.05	ClO ₄	10.1	70.5	9.73	58.2±2.7
25.04	ClO ₄	14.1	52.6	13.9	(65.9±1.7)
25.01	ClO ₄	16.1	58.3	15.8	106.0±6.4

Table 11-A-2. $\text{Co(en)}_3^{+3} + \text{O}_2^-$

T(°C)	$[\text{Co(III)}]$ $\times 10^4, \underline{\text{M}}$	$[\text{O}_2^-],$ $\underline{\mu\text{M}}$	$[\text{Co(III)}]$ $\times 10^4, \underline{\text{M}}$	$k_{\text{obs}} \times 10^3,$ s^{-1}a
(a) Under O_2 ^{b,c}				
25.06	3.29	63.2	3.00	9.04±.5
25.00	6.05	93.6	5.58	14.1±.3
25.01	6.05	63.2	5.73	14.2±.6
25.01	9.04	101.3	8.53	19.4±1.3
25.04	11.3	102.7	10.8	25.4±1.4
25.03	17.9	99.7	17.4	41.3±2.0
16.81	7.79	94.3	7.31	10.8±.5
5.40	7.79	80.1	7.38	4.44±.20
5.37	7.79	79.4	7.39	5.10±.35
(b) Under N_2 ^{b,d}				
24.98	5.15	62.6	4.99	20.9±1.0
24.97	8.58	41.6	8.48	37.0±3.0
25.05	10.3	61.0	10.15	51.0±.4
24.99	13.7	51.8	13.57	62.3±.5
24.97	17.2	47.3	17.08	83.9±.4

^aLess reliable data in parentheses.

^bpH, 11.3-11.7.

^cData for $\text{Co(en)}_3\text{Cl}_3$.

^dData for both $\text{Co(en)}_3\text{Cl}_3$ and $\text{Co(en)}_3(\text{ClO}_4)_3$.

Table 11-A-3. $\text{Co}(\text{chxn})_3 + \text{O}_2^-$

$T(^{\circ}\text{C})$	$[\text{Co}(\text{III})]$ $\times 10^4, \text{ M}$	$[\text{O}_2^-],$ μM	$[\text{Co}(\text{III})]$ $\times 10^4, \text{ M}$	$k_{\text{obs}} \times 10^3$ $\text{s}^{-1\text{a}}$
(a) Under O_2^{b}				
25.06	2.13	34.8	1.96	$3.43 \pm .22$
24.98	2.13	32.1	1.97	$3.52 \pm .31$
24.97	4.24	61.5	3.93	$6.52 \pm .40$
24.96	4.71	114.9	4.13	(10.1 ± 0.3)
25.00	6.56	101.4	6.24	10.2 ± 0.6
25.02	6.56	61.5	6.26	9.47 ± 0.81
24.97	9.13	64.9	8.82	15.0 ± 0.7
19.10	5.40	75.7	5.02	(25.5 ± 2.7)
15.22	5.40	61.2	5.09	$4.50 \pm .08$
9.01	5.40	62.2	5.09	$2.88 \pm .32$
6.16	5.32	64.2	5.00	$2.39 \pm .14$
(b) Under N_2^{b}				
25.00	2.64	50.5	2.51	$7.54 \pm .31$
24.98	3.97	65.2	3.81	$11.7 \pm .89$
24.97	4.87	30.1	4.79	15.2 ± 1.3

^aLess reliable data in parentheses.

^b Cl^- compound, $\text{pH} = 11.7$.

Table II-A-4. Data for calibration curve (Figure II-5), $[O_2^-]$ vs. photolysis time^{a,b}

Photolysis time (s)	$[O_2^-]$, μM	$\overline{[O_2^-]}$, μM
3	8.8	8.8
5	17.6	17.6
6	18.3	18.3
7	24.4	24.4
8	23.8	23.8
10	30.7, 32.1, 33.2, 34.3, 34.8	33.0±1.7
15	45.5, 49.3	47.4±2.7
17	55.3	55.3
20	61.2, 61.5, 61.5, 62.2, 64.9, 66.6, 75.1, 79.4	66.6±7.0
22	70.6, 80.0	75.3±3.3
25	75.7, 81.4, 86.8, 89.1, 99.2, 99.2, 99.2	90.1±9.5
28	93.2	93.2
30	88.5, 91.9, 94.9, 98.9, 100.7, 101.4	96.1±5.1
35	94.9, 96.6, 98.7, 102.8, 106.6, 109.4, 111.8, 112.1, 112.6, 113.5, 114.0, 114.9, 114.9, 115.7, 115.7, 116.2, 116.4, 117.5, 121.3, 121.6, 123.0, 123.0, 123.3, 131.4, 131.5, 132.1	115.1±9.8
40	128.3	128.3

^apH 11.7, 1.0 M 2-propanol, 4-6 μM Ph_2CO , 19-21 μM Na_2EDTA , 2.0-cm cell, excitation wavelength λ_{254} nm.

^bData give the following equation: $[O_2^-] = 3.30 t + 0.0$.

Table 11-A-5. $\text{FeCp}_2^+ + \text{O}_2^{-\text{a,b}}$

Flash energy (J)	$[\text{FeCp}_2^+]$, μM	$k_{\text{obs}} \times 10^{-2}$, $\text{s}^{-1\text{c}}$
25	28.6	2.64 \pm .01
25	28.6	(3.58 \pm .02)
25	57.5	4.50 \pm .13
50	57.5	4.68 \pm .03
25	57.5	5.36 \pm .12
50	57.5	5.53 \pm .19
25	75.0	(4.67 \pm .06)
50	75.0	5.63 \pm .04
50	75.0	5.95 \pm .05
25	75.0	6.14 \pm .09
25	78.3	7.11 \pm .09
25	78.3	7.45 \pm .11
25	104.0	(6.36 \pm .37)
25	104.0	8.68 \pm .15
25	104.0	8.79 \pm .21

^aT = 25.0 \pm 0.5°C, pH = 11.0, 1.0 M 2-propanol.

^b[O₂⁻] = 4-6 μM .

^cLess reliable data in parentheses.

PART III. REACTIONS OF BIS(DIMETHYLGLYOXIMATO)COBALT(II)
COMPLEXES WITH POLYHALOMETHANES

STATEMENT OF THE PROBLEM

It is proposed that one of the key reaction steps in the overall mechanism of the polyhalomethane-organocobaloxime(III) (Figure III-1) reaction is the reaction of the polyhalomethane with the cobaloxime(II) species. A number of literature precedents exist to suggest and support such a reaction, but no direct studies on this reaction have been made.

It is intended to examine this reaction in some detail, including: (1) The rates of reaction between a series of cobaloxime(II) complexes and the polyhalomethanes CCl_4 , BrCCl_3 , CBr_4 , and CHBr_3 in acetone and benzene, (2) the effect due to the nature of the axial base of the cobaloxime(II) complex, and (3) the effect due to temperature (activation parameters).

The radical nature of the mechanism will be probed through the use of known radical scavenging agents. This aspect permits a further examination through computer modeling of the proposed reaction sequence.

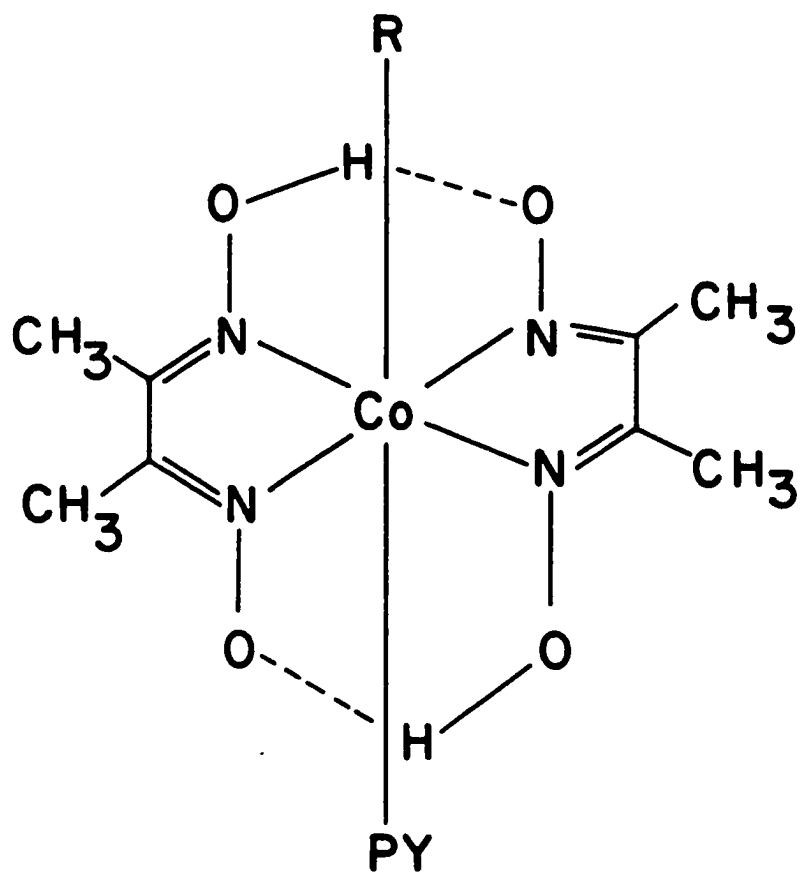


Figure III-1. Molecular structure of an organocobaloxime, where R = alkyl or aryl group

HISTORICAL BACKGROUND

Halogen atom abstraction from organic halides by transition metal containing complexes has long been of interest in inorganic and organometallic chemistry. However, this reaction has recently drawn attention from the field of organic chemistry, in particular the area of organic synthesis. The reaction of various organocobalt(III) complexes with organic halides such as polyhalogenomethanes,¹ aryl and alkyl sulphenyl halides,² and α -halogenoesters³ to produce organic compounds are proposed to occur by a free radical mechanism involving halogen atom abstraction by a transition metal complex as a key step.

The transition metal containing complexes used in these syntheses are the bis(dimethylglyoximate) complexes of cobalt.⁴ The general structures for the five-coordinate cobaloxime(II), as they are commonly referred to as, and the six coordinate cobaloxime(III) are shown in Figure III-1. The predominant feature of all cobaloximes is the pseudo-macrocyclic ring structure about the cobalt ion center formed by the two dimethylglyoximate chelates. The structure of the cobaloximes is very similar to that of another cobalt containing complex, the naturally occurring Vitamin B₁₂ molecule (Figure III-2).⁵ In the co-enzyme, the cobalt ion center lies in a corrin ring structure consisting of four pyrrole units. It is not surprising that the similarity in structure leads to similarity in chemical and physical properties such as reactivity patterns and because of this, chemistry of the cobaloximes are considered in many instances to be models of the chemistry of Vitamin B₁₂, or cobalamins as they are often referred to as.

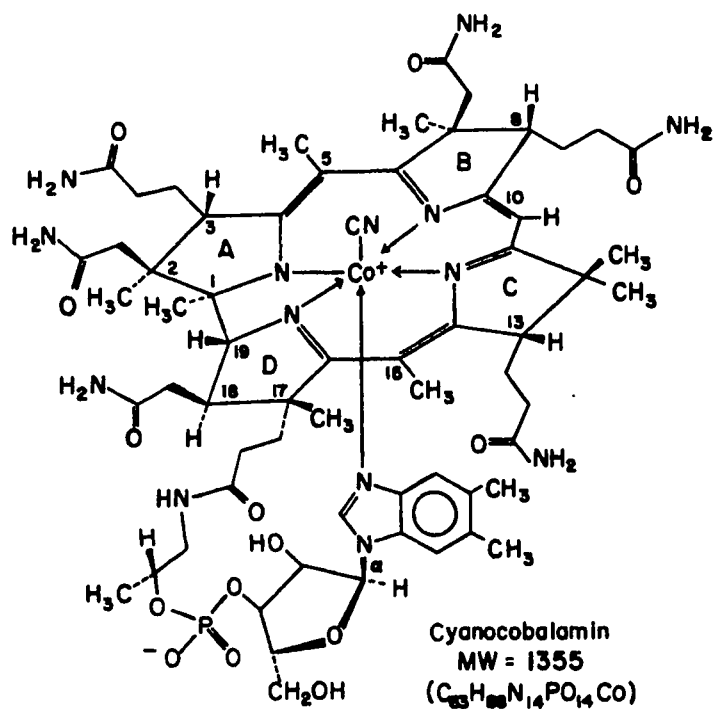


Figure III-2. Molecular structure of vitamin B₁₂. The positive charges of the cobalt(III) ion are balanced by the negative charges on the corrin ring, the cyanide, and the phosphate

One property of the cobaloximes, and also of the cobalamins is the ability to form very stable organocobalt(III) complexes containing a cobalt-carbon sigma bond. Although thermodynamically weak, several factors contribute to the stability of the organometallic bond. Loss of the σ -bound carbanion ligand is not a facile process as the cobalt is in the substitutionally inert oxidation state of three. The macrocyclic or pseudomacrocyclic ring structures kinetically stabilize the organometallic complexes by occupying the coordination sites adjacent to the cobalt-carbon bond, preventing the approach of a displacing ligand to the carbanion ligand.

The organocobaloximes(III) may be prepared in a variety of methods. Schrauzer⁶ first synthesized methyl(pyridine)cobaloxime(III) by the reaction of dimethylsulphate and (pyridine)cobaloxime(I), formed by the reduction of (pyridine)cobaloxime(II) and sodium borohydride. This earliest method is the current method of choice for most organocobaloxime(III) preparations. The use of alkyl halides has supplanted the use of the dialkylsulphates. Recently, an organocobaloxime(III) synthesis was devised by Randaccio et al.⁷ involving the inorganic chloro(pyridine)cobaloxime(III), nitromethane, and silver(I) oxide. This reaction leads to the formation of nitromethyl(pyridine)cobaloxime(III).

The cobaloxime(II) can also be employed as the starting reagent in organocobaloxime(III) syntheses. It is the reaction of cobaloxime(II) and organic halides, in particular the polyhalogenomethanes, the study presented here concerns itself with.

The production of organocobaloxime(III) from cobaloxime(II) and organic halides proceeds by a two-metal center overall one-electron change oxidative-addition reaction, as shown in equation 1.



The products of this reaction are the organometallic product and an inorganic halocomplex. This oxidative-addition process differs from the more common one-metal center overall two-electron change oxidative-addition in that the organic halide is fragmented between two metal centers, yielding two products, rather than adding across one metal center, as shown in equation 2.



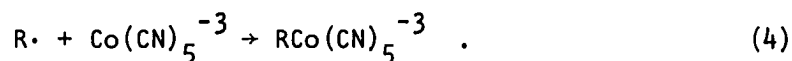
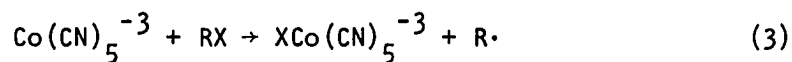
The two-metal center overall one-electron change oxidative-addition by which the cobaloxime(II) and organic halide react is not unique to the cobaloxime(II), but occurs with a variety of cobalt (II) containing complexes as well as other transition metal containing complexes.

One of the earliest cobalt (II) containing complexes to be shown to undergo oxidative-addition with an organic halide was the pentacyanocobaltate(II). In 1964, Halpern and Maher⁸ added benzyl bromide to a water-methanol solution of pentacyanocobaltate(II) resulting in the formation of the pentacyanobenzylcobaltate(III) anion and various inorganic pentacyanocobaltates(III), including the bromo complex. The preparation of the pentacyanomethylcobaltate(III) was also accomplished employing methyl iodide in the place of benzyl bromide.

Since the initial preparation of the pentacyanoalkyl cobaltates(III), an entire series of these organometallic anionic complexes has been synthesized from the pentacyanocobaltate(II) and organic halides. Kwiatek and Seyler,^{9,10} also in 1964, prepared such pentacyanocobaltates(III) as the allyl and crotyl derivatives, the acrylonitrile derivative, the phenacyl and α -propiophenone derivatives, and various linear alkyl derivatives such as the methyl, ethyl and propyl as well as the branched alkyl isobutyl derivative. Also organometallic pentacyanocobaltates(III) containing alkyl groups bound through bridgehead carbons, such as the 1-adamantyl¹¹ and 1-(2,4-dimethyl-bicyclo[2.2.2]octyl)¹² complexes among others have been prepared. All of these complexes were prepared, as mentioned earlier, from the corresponding organic halide, usually the bromide or iodide, and pentacyanocobaltate(III).

A mechanistic study of the reaction of pentacyanocobaltate(II) and various organic halides such as halo substituted carboxylic acids, esters, amides, methyl sulfonates, and alkyl and benzyl halides has been done.^{13,14} The results of their studies indicated a reactivity order of $k_{RI} > k_{RBr} > k_{RCI}$ for the rate of reaction between organic halide and pentacyanocobaltate(II). In addition, it was proposed that the mechanism of this reaction follows a two step free radical process. The initial and rate-determining step is the abstraction of halogen atom from the organic halide by pentacyanocobaltate(II) to yield an organic radical and halopentacyanocobaltate(III). The second faster step is the coupling reaction of two radicals, the organic radical generated in the first step and a second pentacyanocobaltate(II)

complex, considered as an "inorganic" radical in its being a seventeen-electron system and hence having an unpaired electron. Equations 3 and 4 outline the mechanism:



The kinetic studies indicated that the rate of reaction between the cobalt(II) complex and organic halide was first order in each, consistent with the proposal that halogen atom abstraction is the rate limiting step. This led to the rate law given in equation 5. The factor of two in the rate law arises from the stoichiometry of the net

$$\frac{-d[\text{Co(CN)}_5^{-3}]}{dt} = 2k[\text{Co(CN)}_5^{-3}][\text{RX}] \quad (5)$$

reaction--two pentacyanocobaltates(II) for every one organic halide. The interpretation presented by Halpern et al. for this reaction is consistent with the one put forth by Kwiatek and Seyler.^{9,10}

The cobaloxime(II) has been shown to undergo reaction with several different organic halides in a fashion completely analogous to the pentacyanocobaltate(II) reactions. The reaction of cobaloxime(II) and benzyl halides in organic solvents such as benzene and acetone has been studied.^{15,16} The rate of reaction was again seen to follow the order $k_{\text{PhCH}_2\text{I}} > k_{\text{PhCH}_2\text{Br}} > k_{\text{PhCH}_2\text{Cl}}$ and substitution of electron withdrawing groups in the para position resulted in reactivity enhancement. Modification of the pseudomacrocyclic ligand (replacement of

methyl groups by a cyclohexyl ring for example) resulted in little or no change in reaction rate. The effect of the axial base ligand was also studied with an increase in reaction rate concurrent with an increase in the value of the pka for the axial base ligand, i.e., the 4-methylpyridine (pka = 6.1) derivative reacts with benzyl bromide at a rate of $0.43 \text{ M}^{-1} \text{ s}^{-1}$ while the pyridine (pka = 5.3) derivative reacts at a rate of $0.28 \text{ M}^{-1} \text{ s}^{-1}$ and the triphenylphosphine (pka = 2.7) derivative at a rate of $0.042 \text{ M}^{-1} \text{ s}^{-1}$.

In 1970, Schrauzer et al.¹⁷ reported very briefly upon the formation of trihalomethylcobaloxime(III) when tetrahalogenomethanes are added to methylene chloride solutions of cobaloxime(II). The rapid decomposition of the trihalomethylcobaloximes(III) by aqueous hydroxide is also reported.

Roussi and Widdowson¹⁸ developed the halogen atom abstraction oxidative-addition reaction cobaloxime(II) undergoes into a complete method of synthesis for organocobaloximes(III). Reaction of organic halides with cobaloxime(II) in benzene in the presence of zinc metal gives superior yields of organocobaloxime(III) to the Schrauzer⁶ method of alkylation of cobaloxime(I). The zinc metal is present to reduce the halocobaloxime(III) back to cobaloxime(II) and leads to complete conversion (>90% in many instances) of cobaloxime(II) to organocobaloxime(III). The disadvantage to this synthesis as to the Schrauzer cobaloxime(I) method is that not all organic halides are applicable but rather only activated ones such as α -halogeno esters, α -halogeno nitriles, α -halogeno nitro compounds, and phenacyl halides. Isopropyl

iodide gave trace organocobaloxime(III) product over a period of three days at elevated temperature (60°C). Methyl iodide, though, gave an excellent yield of 95% over a period of one day at 40°C.

Recently, Pinault and Crumbliss¹⁹ have demonstrated that cobaloxime(II) initiates coupling of α,α,α -trihalomethylbenzenes. The process is proposed to follow the two step free radical halogen atom abstraction mechanism outlined earlier. The α,α -dihalobenzyl cobaloxime(III) formed in the second step of "radical" coupling is too unstable to be isolated and quickly undergoes decomposition to give organic products and inorganic cobaloxime(III). When the α,α -dihalomethylbenzene was employed in place of the α,α,α -trihalomethylbenzene, halocobaloxime(III) and α -halobenzylcobaloxime(III) were isolated in moderately high yield.

As mentioned earlier, the cobaloximes and their chemistry are considered as models for cobalamin chemistry. It is not surprising then that B_{12r} (cobalt in the +2 oxidation state) also undergoes halogen atom abstraction oxidative-addition with organic halides. Halpern and Blaser²⁰ examined a wide range of organic halides. In methanol solution, the kinetics follow the rate law in equation 6:

$$\frac{-d[B_{12r}]}{dt} = 2k [B_{12r}][RX] \quad (6)$$

This is identical to the cobaloxime(II) and other cobalt(II) containing complexes. The same mechanism is postulated for B_{12r} as is for the cobaloxime(II) (equations 7, 8, 9):



The same reactivity patterns for the inorganic cobalt (II) complexes are noted for B_{12r} , i.e., the following sequence indicates reactivity towards alkyl halides, $k_{RCI} < k_{RBr} < k_{RI}$, $k_{R_2CHX} < k_{R_2C(CH_3)X}$ and $k_{R_2CHX} < k_{R_2CCIX}$. The rates of reaction of B_{12r} are approximately one order of magnitude slower than the cobaloxime(II) for reaction with the same organic halide.

Marzilli et al.²¹ has also demonstrated that Schiff's base complexes of cobalt(II), in particular the saloph derivative, react in an entirely analogous fashion to all the other cobalt(II) containing complexes discussed here. P-cyanobenzyl halides afforded the p-cyanobenzylCo(saloph) complexes in methylene chloride.

As mentioned earlier, transition metal complexes containing a metal other than cobalt also undergo the halogen atom abstraction. Rhodium(II) complexes were shown by Espenson and Tinner²² to abstract halogen atom from organic halides. The complex studied was the rhodium analog of cobaloxime(II), the rhodoxime(II). Because of the rhodoxime(II) tendency to form a dimer, the monomeric species was generated by flash photolysis of the dimer or of an alkylrhodoxime(III), such as the isopropyl derivative. When done in the presence of organic halide, the rate of halogen atom abstraction can be obtained. Organic halides such

as CHBr_3 , CCl_4 , PhCH_2Br , CH_2Br_2 , $i\text{-C}_3\text{H}_7\text{Br}$, and CHCl_3 were examined.

Complexes of chromium(II) have been extensively studied with respect to atom transfer from organic halides to chromium(II).

The earliest studied chromium(II) complex was the simplest one possible, the hexaquo chromium(II) cation in aqueous perchloric acid. In 1957, Anet and LeBlanc²³ reported the formation of yellow solution when benzyl halide was added to a solution of chromous perchlorate in perchloric acid. Products of this reaction were identified as the halochromium(III) cation and the benzylchromium(III) cation.

A study by Kochi and Davis²⁴ in 1964 proposed that the formation of benzylchromium(III) occurred via the two step free radical mechanism given for the cobalt(II) complex reactions. Attempts were made at trapping the benzyl radical intermediate but proved inconclusive. Acrylonitrile and butadiene were employed as traps for the radical but it was found that benzylchromium(III) also reacts with these unsaturated compounds. The synthesis of several ring-substituted benzylchromium(III) cations was presented, again prepared by addition of the corresponding benzyl halide to chromous ion in aqueous perchloric acid.

The pentaquopyridinomethylchromium(III) ion preparation was described by Coombes et al.²⁵ Solutions of chromous sulphate reacted with 2-, 3-, or 4-bromomethyl pyridinium bromide to give the organochromium(III) cation. Dodd and Johnson²⁶ in 1968 prepared the mono- and dihalogenomethylchromium(III) cations from the corresponding methylene dihalides or halogenoforms. For example, bromoform gave the dibromomethylchromium(III) cation. Again, the two step free radical process

is credited as the mechanism of formation.

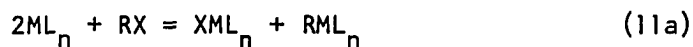
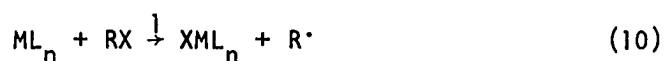
Several other organochromium(III) cationic complexes have been prepared by halogen atom abstraction, including those derived from the halogenoacetic acids²⁷ and carbon tetrachloride.²⁸ Pohl and Espenson²⁹ prepared a family of difunctional complexes of bis(benzylchromium) cations by reaction of chromous ion with organic halides such as α,α' -dibromo-m-xylene and α,α' -dibromo-p-xylene. Marty and Espenson³⁰ prepared the 3,3'-oxybis(chromiomethyl)benzene cation, $(\text{CrCH}_2\text{C}_6\text{H}_4)_2\text{O}^{+4}$, by reaction with bis[m-(bromomethyl)-phenyl] ether.

The reduction of alkyl halides to alkanes by chromous ion in solutions containing ethylenediamine or other β -amines has been studied.^{31,32} The presence of the β -amine enhances the reducing ability/abstracting power of the chromium(II) ion. The reactive species is believed to be the mono(β -amine)chromium(II) complex and reacts with organic halides to produce the halo complex and the organometallic complex. The organometallic complexes are hydrolytically unstable and decompose rapidly. Spectral evidence supports the claim of alkyl(ethylenediamine)chromium(III) intermediates. The enhancement of reducing power by chelation of the chromium(II) ion by β -amines is acknowledged by reduction of n-butyl bromide to n-butane, a reduction not observed when only the hexaaquochromium(II) ion is used.

Finally, macrocyclic complexes of chromium(II) have been shown to be powerful reductants/halogen atom abstractors towards organic halides. Samuels and Espenson^{33,34} studied the reaction of (1,4,8,12-tetraazacyclopentadecane)chromium(II) with several alkyl halides.

The mechanism of reaction is the two step process already given numerous times. A competition study was conducted to determine the rate of the second step, that of radical coupling. 6-bromo-1-hexene was reacted with the macrocyclic chromium(II) complex. The resulting organic radical can either couple with another chromium(II) complex or may undergo a rearrangement to cyclopentyl methyl radical³⁵ before coupling with a second metal complex. The ratio of products lead to a value of $(0.9 \pm 0.2) \times 10^7 \text{ M}^{-1} \text{ s}^{-1}$ for this coupling rate. A similar study³² on the ethylene diamine chromium(II) complexes leads to a value of $4 \times 10^7 \text{ M}^{-1}$ for the ω -hexanyl radical and the β -amine complex of chromium(II). This value is consistent with the inability of the β -amine complex of chromium(II) to capture cyclopropylmethyl radical before it isomerizes to γ -butenyl radical, a rate estimated at greater than 10^{+8} s^{-1} .³⁶

The reactions discussed above follow the same mechanism, a two step free radical process shown in equations 10 and 11, and a rate law given in equation 12.



$$\frac{-d[\text{ML}_n]}{dt} = 2k_1 [\text{ML}_n][\text{RX}] \quad (12)$$

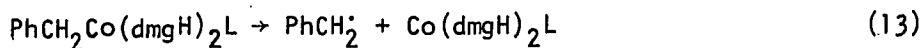
The reaction to be investigated in the studies here is the

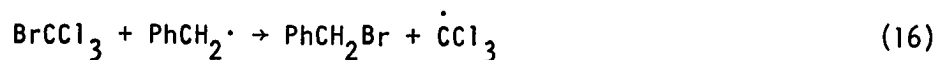
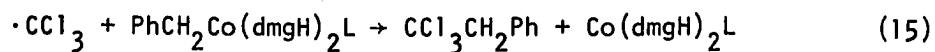
cobaloxime(II) reaction with polyhalogenomethanes. This reaction, as mentioned in the opening paragraph, is a key step in the work of Johnson and coworkers. It is believed to follow all the precedents put forth by the previously studied halogen atom abstraction reactions. It is of interest though because it is one of the unverified steps in the chain mechanism of Johnson et al.'s work.

Johnson and coworkers have reported, in a series of papers,^{1,2,37-41} several different reactions involving homolytic displacements at carbon centers. Among these reactions are studies involving SO₂ insertions into metal-carbon sigma bonds,³⁸ regiospecific syntheses of alkyl sulphenes from allylcobaloxime(III) and organosulphenyl chlorides,² and two studies of interest here, the reaction of alkyl- and allenylcobaloxime with polyhalogenomethanes¹ and the syntheses of trichloroethylbenzenes from benzylcobaloxime(III).⁴⁰

In the first study of interest, the allyl- and allenylcobaloxime(III) systems, reaction of these complexes with bromotrichloromethane yielded 4,4,4-trichlorobutene and 4,4,4-trichlorobutyne, respectively, as well as bromocobaloxime(III). The second study with benzylcobaloxime(III) produced trichloroethylbenzene where bromotrichloromethane was added to it as well as bromocobaloxime(III) once again.

The mechanism for the benzylcobaloxime(III) reaction is outlined below in equations 13-18.





The reaction of benzylcobaloxime(III) and bromotrichloromethane occurs at an elevated temperature (50°C-90°C in CHCl_3) and the initial homolysis of the organocobaloxime(III) in equation 13 is completely reasonable. The metal-carbon bond in organocobaloximes(III) are not thermodynamically robust and thermolysis readily leads to homolytic cleavage. Traces of the cobaloxime(II) may also arise either as an impurity in the organocobaloxime(III) species or from homolysis of the Co-C bond due to photolysis.

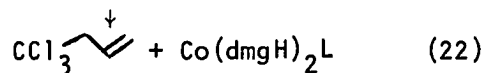
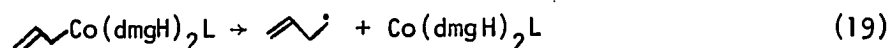
The next step, that of halogen atom abstraction by the cobaloxime(II) formed upon homolysis, is the reaction undertaken as the study in this dissertation. Based upon the precedents cited in the first half of this section, the reaction is once again reasonable and expected under the given conditions (high concentration of bromotrichloromethane and low concentration of cobaloxime(II)).

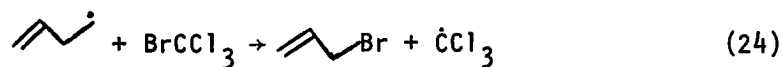
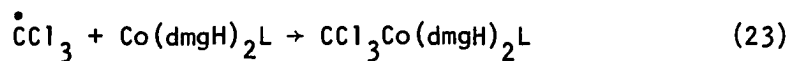
Equation 15 accounts for the production of the trichloroethylbenzene. This reaction is attack at the α -carbon of the benzyl ligand by the trichloromethyl radical. This requires that the cobaloxime(II) moiety to be an excellent leaving group in an $\text{S}_{\text{N}}2$ fashion. Dodd et al.⁴² have shown that alkyl transfer from organocobaloxime(III) to

cobaloxime(II) is a very facile and rapid process in many instances. This is indicative of the ability of cobaloxime(II) to behave as an excellent leaving group in a displacement reaction.

Equations 14 and 15 then constitute a chain mechanism involving cobaloxime(II) as a chain carrying species. Equation 16 is included to account for the benzyl bromide formed in the reaction. This yield of benzyl bromide and subsequently of trichloroethylbenzene is dependent upon the nature of the axial ligand. Equations 17 and 18 are possible termination steps for this chain sequence. Both are viewed as radical coupling reactions. Equation 17, the formation of trichloromethylcobaloxime(III) could be more than simply a termination step. Trichloromethylcobaloxime(III) can be viewed as a storage well for the trichloromethyl radical and therefore equation 17 can possibly be reversible. In view of the elevated temperatures this reaction is run under, homolysis of the cobalt-carbon bond in trichloromethylcobaloxime(III) is reasonable and expected.

The reaction of the allyl- and allenylcobaloxime(III) follow a similar mechanism. Equations 19-25 give the allyl cobaloxime(III) mechanism:





The same interpretation as for the benzylcobaloxime(III) reaction may be presented here also. Photolysis or thermolysis of allylcobaloxime(III) initiates the chain in equation 19. Halogen atom abstraction occurs followed by attack of the trichloromethyl radical on the terminal carbon of the allylcobaloxime(III) rather than α -attack as in the benzylcobaloxime(III) reactions. Loss of cobaloxime(II) in equation 22 sets up the chain mechanism. Equations 23 and 25 are again probable termination steps and equation 24 accounts for the small amount of allyl bromide produced.

A similar mechanism can be presented for the allenylcobaloxime(III) reactions.

The reaction of cobaloxime(II) and polyhalogenomethanes (bromo-trichloromethane is not the only organic halide that reacts under these conditions-- CHBr_3 , CCl_3CN , CCl_4 , CBr_4 , CHBr_2CN have all been demonstrated to react analogously to BrCCl_3 with benzyl-, allyl-, and allenylcobaloxime(III)) then is a very important step in the Johnson scheme. Although adequate studies have been done to support the abstraction of halogen atom from polyhalogenomethanes by cobaloxime(II), no actual mechanistic studies have been done.

It is with this reasoning the study of cobaloxime(II) and various polyhalogenomethanes (CCl_4 , BrCCl_3 , CBr_4 , CHBr_3) is performed. The

rate of reaction as well as thermodynamic data are obtained for these reactions, allowing correlations between rate, activation parameters, and thermodynamic quantities such as bond dissociation energies.

In addition, the radical nature of the mechanism is probed in a different manner than previously attempted. Suitable scavenging agents are employed to kinetically alter the mechanism and therefore rate of reaction. Computer simulation of the experimental data allows speculation about the rate of radical coupling between cobaloxime(II) and the radical intermediate.

RESULTS AND DISCUSSION

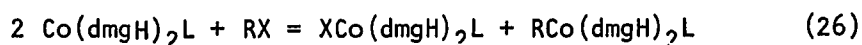
Solvents

The kinetics and mechanism of the reactions between cobaloxime(II) and several polyhalomethanes were studied in acetone and benzene as solvents. The majority of the experiments were performed in the latter solvent as it proved the more easily handled. Several reasons exist for the selection of acetone and benzene over several other solvents.

They provide very stable solutions of cobaloxime(II) as very little decomposition is noted over a period of several hours. Alcoholic solvents such as methanol or ethanol provided very unstable solutions in that most of the cobaloxime(II) was lost in less than an hour's time. This has also been observed by Schneider et al. in their cobaloxime(II) studies.¹⁵ The use of methylene chloride and chloroform was also rejected as they do react very slowly with cobaloxime(II) in the same manner as higher polyhalomethanes (see below).

Stoichiometry and the Products of Reaction

A very limited number of stoichiometric studies was done as previous work^{15,16,21,43} has established the overall stoichiometry of the cobaloxime(II)/alkyl halide reaction as 2:1. One determination was conducted in each solvent. Spectrophotometric titrations with BrCCl_3 of $\text{Co}(\text{dmgH})_2\text{py}$ in benzene (Figure III-3A) gave an average ratio of 2.05 ± 0.13 while $\text{Co}(\text{dmgH})_2\text{PPh}_3$ in acetone gave an average ratio of 2.16 ± 0.06 . Equation 26 presents the stoichiometry of reaction.



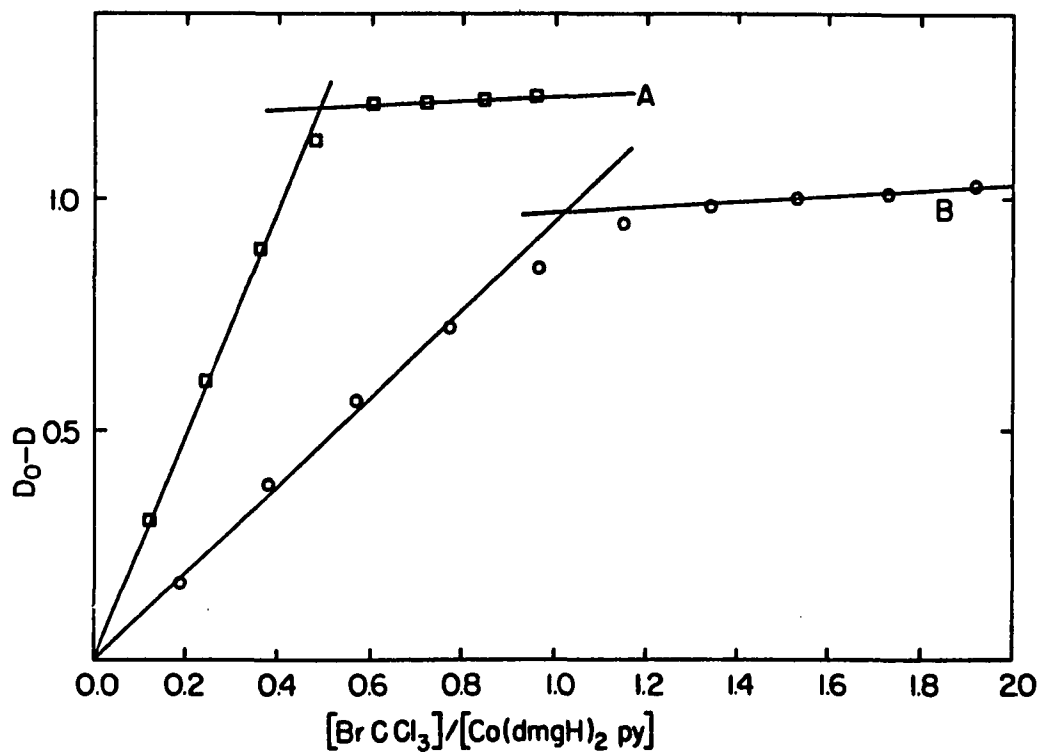


Figure III-3. Illustrating the results of spectrophotometric titrations of $\text{Co}(\text{dmgh})_2\text{py}$ by BrCCl_3 : (a) No added radical scavenger; (b) in the presence of excess 4-HTMPO

Table III-1 contains the pertinent data.

Table III-1. Stoichiometry of the cobaloxime(II)-polyhalogenomethane reaction^{a,b}

Solvent	Axial base	Polyhalogenomethane	Cobaloxime (II): Polyhalogenomethane
(CH ₃) ₂ CO	PPh ₃	BrCCl ₃	2.13, 2.27, 2.08:1 Avg: 2.16±.06:1
C ₆ H ₆	C ₅ H ₅ N	BrCCl ₃	2.06, 1.92, 3.18:1 Avg: 2.05±.13:1
C ₆ H ₆	C ₅ H ₅ N	BrCCl ₃	.98, 1.00, 1.00:1 Avg: .993±.012:1 ^c

^a25.0±.1°C.

^bDetermined by spectrophotometric titration at λ460 nm (PPh₃) and λ420 nm (C₅H₅N).

^cIn presence of excess radical scavenging agent 4-HTMPO.

The products of reaction were not readily isolated in pure form. The standard chromatographic procedures that have proven highly successful for other mixtures of halocobaloxime(III) and alkylcobaloxime(III) were unsuccessful with the mixture of halocobaloxime(III) and trihalomethylcobaloxime(III). This is not too surprising in the light that both complexes are very similar if one views the trihalomethyl group as one "large halide" ligand and that silica gel separates on the basis of polarity and H-bonding.

Attempts were made to isolate the trihalomethylcobaloximes(III) by conversion of the halocobaloxime(III) to other species. Ag⁺ salts were added to the product mixture with the hope of converting the

halocobaloxime(III) to a (solvato)cobaloxime(III) that carries a +1 charge. These cationic cobaloximes(III) do not readily elute down chromatographic columns and would provide very facile separation. Unfortunately, the Ag^+ also seems to attack the trihalomethylcobaloximes(III) as they are not recovered as evidenced by ^1H NMR (see below).

The methodology of Roussi and Widdowson¹⁸ was applied in that Zn dust was added to reduce the halocobaloxime(III) to cobaloxime(II) without affecting the organocobaloxime(III). For reasons unknown, very little halocobaloxime(III) was removed. The use of elevated temperatures (40-50°C) to facilitate the process resulted in recovery of only inorganic cobaloximes(III), due most likely to the homolysis of the organocobaloximes(III).

A third attempt at separation of these products was to convert the axial base of the alkylcobaloxime(III) to a different one from that on the halocobaloxime(III). Although in the substitutionally inert oxidation state of +3, the Co center experiences a very large translabilization effect due to the alkyl ligand in organocobaloximes(III).⁴⁴ It was reasoned then that addition of pyridine to a mixture of the triphenylphosphine adducts of bromocobaloxime(III) and trichloromethylcobaloxime(III) would result in a mixture of bromo(triphenylphosphine)cobaloxime(III) and trichloromethyl(pyridine)cobaloxime(III). This mixture should then be readily separable on silica gel. Unfortunately, in solvents such as benzene and acetone, the halocobaloxime(III) also exchanges axial bases rapidly and quantitatively and the net result was substitution of axial bases in both

complexes.

After these failures at separation and isolation, the products were identified on the basis of their ^1H NMR and known chemical reactions.

The ^1H NMR spectrum of a product mixture from the reaction of cobaloxime(II) and excess polyhalomethane in benzene or acetone showed two singlets in the region where the methyl groups of the dimethylglyoximate ligands resonate. They occurred at $\delta 2.25$ and $\delta 2.35$ (relative to TMS, $\delta 0.0$) and were roughly equal in peak height and area. The former is assigned to the halocobaloxime(III) based on a comparison with an authentic sample. The latter is then assigned to the alkylcobaloxime(III). This is supported by the observation that addition of aqueous alkali resulted in the loss of the $\delta 2.35$ signal and enhancement in the $\delta 2.25$ signal. This is consistent with the reported decomposition of trihalomethylcobaloximes(III) by aqueous base.¹⁷ The equality of the size of the peaks is a further confirmation of the stoichiometry of equation 26.

The reactions of bromoform with cobaloxime(II) was free of the complications experienced with the tetrahalomethanes in that product mixtures were easily separated by silica gel chromatography and isolated in pure form. For details, see the Experimental section.

Kinetics

Pseudo-first-order rate constants were determined in the presence of a large excess of polyhalomethane. They represent the quantity defined in equation 27.

$$k_{\text{obsd}} = -d \ln [\text{Co}(\text{dmgH})_2\text{L}]/dt \quad . \quad (27)$$

Figure III-4 represents several typical sets of data. All plots of k_{obsd} vs. $[\text{RX}]$ are linear and pass through the origin. Assuming that the rate determining step is halogen atom abstraction, the net rate of reaction is given in equation 28a:

$$\frac{-d[\text{Co}(\text{dmgH})_2\text{L}]}{dt} = \frac{-2d[\text{RX}]}{dt} = 2k_1 [\text{Co}(\text{dmgH})_2\text{L}][\text{RX}] \quad . \quad (28a)$$

The values of k_1 are calculated as $k_1 = k_{\text{obsd}}/2[\overline{\text{RX}}]$. The data are summarized in Table III-2 for the polyhalomethanes CCl_4 , BrCCl_3 , CBr_4 , and CHBr_3 in acetone and benzene. As is evident, the reactions were also studied as a function of temperature. Table III-3 gives the activation parameters for these reactions.

Reaction in the Presence of Radical Scavenging Agents

The effect of the addition of possible scavenging agents to the system was investigated by employing a diverse group of reagents.

Inorganic scavenging agents such as Cu^{+2} were not successful because of their limited solubilities in acetone and benzene, possible redox reactions with cobaloxime(II) and the possibility of hydrolysis reactions involving the waters they introduce into the system and consequently attack on the trihalomethylcobaloxime(III).

Olefinic complexes such as 1-octene, acrylonitrile, and 1,3-cyclohexadiene were also unsuccessful. The presence of these compounds, even in very high excess over cobaloxime(II), caused no discernible effects in the kinetics of the reaction. For example, a 135-fold excess of

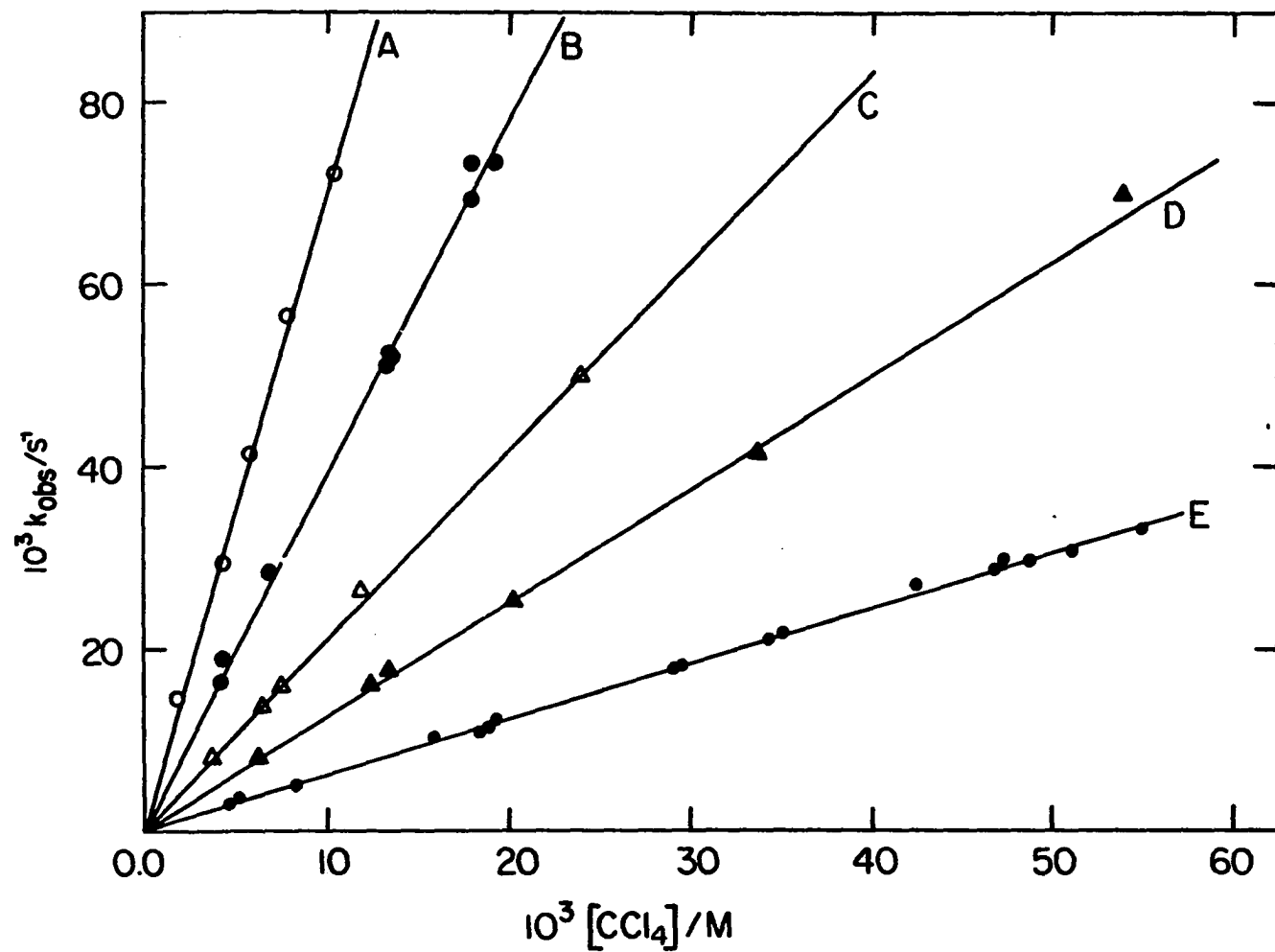


Figure III-4. Plots of the pseudo-first-order rate constants at 25.0°C vs. $[\text{CCl}_4]$ for its reaction with $\text{Co}(\text{dmgH})_2\text{L}$ in acetone (A, B, E) and benzene (C, D) for L = 4-picoline (A, C), pyridine (B, D), and triphenylphosphine (E)

Table III-2. Values of the second-order rate constants k_1 for the reaction of $\text{Co}(\text{dmgH})_2\text{L}$ with polyhalomethanes^a

RX	$k_1/\text{M}^{-1}\text{s}^{-1}$ (T/°C)			
	$\text{Co}(\text{dmgH})_2\text{py}$		$\text{Co}(\text{dmgH})_2\text{PPh}_3$	
	acetone	benzene	acetone	benzene
CCl_4		0.199 (10.88)	0.161 (15.74)	0.0835 (19.67)
	1.90 (25.00)	0.558 (25.01)	0.304 (25.01)	0.106 (24.91)
		1.18 (34.77)	0.571 (34.61)	0.212 (34.44) ^b
		[3.53 (25.00)] ^b	[1.06 (25.00)] ^b	
CHBr_3		0.274 (14.49)		
	1.12 (25.00)	0.515 (25.00)	0.231 (25.00)	0.0755 (25.00)
		0.814 (34.78)		
BrCCl_3		614 (14.89)		
		938 (25.35)		
		1280 (34.56)		
CBr_4		1900 (5.91)		
		2580 (14.21)		
		4580 (25.02)		

^aDetails of the kinetic results are given elsewhere.

^bL = 4-methylpyridine.

Table III-3. Activation parameters for the reaction of $\text{Co}(\text{dmgH})_2\text{L}$ with polyhalomethanes

RX	L	Solvent	$\Delta H^\ddagger/\text{kcal mol}^{-1}$	$\Delta S^\ddagger/\text{cal mol}^{-1}\text{K}^{-1}$
CCl_4	PPh_3	Acetone	11.26 ± 0.10	-23.13 ± 0.33
CCl_4	PPh_3	Benzene	10.42 ± 0.90	-27.6 ± 3.0
CCl_4	$\text{C}_5\text{H}_5\text{N}$	Benzene	12.01 ± 0.25	-19.33 ± 0.85
CHBr_3	$\text{C}_5\text{H}_5\text{N}$	Benzene	8.87 ± 0.49	-30.16 ± 1.63
BrCCl_3	$\text{C}_5\text{H}_5\text{N}$	Benzene	5.94 ± 0.23	-25.06 ± 0.76
CBr_4	$\text{C}_5\text{H}_5\text{N}$	Benzene	6.97 ± 0.88	-18.5 ± 3.0

1-octene over $\text{Co}(\text{dmgH})_2\text{PPh}_3$ in benzene gave the same rate of reaction with CCl_4 as if no 1-octene were added.

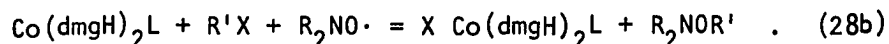
The class of organic compounds known as the nitrones was also tried. These complexes scavenge radical intermediates by forming stable nitroxide species with them. N-t-butyl- α -phenyl-nitrone was the particular reagent used. As with the olefins, the presence of this material made no difference upon the rate of reaction. It is not certain whether or not the nitrone is trapping the radical species as the reverse of the trapping reaction is very facile and enhanced by visible light irradiation. It could also be that the nitrones are too slowly reacting.⁴⁵

The class of organic compounds known as the nitroxides proved most successful in trapping the radical intermediate. Two particular nitroxides were used. The first was the di-t-butyl nitroxide.

Blank experiments indicated that di-t-butyl nitroxide was unreactive towards the polyhalomethane as well as the cobaloxime(II) reagent. The addition of di-t-butyl nitroxide to a solution of cobaloxime(II) and excess carbon tetrachloride produced a kinetic trace decidedly different from simple first order behavior. It is obvious that the nitroxide is altering the course of the reaction in that it is intercepting some of the radical intermediate before cobaloxime(II) reacts with it. A large enough excess of nitroxide over cobaloxime(II) would be expected to return to first order behavior as the radical intermediate would have only one option in its reaction. A 300-fold excess failed to achieve this.

More successful was the use of the compound 4-hydroxy-2,2,6,6-tetramethylpiperidinoxy (4-HTMPO) in the system. Blank experiments also proved this compound unreactive towards the other starting materials in the system.

Figure III-3B shows the effect an excess of 4-HTMPO has upon the stoichiometry of the cobaloxime(II)/polyhalomethane reaction. As seen here and in Table III-1, the stoichiometry changed from 2:1 cobaloxime(II)/RX to 1:1 cobaloxime(II)/RX. The new stoichiometric reaction is given in equation 28b:



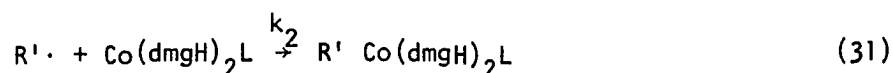
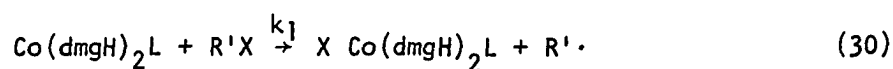
The kinetics of the reaction also change markedly by the presence of 4-HTMPO. Three cases must be examined: (1) no 4-HTMPO present; (2) large excess of 4-HTMPO present; and (3) an intermediate concentration of 4-HTMPO where both cobaloxime(II) and 4-HTMPO compete for the radical intermediate. The first case has already been discussed above.

The second case where 4-HTMPO is sufficiently high in excess of cobaloxime(II) to completely scavenge the radical intermediate is a relatively straightforward situation. Very clean first order decay was again noted just as in the case where no scavenging agent was present. The major difference is that the rate in the scavenger present system is lower by a factor of 2.0 than in the system without. As an example, the reaction between $\text{Co}(\text{dmgH})_2\text{py}$ and BrCCl_3 in benzene has $k_{\text{obsd}}/[\text{BrCCl}_3] = (1.88 \pm 0.06) \times 10^3 \text{ M}^{-1} \text{ s}^{-1}$ at 25.35°C without 4-HTMPO and $(9.13 \pm 0.09) \times 10^2 \text{ M}^{-1} \text{ s}^{-1}$ at 25.00°C with $(5.6) \times 10^{-3} \text{ M}$ 4-HTMPO present.

The ratio of these two rate constants is 2.05 ± 0.09 . This is entirely consistent with what has gone on in the scavenger absent system. In the system with no 4-HTMPO, k_1 is defined as $k_{\text{obsd}}/2[\text{BrCCl}_3]$ and has a value of $(9.38 \pm 0.3) \times 10^2 \text{ M}^{-1} \text{ s}^{-1}$. These two values are the same within acceptable limits. Therefore, when a large excess of 4-HTMPO is present, the rate law is as given in equation 29:

$$\frac{-d[\text{Co}(\text{dmgH})_2\text{L}]}{dt} = \frac{-d[\text{RX}]}{dt} = k_1 [\text{Co}(\text{dmgH})_2\text{L}][\text{RX}] \quad (29)$$

The situation where effective competition between cobaloxime(II) and 4-HTMPO is occurring is a much more complex one than the two extremes above. The overall mechanism of concern is given in equations 30-32. For simplicity and consistency, the rate constants will be



assigned as k_1 for equation 30, k_2 for 31, and k_3 for 32.

When the steady-state approximation is made for $[\text{R}' \cdot]$, the rate of reaction by equations 30-32 is given in equations 33 and 34:

$$\frac{-d[\text{Co}(\text{dmgH})_2\text{L}]}{dt} = k_1 \left(\frac{2+\alpha}{1+\alpha} \right) [\text{Co}(\text{dmgH})_2\text{L}][\text{RX}] \quad (33)$$

$$\alpha = k_3[4\text{-HTMPO}]/k_2[\text{Co}(\text{dmgH})_2\text{L}] \quad (34)$$

The two correct limiting forms, equations 28 and 29, are derived from equations 33 and 34 at the extreme [4-HTMPO] concentrations of zero $\{(\frac{2+\alpha}{1+\alpha}) = 2\}$ and infinity $\{(\frac{2+\alpha}{1+\alpha}) = 1\}$. In the intermediate region, a more complicated analysis is required.

Define the quantity m as in equation 35 from k_{obsd} and the

$$m = \frac{k_{obsd}}{k_1[RX]} = \frac{2+\alpha}{1+\alpha} \quad (35)$$

independently known value of k_1 . The value of m then should be the same for different compounds that lead to the same free radical (e.g. $BrCCl_3$ and CCl_4) at a given value of α as k_2 and k_3 are independent of the variation of X .

Figure III-5 depicts the variation of m with the initial concentration ratio of $[4-HTMPO]/[Co(dmgH)_2L]$. The result that data from conventional methods involving CCl_4 and flash photolytic methods involving $BrCCl_3$ lie in the same curve establishes the expected congruence for the case $R\cdot = CCl_3\cdot$.

Before leaving this section, a comment or two is necessary. Unlike the di-*t*-butyl nitroxide experiments, no curvature or at best very minor bowing was noted in the $\ln(D_t - D_\infty)$ vs. time plots used to determine the pseudo first order rate constants k_{obsd} . This is most unusual and unexpected given the complex nature of equation 33 which defines the rate law in the intermediate 4-HTMPO concentrations. Inspection of equation 33 should lead to behavior far from first order, but this is the exact opposite of the observed behavior. This point is rectified in the next section on the computer simulations of the system.

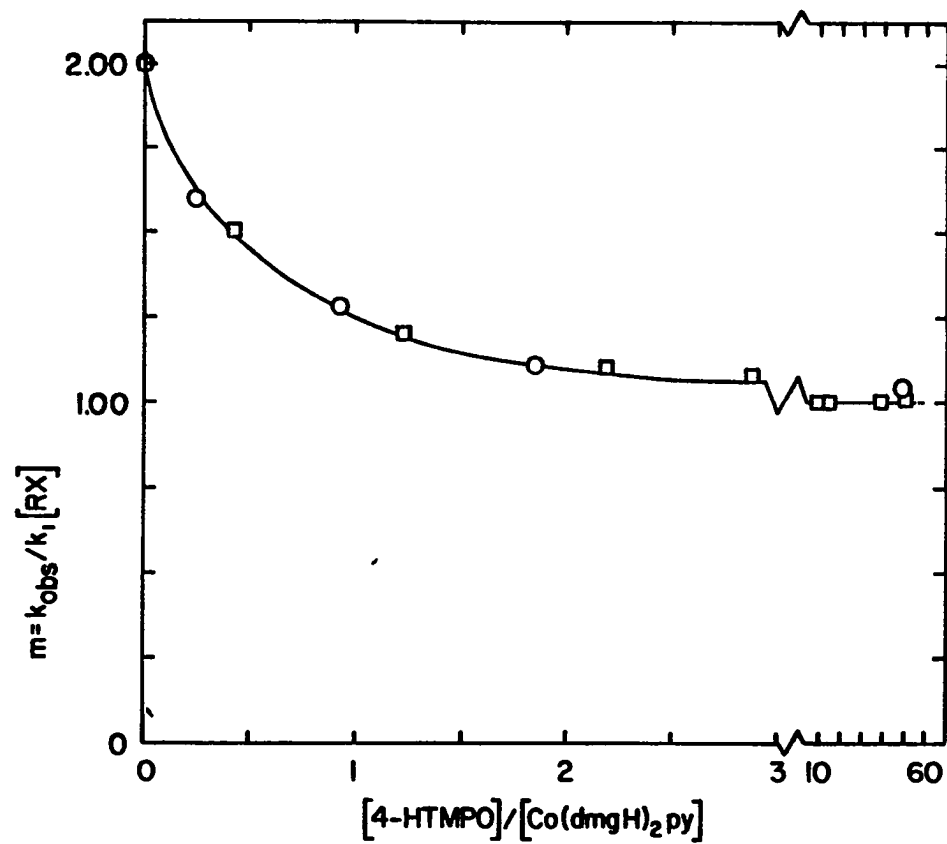


Figure III-5. Competitive reactivity of 4-HTMPO and Co(dmgh)₂py toward •CCl₃, generated from BrCCl₃ (○) and from CCl₄ (□) as illustrated by the variation of m (equation 11) with the ratio of initial concentrations. The solid line shows the same quantity using kinetic data simulated by forward integration techniques for the ratio $k_3/k_2 = 1.8$

Mathematical Simulations

The treatment given in the above section on the intermediate scavenging reactions of 4-HTMPO is imprecise on two counts. The first is that the values of α and m (equations 34 and 35) were assumed to be constant during the kinetic run. In actuality, both should vary during the kinetic run as the consumption of 4-HTMPO and $\text{Co}(\text{dmgH})_2\text{L}$ occur at different rates. This is the oddity mentioned above concerning the unexpected pseudo-first-order behavior. The factor $(2+\alpha/1+\alpha)$ in equation 33 should be changing with time leading to nonpseudo-first-order kinetics. The second point is that the description of m as a function of the initial concentration ratio $[4\text{-HTMPO}]/[\text{Co}(\text{dmgH})_2\text{L}]$ can only be approximate since this ratio changes during the course of the kinetic run.

To better understand these effects and their importance in the total analysis, the kinetic situation represented by equations 30-32 was examined mathematically. The differential rate equations used in the analysis are given in equations 36-40.

$$\frac{-d[\text{Co}(\text{II})]}{dt} = k_1[\text{Co}(\text{II})][\text{R}'\text{X}] + k_2[\text{Co}(\text{II})][\text{R}\cdot'] \quad (36)$$

$$\frac{d[\text{R}'\text{Co}(\text{III})]}{dt} = k_2[\text{Co}(\text{II})][\text{R}\cdot'] \quad (37)$$

$$\frac{d[\text{XCo}(\text{III})]}{dt} = k_1[\text{Co}(\text{II})][\text{R}'\text{X}] \quad (38)$$

$$\frac{d[\text{R}\cdot']}{dt} = k_1[\text{Co}(\text{II})][\text{R}'\text{X}] - k_2[\text{Co}(\text{II})][\text{R}\cdot'] - k_3[\text{R}_2\text{NO}\cdot][\text{R}\cdot'] \quad (39)$$

$$\frac{d[\text{R}_2\text{NOR}']}{dt} = k_3[\text{R}_2\text{NO}\cdot][\text{R}\cdot'] \quad (40)$$

Numerical forward integration techniques were applied to the solution of the above equations. The fourth order Runge-Kutta method proved to be highly inefficient in their solution. This was due to k_2 and k_3 being so much larger than k_1 that minute time increments were necessary and consequently, the analyses required computer calculations that were too lengthy and costly. This type of situation is referred to as involving a "stiff" set of differential equations and is a situation best suited for Gear's predictor-corrector method.^{46,47} Therefore, this was the chosen method of analysis.

Initial values of all reactant concentrations were chosen for each calculation corresponding to the different experimental conditions used. The rate constant k_1 was held fixed at its experimentally determined value of $0.558 \text{ M}^{-1} \text{ s}^{-1}$ for CCl_4 in benzene at 25.0°C . The rate constants k_2 and k_3 are unknown but are expected to be large and were appropriately set in the range 10^7 - $10^9 \text{ M}^{-1} \text{ s}^{-1}$. The actual values of k_2 and k_3 are unimportant only relative to each other and need only be larger than k_1 .

The computer program used generated a concentration vs. time profile at frequent time intervals for all species involved--reactants, products, and intermediates. A simulated absorbance vs. time curve was also produced by using the known molar absorptivities of every species (at $\lambda 420 \text{ nm}$, $\epsilon(\text{Co}(\text{dmgH})_2\text{py}) = 3.55 \times 10^3 \text{ M}^{-1} \text{ cm}^{-1}$, $\epsilon(4\text{-HTMPO}) = 9.4 \text{ M}^{-1} \text{ cm}^{-1}$, $\epsilon(\text{ClCo}(\text{dmgH})_2\text{py}) = 6.82 \times 10^2 \text{ M}^{-1} \text{ cm}^{-1}$, and $\epsilon(\text{CCl}_3\text{Co}(\text{dmgH})_2\text{py}) = 7.89 \times 10^2 \text{ M}^{-1} \text{ cm}^{-1}$, all other species have molar absorptivities of zero at this wavelength).

The results of these calculations are as follows. (1) Simulated absorbance vs. time traces are identical with the actual traces for at least the first three half-lives. Beyond this point, differences set in due to a secondary reaction in the actual kinetic run not compensated for in the mathematical model. (2) The simulated concentration of the intermediate $\cdot\text{CCl}_3$ radical species remains at very low steady state concentration throughout, $\sim 10^{-4}\%$ of the $[\text{Co}(\text{dmgH})_2\text{py}]_0$. (3) Without any 4-HTMPO present or with a very large excess of it over Co(II), precise pseudo-first-order data are generated. Consistent with the experimental findings, values of $k_{\text{obsd}}/[\text{CCl}_4]$ differ exactly by a factor of 2.00 at these extremes. (4) At intermediate concentrations of 4-HTMPO, the simulated data are not precisely pseudo-first-order in nature. The values of k_{obsd} at a given $[\text{CCl}_4]$ concentration decrease slightly throughout the run. The extent of this curvature is not very large in the pseudo-first-order plots and becomes linear with a very small adjustment in the predicted D-infinity. This is why in the experimental data where competition of the radical intermediate exists, linear plots are still realized due to a compensation in the D-infinity during analysis. (5) Each simulation, after adjustment of D-infinity to force a first-order fit, yields a value of k_{obsd} and (by equation 35) a value of m . The variation of m with the initial concentration ratio for the simulated data was compared to that found experimentally, as shown in Figure III-4. The best agreement occurred at the ratio of $k_3/k_2 = 1.8 \pm 0.1$. This agreement proved independent of the actual values of the rate constants k_2

and k_3 provided they were sufficiently large compared to k_1 (a factor of 10^3) and were in the ratio of 1.8.

INTERPRETATION

As indicated in the introduction to this part of the thesis, a great amount of study has gone on before to fully establish the generality of the mechanism given in equations 10 and 11 in the case of other alkyl and aryl halides. The results found here are in complete agreement with these previous findings. The stoichiometry and the products are in accord with equation 11a, and the rate law establishes the bimolecularity of the rate limiting step.

An alternative mechanism to the one proposed in equations 30 and 31 exists and should be considered. Rather than the abstraction of halogen atom with the formation of a carbon centered radical as the rate limiting step, the transfer of the alkyl group to the cobaloxime(II) with the formation of halogen atom could occur. This is highly unlikely in light of the results of the trapping experiments which include the change in stoichiometry and reaction rates. The only product observed when a large excess of 4-HTMPO was present was the halocobaloxime(III). It would be most unexpected for the polyhalomethanes to react differently from other alkyl halides. Further support of the mechanism given in equations 30 and 31 is the minor decrease in rate concurrent with a change in solvent polarity in going from benzene to acetone. This is indicative of a nonionic transition state consistent with the rate limiting step of halogen atom abstraction.

The rate of reaction between a given halide RX and the complex $\text{Co}(\text{dmgH})_2\text{L}$ is very dependent upon the nature of the axial base L. The

reaction rate order was found to be $\text{PPh}_3 < \text{pyridine} < 4\text{-methylpyridine}$, also consistent with earlier work.^{15,16} Ligand basicity increases in the same order, as measured by pKa values, which are 2.7, 5.3, and 6.1, respectively.^{48,49} This trend in reactivity is in full agreement with a transition state for equation 30 in which electron transfer from Co(II) is enhanced by electron donation from L onto the metal. The increases in rate with increasing ligand basicity are not great, with only one order of magnitude between the extreme members. This is very comparable to the analogous reactions involving the benzyl halides.^{15,16}

Variation of the organic halide gives rise to very pronounced differences in the rate constant k_1 (for equation 30) and the associated value of ΔH^\ddagger . For proper comparison of these values, the rate constants must undergo a statistical correction based upon the number of equivalent reactive C-X bonds. On such a standard, the reactivity order (and k_1^{Corr} values for the reaction of $\text{Co(dmgH)}_2\text{py}$ in benzene) is CCl_4 (0.14 $\text{M}^{-1} \text{s}^{-1}$) $< \text{CHBr}_3$ (0.17) $\ll \text{BrCCl}_3$ (938) $< \text{CBr}_4$ (1145). This is another trend totally in agreement with previous investigations.^{14,16,22,32,33} Carbon-bromine bond cleavage occurs more readily than carbon-chlorine bond cleavage in comparable compounds. The very large difference between bromoform and the two more reactive bromine containing polyhalomethanes is apparently due to the differences in the carbon-bromine bond strength.

Analysis of variations such as these that arise in a homologous series can be sought through the bond dissociation enthalpy of the carbon-halogen bond. Values for the latter are well-established and

given in Table III-4 along with the corresponding enthalpy of activation values.

Table III-4. Comparison between enthalpy of activation for the cobaloxime(II)-polyhalogenomethane reaction and the bond dissociation energy of the C-X bond

Reaction	Solvent	H^\ddagger (kcal/mole)	B.D.E. (kcal/mole)
$\text{Co}(\text{dmgH})_2\text{py} + \text{CCl}_4$	C_6H_6	$12.01 \pm .25$	70.4 ± 1^{50}
$\text{Co}(\text{dmgH})_2\text{py} + \text{CHBr}_3$	C_6H_6	$8.87 \pm .49$	62^{51}
$\text{Co}(\text{dmgH})_2\text{py} + \text{CBr}_4$	C_6H_6	$6.97 \pm .88$	56.2 ± 1.8^{52}
$\text{Co}(\text{dmgH})_2\text{py} + \text{BrCCl}_3$	C_6H_6	$5.94 \pm .23$	55.7 ± 1^{50}

In Figure III-6 is a comparison of these two quantities. As is evident, a good linear correlation exists. Caution must be used, however, in analyses such as these. If the comparison is extended outside the homologous series to similarly reacting compounds, the correlation becomes lost. The value off the line in Figure III-6 is for PhCH_2Br . The reason for this is the stability differences among the different carbon-centered free radicals being formed at the transition state. These now play a deciding role in influencing the activation and bond enthalpies.

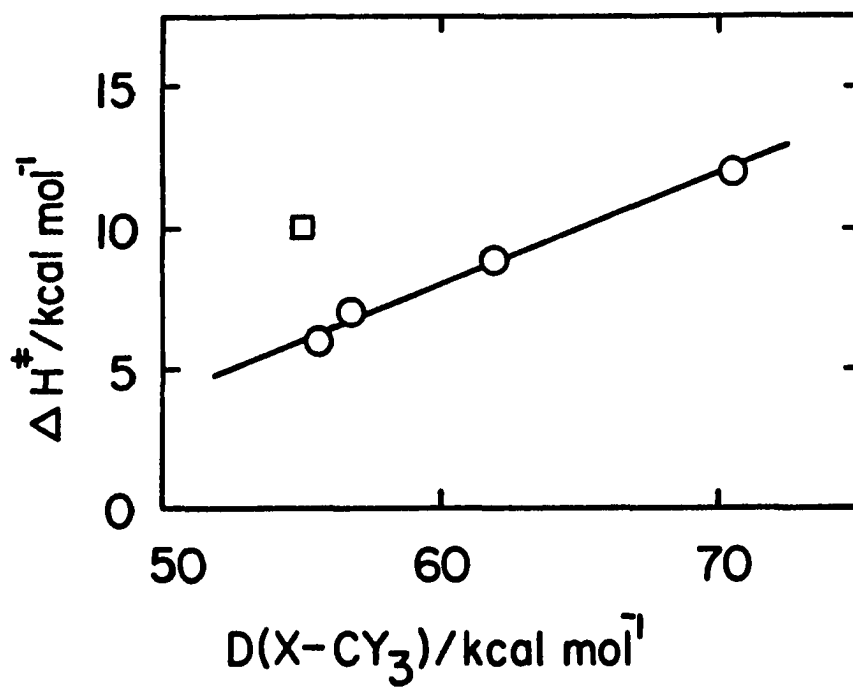


Figure III-6. The enthalpy of activation associated with halogen atom abstraction reaction of equation 1 is linearly correlated with the bond dissociation enthalpy for the given polyhalomethane (○). The correlation does not extend to benzyl bromide, however (◻)

The entropy of activation values, ΔS^\ddagger , are very negative, -19 to -30 cal mol⁻¹ k⁻¹ (see Table III-3). Again, in total agreement with earlier studies, such as the analogous reactions of benzyl bromide with Co(dmgh)₂PPh₃ (-32 cal mol⁻¹ k⁻¹) and Co(dmgh)₂py (-29 cal mol⁻¹ k⁻¹).¹⁶ Solvation effects cannot account for these values since the reaction is nonionic in character and the results were obtained in the relatively unpolar solvents acetone and benzene. Instead, these values imply a very highly ordered transition state. Within the solvent cage, many possible collision complexes will form during the encounter of Co(dmgh)₂L and RX. Of these collisions, a very small proportion would be likely to occur with an orientation suitable for halogen atom transfer. Additionally, it is known that the participants in a gas-phase association reaction will experience a large loss of translational entropy in their combination.

The presence of 4-HTMPO and its effect upon the reaction kinetics is successfully and accurately modeled as following equations 30-32. An estimate of k_3/k_2 was found to be 1.8 from the simulations. The absolute values of either of these two radical coupling reactions are not known, but sufficient data exist to make reasonable estimates. The rate constant k_3 is estimated at $1.5 \times 10^8 \text{ M}^{-1} \text{ s}^{-1}$ based on the value for the coupling of C-C₅H₉ and other aliphatic radicals to 4-HTMPO.⁵³ This leads to an estimate of $k_2 \sim 8.0 \times 10^7 \text{ M}^{-1} \text{ s}^{-1}$. This latter value can be compared with the rate constants for the capture of other aliphatic radicals by other Co(II) macrocyclic complexes leading to the formation

of Co-C bonds $R \cdot + \text{Co}(\text{Me}_6[14]\text{ane-4,11-diene } N_4)(\text{OH}_2)_2^{+2}$, $(1-7) \times 10^8 \text{ M}^{-1} \text{ s}^{-1}$ ($R = \text{CH}_3$),^{54,55} 8×10^7 ($R = \text{CH}_2\text{CHO}$),⁵⁶ 7×10^7 ($R = \text{CH}_2\text{OH}$),⁵⁶ 3×10^7 ($R = \text{CH}(\text{CH}_3)\text{OH}$),⁵⁶ 4×10^7 ($R = \text{CH}(\text{CH}_2\text{NH}_3^+)\text{OH}$),⁵⁶ and 1×10^7 ($R = \text{CHOHCH}_2\text{OH}$).⁵⁶ It is reasonable then to state that these estimates of $k_2 = 8.0 \times 10^7 \text{ M}^{-1} \text{ s}^{-1}$ and $k_3 = 1.5 \times 10^8 \text{ M}^{-1} \text{ s}^{-1}$ are roughly correct.

The final comments will concern the lack of effect upon the reaction rates of 1-octene. The inability of a 135-fold excess of 1-octene over cobaloxime(II) to alter the kinetics of the reaction is a reflection of its inability to successfully compete with cobaloxime(II) for the trihalomethyl radical intermediate. Taking into consideration the level of experimental uncertainty, an upper limit of $6 \times 10^4 \text{ M}^{-1} \text{ s}^{-1}$ is placed on the second order rate constant for the addition of $\cdot\text{CCl}_3$ to 1-octene. The actual value for this rate constant is presently not known, but values are known for the similar reaction of methyl radical addition to olefins. These values lie in the range of $(5-30) \times 10^3 \text{ M}^{-1} \text{ s}^{-1}$.⁵⁷ This upper limit is then reasonable and simply reinforces the argument that 1-octene is too low in reactivity towards $\cdot\text{CCl}_3$ to be an effective scavenger.

EXPERIMENTAL

Materials

Solvents

For most kinetic experiments, reagent grade acetone (Fischer Scientific) and benzene (Fischer Scientific) were employed. Spectrophotometric grade acetone (Aldrich) was used for some measurements. Acetone and benzene purified in the manners described below were also used for some reactions. Identical results were achieved regardless of the history and nature of the solvent.

Acetone was purified by saturating 1 liter of the neat liquid with NaI at room temperature. The solution was then decanted and cooled to -10°C in an acetone/dry ice slurry. Crystals of the NaI complex precipitated and were collected on a glass frit by suction filtration. The crystals were then added to a distillation flask and gently warmed to 30°C . The resulting liquid was then distilled onto Molecular Sieves 4A.

Benzene was purified by first shaking with sulfuric acid (concentrated) until no darkening appeared in the acid layer. The benzene was then added to a distillation flask and distilled onto calcium chloride (anhydrous).

A small quantity of very high purity benzene was obtained by fractional crystallization from ethanol, followed by distillation onto anhydrous CaCl_2 .

Solvents for syntheses (methanol, benzene, tetrahydrofuran, ethanol, methylene chloride, hexanes, acetone) were all reagent grade and used as

received. Chromatographic solvents (ethyl acetate, chloroform, methanol, carbon tetrachloride) were also all reagent grade and used without purification.

Polyhalogenomethanes

Carbon tetrachloride (Fischer Scientific) The bulk liquid was dried over CaCl_2 (anh), followed by distillation from P_2O_5 at 76°C into an amber colored bottle. The liquid was stored under an atmosphere of either nitrogen or argon.

Bromotrichloromethane (Aldrich) The same procedure for carbon tetrachloride was employed, distilling the liquid at 105°C .

Carbon tetrabromide (Eastman) The solid was recrystallized three times from absolute ethanol, followed by prolonged drying under vacuum in a desiccator. This process was repeated twice. The final sample gave an infrared spectrum that agreed very well with the published spectrum of Aldrich's. Proton NMR in $d\text{-CHCl}_3$ gave no signal.

Bromoform (Aldrich) The neat liquid is bulk dried first with CaCl_2 (anh), followed by distillation at 51°C under reduced pressure from CaCl_2 (anh) onto anhydrous $\text{Ba}(\text{ClO}_4)_2$. The liquid is then stored either in an amber colored bottle or in bottles wrapped in foil and stored in the dark. An inert atmosphere is placed above the liquid.

Cobaloxime(II) reagents

The bis(ligand)cobaloxime(II) complexes were prepared in a manner similar to that of Schrauzer.⁶ All chemicals used are of reagent grade quality. A typical synthesis is outlined below.

$\text{Co}(\text{C}_2\text{H}_3\text{O}_2)_2 \cdot 4\text{H}_2\text{O}$ (x mole) is added to a thoroughly deoxygenated suspension of dimethylglyoxime (2x mole) in MeOH. A two or three necked round bottom flask equipped with a magnetic stirring bar is used. After 40 minutes of stirring under nitrogen (or argon), a brick red suspension is obtained. The desired axial base (6x mole) is then added. If the axial base is a liquid, the neat deoxygenated liquid is directly added to the reaction mixture. If the axial base is a solid, two options were employed. If the solid was sufficiently soluble in methanol, it is added as a deoxygenated solution in methanol (25-30 mL). This proved most successful in the case of solid nitrogen bases, such as nicotinamide. In the event the solid proved too insoluble, as with phosphorus bases such as triphenylphosphine, the solid is added to a solid addition funnel, deoxygenated for 40 minutes, and then attached to the reaction vessel containing the cobaloxime(II). The addition funnel is inverted and gentle tapping of its side drives the solid into the reaction slurry. After complete addition of any axial base, the reaction mixture turns black. Thirty more minutes of stirring precede filtration under inert atmosphere. The black solid is collected on a glass fit and washed thoroughly with diethyl ether (deoxygenated). In the case of pyridine and the substituted pyridine adducts, the diethyl ether washes contained 15-20% of the free ligand to prevent loss of the axial base during washing. Four hours of a strong argon flow through the solid dries the material. Once dry, the solids are air-stable and are easily handled. When not in use, the solids are stored in a desiccator under nitrogen or argon. Yields obtained were normally 90% or better

of the theoretical.

Analyses of the cobaloxime(II) reagents are found in Table III-5.

Table III-5. Analyses of bis (ligand)cobaloxime(II) complexes

Ligand	Molecular weight	% yield	% Co	% C	% H	% N
Pyridine	447.4	93.0	13.76±.32 ^a (13.17) ^b	48.41 (48.31)	5.43 (5.41)	18.67 (18.77)
Nicotinamide	533.5	95.2	10.92±.08 (11.05)	--	--	--
4 picoline	475.5	95.2	12.57±.10 (12.39)	--	--	--
Triphenylphosphine	813.7	94.6	7.01±.12 ^c (7.24)	64.70 (64.90)	5.48 (5.45)	6.93 (6.89)

^aOther preparations of this complex gave % Co values of 12.74±.28 and 12.77±.18.

^bValues in parentheses are the calculated percentages for Co(dmgH)₂·2L.

^cAnother preparation of this complex gave % Co value of 7.24±.12 and a third gave a C,H,N analysis of 65.00, 5.43, and 6.73, respectively.

Organocobaloxime(III) reagents

Cobaloxime(I) procedure The method of Schrauzer⁶ was used to prepare the following complexes: methyl-, monobromomethyl-, dibromomethyl-, and allyl(pyridine)cobaloxime(III). The methyl(aquo)-cobaloxime(III) complex was prepared following the same procedure only no pyridine was used.

OH⁻ disproportionation The method of Yamazaki and Hohokabe⁵⁸ was used to prepare the following complexes: methyl(aquo)-, isopropyl-(pyridine)-, and n-octyl(pyridine)cobaloxime(III).

Zn reduction method Benzyl(triphenylphosphine)cobaloxime(III) was prepared using the procedure of Roussi and Widdowson.¹⁸

CH₃Co(dmgh)₂PPh₃ preparation 0.96 g (.003 mole) CH₃Co(dmgh)₂H₂O is suspended in 15 mL CH₂Cl₂. 0.80 g (.0031 mole) P(C₆H₅)₃ is added and stirred for 10 minutes. The solutions turned homogeneous. 40 mL hexanes is added and the solution rotovapped at low heat until crystals began to form. One additional minute of rotary evaporation is done and the bright orange crystals are filtered and washed thoroughly with hexanes.

Analyses Table III-6 lists the analyses of the various organo-cobaloxime(III) complexes prepared. All complexes were also analyzed by NMR and proved to be pure as no extraneous peaks were noted.

Inorganic cobaloxime(III) reagents

Schrauzer method Bromo- and chloro(pyridine)cobaloxime(III) were prepared by the procedure of Schrauzer.⁶

Burkhardt method Bromo- and chloro(triphenylphosphine)-cobaloxime(III) were synthesized by the method of Burkhardt and Burmeister.⁵⁹

Analyses Table III-7 gives the cobalt analyses for these complexes.

Table III-6. Analyses of organocobaloxime(III) complexes

Complex	Synthetic method	Molecular weight	% Co
$C_3H_5Co(dmgh)_2py$	Cobaloxime(I)	409.4	14.31±.19 (14.40) ^a
$CHBr_2Co(dmgh)_2py$	Cobaloxime(I)	541.4	11.16±.18 (10.89)
$CHBr_2Co(dmgh)_2py$	Cobaloxime(I)	462.2	12.55±.21 (12.75)
$CH_3Co(dmgh)_2py$	Cobaloxime(I)	383.3	--
$CH_3Co(dmgh)_2H_2O$	OH^- disproportionation	322.2	--
$n-C_8H_{17}Co(dmgh)_2py$	OH^- disproportionation	481.5	11.91±.10 (12.22)
$i-C_3H_7Co(dmgh)_2py$	OH^- disproportionation	411.4	14.23±.84 (14.32)
$PhCH_2Co(dmgh)_2PPh_3$	Zn reduction	642.6	8.13±.14 (9.18) ^b
$CH_3Co(dmgh)_2PPh_3$	$CH_3Co(dmgh)_2H_2O + PPh_3$	566.2	10.25±.26 (10.41)

^aCalculated percentage values in parentheses for $RCo(dmgh)_2L$.

^bContaminated with $BrCo(dmgh)_2PPh_3$.

Table III-7. Cobalt analyses for inorganic cobaloxime(III) complexes

Complex	Method	Molecular weight	% Co
$ClCo(dmgh)_2py$	Schrauzer	403.8	--
$BrCo(dmgh)_2py$	Schrauzer	448.2	12.99±.27 (13.15) ^a
$ClCo(dmgh)_2PPh_3$	Burkhardt	587.0	10.08±.32 ^b (10.04)
$BrCo(dmgh)_2PPh_3$	Burkhardt	631.3	9.31±.006 (9.33)

^aCalculated percentage values in parentheses for $XCo(dmgh)_2L$.

^bA second preparation gave a product with 9.82±.05 cobalt percentage.

Scavenging agents

Acrylonitrile (Aldrich), 1,3-cyclohexadiene (Aldrich), di-N-t-butyl nitroxide (Eastman), α -phenyl-N-t-butyl nitroxide (Aldrich) were all used as received.

4-Hydroxy-2,2,6,6-tetramethylpiperidinoxy (Aldrich) was recrystallized twice from acetone. 1-Octene (Aldrich) was dried over MgSO_4 (anh) and distilled onto CaCl_2 (anh) at 121°C .

Stoichiometric Studies

Stock solutions were prepared as follows. The desired amount of cobaloxime(II) reagent is measured out and added to a volumetric flask, followed by a thorough flushing with argon. The desired solvent (acetone or benzene) is then added via transfer needle to mark. Thorough mixing is ensured by passage of a mild flow of argon through the solution for 20 seconds. The 4-hydroxy-2,2,6,6-tetramethylpiperidinoxy stock solution is prepared similarly.

The bromotrichloromethane stock solution is prepared by filling a 10 mL volumetric flask with deaerated solvent; 2.5 μL of the polyhalogenomethane is injected into the solution.

All stocks solutions are maintained under a constant positive pressure of argon by leaving the flasks attached to the inert gas line with no exit port.

Reaction cells (2.0-cm quartz cells) are prepared by adding 0.6 mL of the cobaloxime(II) stock solution to either 5.4 mL of the pure solvent (experiments with no scavenging agent) or 5.4 mL of the 4-hydroxy-2,2,6,6-tetramethylpiperidinoxy stock solutions.

Alternatively, 6.0 mL of a dilute cobaloxime(II) solution is added to the reaction cell. Final concentrations of reagents are $2.0-4.0 \times 10^{-4}$ M for the cobaloxime(II) complexes and 2.87×10^{-2} M for the scavenging agent.

The spectrum of the solution in the Cary cell is measured from $\lambda 600$ nm to $\lambda 420$ nm (triphenylphosphine complex in acetone titration) to $\lambda 380$ nm (pyridine complex in benzene titration). 5 μ L injections of the bromotrichloromethane solution are made until 4 or 5 consecutive injections lead to minor or no changes in the spectrum.

Absorbance readings are taken at the maxima for the cobaloxime(II) species, $\lambda 420$ nm for (pyridine)cobaloxime(II) in benzene and $\lambda 460$ nm for (triphenylphosphine)cobaloxime(II) in acetone. The absorbance change, $D_0 - D_i$, is plotted against the ratio moles BrCCl_3 /moles cobaloxime(II). The intersection of the two straight lines defined by the data, when plotted in the manner above, is taken as the stoichiometry of the reaction.

Identification of Products from $\text{Co}(\text{dmgH})_2\text{py}/\text{CHBr}_3$ Reaction

The following four cobaloxime(III) complexes were prepared in the usual manner: $\text{BrCo}(\text{dmgH})_2\text{py}$, $\text{CH}_3\text{Co}(\text{dmgH})_2\text{py}$, $\text{BrCH}_2\text{Co}(\text{dmgH})_2\text{py}$, and $\text{Br}_2\text{CHCo}(\text{dmgH})_2\text{py}$. All complexes were deemed pure by TLC (silica gel) analysis using 2:2:1 ethyl acetate:chloroform:methanol. Only one spot was seen after development of TLC plates.

UV-Vis spectra

CH₃Co(dmgh)₂py In MeOH, two maxima are noted, $\lambda 438$ nm ($\epsilon=1070$ $\text{M}^{-1} \text{cm}^{-1}$) and $\lambda 373$ nm ($\epsilon=1840$ $\text{M}^{-1} \text{cm}^{-1}$). Addition of two drops concentrated HClO₄ causes a shift in both maxima to higher wavelengths: $\lambda 447$ nm ($\epsilon=1270$ $\text{M}^{-1} \text{cm}^{-1}$) and $\lambda 392$ nm ($\epsilon=1800$ $\text{M}^{-1} \text{cm}^{-1}$).

In C₆H₆, CH₃Co(dmgh)₂py exhibits a shoulder at $\lambda 420$ nm ($\epsilon=1260$ $\text{M}^{-1} \text{cm}^{-1}$) and a maximum at $\lambda 392$ nm ($\epsilon=5490$ $\text{M}^{-1} \text{cm}^{-1}$).

BrCH₂Co(dmgh)₂py Methanolic solutions of BrCH₂Co(dmgh)₂py exhibit two shoulders, the first at $\lambda 420$ nm ($\epsilon=550$ $\text{M}^{-1} \text{cm}^{-1}$), the second at $\lambda 360$ nm ($\epsilon=1850$ $\text{M}^{-1} \text{cm}^{-1}$). The second shoulder is a very weakly resolved feature of the spectrum. Acidification of the solution with concentrated HClO₄ leads to little resolution in either shoulder and again causes a shift to higher wavelengths of the two spectral features: $\lambda 440$ nm ($\epsilon=457$ $\text{M}^{-1} \text{cm}^{-1}$) and $\lambda 365$ nm ($\epsilon=1850$ $\text{M}^{-1} \text{cm}^{-1}$).

Solutions of BrCH₂Co(dmgh)₂py also exhibit two shoulders. The first is at $\lambda 480$ nm ($\epsilon=145$ $\text{M}^{-1} \text{cm}^{-1}$) and $\lambda 420$ nm ($\epsilon=690$ $\text{M}^{-1} \text{cm}^{-1}$).

Br₂CHCo(dmgh)₂py Two shoulders are observed in methanolic solutions: $\lambda 435$ nm ($\epsilon=380$ $\text{M}^{-1} \text{cm}^{-1}$) and $\lambda 380$ nm ($\epsilon=1085$ $\text{M}^{-1} \text{cm}^{-1}$). Acidification (concentrated HClO₄) results in minor shifts of the two shoulders to higher wavelengths: $\lambda 440$ nm ($\epsilon=360$ $\text{M}^{-1} \text{cm}^{-1}$) and $\lambda 383$ nm ($\epsilon=1085$ $\text{M}^{-1} \text{cm}^{-1}$).

Benzene solutions exhibit two very poorly defined shoulders at $\lambda 435$ nm ($\epsilon=490$ $\text{M}^{-1} \text{cm}^{-1}$) and $\lambda 388$ nm ($\epsilon=1310$ $\text{M}^{-1} \text{cm}^{-1}$).

BrCo(dmgh)₂py Methanolic solutions exhibit little if any features in the region of $\lambda 600$ nm to $\lambda 300$ nm. A possible, very weakly defined

shoulder is noted around $\lambda 375$ nm ($\epsilon=1675 \text{ M}^{-1} \text{ cm}^{-1}$). Acidification with concentration HClO_4 results in no changes in the spectrum.

Solutions in benzene exhibit a well-defined shoulder at $\lambda 380$ nm ($\epsilon=810 \text{ M}^{-1} \text{ cm}^{-1}$).

^1H NMR spectra

Table III-8 lists the signals arising in the ^1H NMR of the four cobaloxime (III) complexes.

Table III-8. ^1H NMR of 4 cobaloximes(III) (CDCl_3 , TMS as reference, 0.0)

Compound	Signal (multiplicity)	Origin
$\text{CH}_3\text{Co}(\text{dmgH})_2\text{py}$	$\delta 0.50$ (singlet) $\delta 2.19$ (singlet) $\delta 7.29$ - $\delta 8.71$ (several peaks)	axial CH_3 group dmgH CH_3 groups axial $\text{C}_5\text{H}_5\text{N}$ group
$\text{BrCH}_2\text{Co}(\text{dmgH})_2\text{py}$	$\delta 2.21$ (singlet) $\delta 4.64$ (singlet) $\delta 7.20$ - $\delta 8.60$ (several peaks)	dmgH CH_3 groups axial CH_2Br group axial $\text{C}_5\text{H}_5\text{N}$ group
$\text{Br}_2\text{CHCo}(\text{dmgH})_2\text{py}$	$\delta 2.18$ (singlet) $\delta 5.71$ (singlet) $\delta 7.08$ - $\delta 8.39$ (several peaks)	dmgH CH_3 groups axial CHBr_2 group axial $\text{C}_5\text{H}_5\text{N}$ group
$\text{BrCo}(\text{dmgH})_2\text{py}$	$\delta 2.40$ (singlet) $\delta 7.03$ - $\delta 8.22$ (several peaks)	dmgH CH_3 groups axial $\text{C}_5\text{H}_5\text{N}$ group

Thin layer chromatography and column chromatography

1. A mixture of $\text{BrCo}(\text{dmgH})_2\text{py}$ and $\text{Br}_2\text{CHCo}(\text{dmgH})_2\text{py}$ is prepared. The composition of this sample is 46.5% $\text{BrCo}(\text{dmgH})_2\text{py}$ and 53.5% $\text{Br}_2\text{CHCo}(\text{dmgH})_2\text{py}$. This is a 1:1 mole mixture of the two complexes and therefore representative of product mixture for the cobaloxime(II)-

bromoform reaction.

Thin layer chromatography (Eastman No. 13181 Silica Gel plates) is performed on the mixture using a variety of eluents. Once a suitable eluent is found, the separation is tried on a column.

Below is a summary of the TLC experiments.

1. 1:1 Ethyl acetate:CHCl₃ - good separation is seen. Tailing in both spots noted, BrCo(dmgh)₂py tailing more than Br₂CHCo(dmgh)₂py.

2. 10:10:3 Ethyl acetate:CHCl₃:EtOH - very poor separation, less tailing than 1:1 ethyl acetate:CHCl₃ (#1).

3. 5:5:2 Ethyl acetate:CHCl₃:CCl₄ - separation similar to 1:1 ethyl acetate:CHCl₃ (#1), tailing similar to 1:1 ethyl acetate:CHCl₃ (#1).

4. 1:1 CH₂Cl₂:Ethyl acetate - two spots are noted but separation is not clean, tail of first spot overlaps with head of second.

5. 1:1:1 Ethyl acetate:CHCl₃:CCl₄ - two spots again are noted. Separation is better than 1:1 CH₂Cl₂:ethyl acetate (#4) but not as good as 1:1 ethyl acetate:CHCl₃ (#1) or 5:5:2 ethyl acetate:CHCl₃:CCl₄ (#3). Tail of first spot may overlap with head of second.

6. 2:1 Ethyl acetate:CHCl₃ - separation similar to 1:1 ethyl acetate:CHCl₃ (#1) with more severe tailing in BrCo(dmgh)₂py spot.

7. 2:1 CHCl₃:Ethyl acetate - separation better than 2:1 ethyl acetate:CHCl₃ (#6) comparable to 1:1 mixture of same (#1). Tailing is notably less than other solvent systems above.

8. 2:2:1 Ethyl acetate:CHCl₃:MeOH - no separation.

9. 2:2:1 Ethyl acetate:CHCl₃:EtOH - slightly better than 2:2:1

ethyl acetate:CHCl₃:MeOH (#8) but spots still overlap.

10. 2:2:1 Ethyl acetate:CHCl₃:i-PrOH - better than EtOH substituted system (#9) but separation still poor at best.

The net result of the TLC work is that the 2:1 CHCl₃:ethyl acetate eluent be used in the column chromatography.

An ion exchange column is employed. A slurry of silica gel (Baker 40-140 mesh) in CHCl₃ is prepared and poured into the ion exchange column. CHCl₃ containing increasing amounts of ethyl acetate is run through the column until the liquid phase of the column is a 2:1 CHCl₃:ethyl acetate mixture.

A sample of the known BrCo(dmgh)₂py/Br₂CHCo(dmgh)₂py mixture (~.15 g) is dissolved in the eluent (20 mL + 3 mL CH₂Cl₂) and loaded onto the column. Elution was then started with 2:1 CHCl₃:ethyl acetate at a 1 drop per second rate.

No separation is observed during elution. A long, smeared band develops in the column, bright yellow at the head, dull brown at the tail. Proton NMR indicates the head of the band to contain mostly CHBr₂Co(dmgh)₂py (singlet at δ2.18) while the tail contains mostly BrCo(dmgh)₂py (singlet at δ2.36). Intermediate fractions off column show a mixture of the cobaloximes(III).

Repetition of this procedure using a variety of elution rates (very fast to very slow) failed to produce a separation of bands. 2:1 CHCl₃:ethyl acetate eluent abandoned.

11. In order to better understand the BrCo(dmgh)₂py/Br₂CHCo(dmgh)₂py system, the BrCo(dmgh)₂py/CH₃Co(dmgh)₂py system is examined. Below is a

summary of the TLC work.

1. 2:2:1 Ethyl acetate:CHCl₃:MeOH - very little separation.
Solvent:5.2 cm R_f (CH₃Co(dmgh)₂py):0.904 R_f (BrCo(dmgh)₂py):0.846.
2. 2:2:1 Ethyl acetate:CHCl₃:MeOH (freshly prepared and with paper envelope in TLC chamber) - very little separation. Solvent:5.1
R_f(CH₃):0.781 R_f(Br):0.754.
3. 2:2:1 Ethyl acetate:CHCl₃:EtOH (with paper envelope) - better than 1 or 2 but tail of first spot overlaps with head of second.
Solvent:5.5 cm. R_f(CH₃) = 0.828 R_f(Br) = 0.727.
4. 2:2:1 Ethyl acetate:CHCl₃:i-PrOH: comparable to 2:2:1 ethyl acetate:CHCl₃:MeOH (#1). Solvent:6.2 cm R_f(CH₃):0.734 R_f(Br):0.661.
5. 40% CCl₄ in i-PrOH: fair separation, tailing in BrCo(dmgh)₂py spot. Solvent:6.0 cm R_f(CH₃):0.750 R_f(Br):0.608.
6. 40% CCl₄ in EtOH: poorer than #5, 40% CCl₄ in i-PrOH. Overlap of bands. Solvent:5.3 cm R_f(CH₃):0.887 R_f(Br):0.792.
7. 50% CCl₄ in i-PrOH: slightly better than 40% mixture, #5.
Solvent:5.4 cm R_f(CH₃):0.870 R_f(Br):0.722.
8. 60% CCl₄ in i-PrOH: better than 50% mixture, #7. Solvent:5.2 cm R_f(CH₃):0.837 R_f(Br):0.644.
9. 70% CCl₄ in i-PrOH: better than 60% mixture, #8. Solvent:5.1 cm R_f(CH₃):0.843 R_f(Br):0.618.
10. 85% CCl₄ in i-PrOH: better than 70% mixture. Solvent:5.7 cm R_f(CH₃):0.632 R_f(Br):0.342.
11. 85% CCl₄ in EtOH: comparable to 85% CCl₄ in i-PrOH, spots

move more rapidly along plate than with i-PrOH mixture. Solvent: 4.9 cm
 $R_f(\text{CH}_3^-):0.735$ $R_f(\text{Br}):0.531$.

A dilute ethanolic solution in CCl_4 is decided upon as eluent. Further TLC work is now performed on the dibromomethyl(pyridine)-cobaloxime(III).

12. R_f values of CH_3^- , BrCH_2^- and $\text{CHBr}_2\text{Co}(\text{dmgH})_2\text{py}$ in 10% EtOH in CCl_4 . Solvent: 6.0 cm $R_f(\text{CH}_3^-):0.533$ $R_f(\text{BrCH}_2^-):0.500$ $R_f(\text{CHBr}_2):0.467$.

The following are now separations (TLC) of $\text{Br}_2\text{CHCo}(\text{dmgH})_2\text{py}$ and $\text{BrCo}(\text{dmgH})_2\text{py}$.

13. 10% EtOH in CCl_4 . Clean separation not achieved, overlapping of spots noted. Solvent: 5.4 cm $R_f(\text{Br}_2\text{CHCo}(\text{dmgH})_2\text{py}):0.537$
 $R_f(\text{BrCo}(\text{dmgH})_2\text{py}):0.370$.

14. 10:1:1 CCl_4 :EtOH:Ethyl acetate - Separation is cleaner than eluent without ethyl acetate, #13, but overlapping still noted.

15. Neat CCl_4 : no movement of $\text{Br}_2\text{CHCo}(\text{dmgH})_2\text{py}$ or $\text{BrCo}(\text{dmgH})_2\text{py}$.

16. 5% EtOH in CCl_4 : good separation. Solvent 5.0 cm.
 $R_f(\text{CHBr}_2):0.470$ $R_f(\text{Br}):0.200$.

17. 5% CH_2Cl_2 in CCl_4 : no movement of $\text{Br}_2\text{CHCo}(\text{dmgH})_2\text{py}$ or $\text{BrCo}(\text{dmgH})_2\text{py}$. TLC final results: Use 4% EtOH in CCl_4 on column.

Column chromatography A four foot 3/4" glass column is packed with silica gel (Baker 40-140 mesh) - 4% EtOH in CCl_4 slurry.

0.1405 g of a 1:1 mole composition mixture of $\text{BrCo}(\text{dmgH})_2\text{py}$ and $\text{Br}_2\text{CHCo}(\text{dmgH})_2\text{py}$ is dissolved in 8 mL 4% EtOH in CCl_4 and 2 mL CH_2Cl_2 . The liquid is loaded onto the column and eluted with 4% EtOH in CCl_4 at the rate of 1 drop/3 second (exiting the column).

Two bands develop. A yellow band, identified as $\text{Br}_2\text{CHCo}(\text{dmgH})_2\text{py}$ by proton NMR (singlet at $\delta 2.21$), elutes first off column followed by a brown band, identified as $\text{BrCo}(\text{dmgH})_2\text{py}$ (singlet at $\delta 2.40$). No yields taken.

Identification of Products of $\text{Co}(\text{dmgH})_2\text{py} + \text{CHBr}_3$
Reaction in C_6H_6

50 mL C_6H_6 is deoxygenated thoroughly with argon in a 1 neck 100 mL round bottom flask. 2.461 g (5.59 mmole) $\text{Co}(\text{dmgH})_2\cdot 2\text{py}$ is added and dissolved by stirring. 8.0 mL (91.5 mmole) deoxygenated CHBr_3 is added with stirring.

After 30 minutes, the reaction mixture is added to 170 mL hexanes in a single neck 500 mL round bottom flask. The volume is reduced to one-half its original by rotovapping. 80 mL hexanes is then added back and the precipitate filtered and washed with 150 mL hexanes. Thorough drying is achieved by storing under vacuum overnight. Yield: 2.495 g.

Proton NMR of yellow brown product mixture shows two singlets in region of interest, $\delta 2.40$ and $\delta 2.19$. Peak height ratio is 71%, the $\delta 2.40$ peak the taller.

0.2872 grams of product is dissolved in 15 mL 4% EtOH in CCl_4 , 5 mL CH_2Cl_2 , and 0.5 mL EtOH. It is loaded onto a four foot, $3/4$ " wide silica gel column, 4% EtOH in CCl_4 being the mobile phase.

Elution with 4% EtOH in CCl_4 is begun at the rate of 1 drop per second. Two bands develop. Separation is approximately 23 cm. The first yellow band is collected as a 100 mL fraction.

After complete elution of the yellow band, the brown band is eluted

off with 25% EtOH in CCl_4 first, followed by 1:1 EtOH: CCl_4 when approximately half the band collected. Total volume of fraction is 500 mL.

Both fractions are rotovapped dry.

Yellow band analyzes as follows: δ 2.22 singlet and δ 5.75 single in ^1H NMR: C,H,N analysis: 30.79% C, 3.74% H, 12.64% N. For $\text{CHBr}_2\text{Co}(\text{dmgH})_2\text{py}$: δ 2.18 + δ 5.71 singlets in ^1H NMR. C,H,N expected 31.1% C, 3.73% H, 12.94% N.

Brown band analysis: δ 2.41 singlet in ^1H NMR. C,H,N analysis: 35.34% C, 4.54% H, 15.58% N. For $\text{BrCo}(\text{dmgH})_2\text{py}$: δ 2.40 singlet in ^1H NMR C,H,N expected: 34.8% C, 4.27% H, 15.6% N.

Result

Cobaloxime(II) reaction with CHBr_3 yields only two products, dibromomethylcobaloxime(III) and bromocobaloxime(III).

Unsuccessful Syntheses of Trihalomethylcobaloximes(III)

Conversion of $\text{XCo}(\text{dmgH})_2\text{py}$ to charged cobaloxime(III) complex with Ag^+

To facilitate the separation of $\text{CX}_3\text{Co}(\text{dmgH})_2\text{py}$ and $\text{XCo}(\text{dmgH})_2\text{py}$, attempts were made to convert $\text{XCo}(\text{dmgH})_2\text{py}$ to a charged complex such as $\text{H}_2\text{OCo}(\text{dmgH})_2\text{py}^+$.

Addition of AgNO_3 to suspensions of $\text{ClCo}(\text{dmgH})_2\text{py}$ in absolute EtOH resulted in little or no formation of AgCl over a period of seven hours. In $(\text{CH}_3)_2\text{CO}$ or CH_3NO_2 , formation of a white precipitate occurred within the first 10 minutes of mixing. After 1 hour of stirring, conversion appeared complete. After filtration through Celite, evaporation of solvent yielded a very pale brown powder. Digestion in concentrated

HNO_3 revealed AgCl to be present in brown product. No analyses were done to determine nature of brown product.

Addition of AgNO_3 to a mixture of $\text{CCl}_3\text{Co}(\text{dmgH})_2\text{py}/\text{ClCo}(\text{dmgH})_2\text{py}$ apparently destroys the organocobaloxime(III) as ^1H NMR of the final product mixture (after filtration through Celite and removal of solvent ($\text{CH}_3)_2\text{CO}$ or CH_3NO_2) shows no signal at $\delta 2.20$. Further attempts along these lines were not tried.

Ag_2O synthesis

Attempts to extend the synthesis for $\text{NO}_2\text{CH}_2\text{Co}(\text{dmgH})_2\text{py}$ to $\text{CX}_3\text{Co}(\text{dmgH})_2\text{py}$ failed.

Following the procedure of Randaccio et al.,⁶⁰ substituting CHI_3 for CH_3NO_2 and using either C_6H_6 or $\text{C}_6\text{H}_5\text{NO}_2$ as solvent, no $\text{Cl}_3\text{Co}(\text{dmgH})_2\text{py}$ was detected even after 72 hours of reaction.

Zn reduction method and Schrauzer methods

Both of these methods proved unfruitful. The Zn reduction method¹⁸ yielded a mixture of $\text{ClCo}(\text{dmgH})_2\text{py}$ and $\text{CCl}_3\text{Co}(\text{dmgH})_2\text{py}$ after several hours of reaction employing a large excess of Zn powder.

The Schrauzer method¹⁷ produced the expected mixture of $\text{ClCo}(\text{dmgH})_2\text{py}$ and $\text{CCl}_3\text{Co}(\text{dmgH})_2\text{py}$, as evidenced by proton NMR.

Washing with 250 mL H_2O resulted in minimal enrichment of the organocobaloxime(III).

Further syntheses of $\text{CX}_3\text{Co}(\text{dmgH})_2\text{py}$ were not tried.

Stoichiometry of the $\text{ClCo}(\text{dmgH})_2\text{PPh}_3/\text{C}_5\text{H}_5\text{N}$ and $\text{ClCo}(\text{dmgH})_2\text{PPh}_3/4\text{-CH}_3\text{C}_5\text{H}_4\text{N}$ reactions

In a benzene solution, $\text{ClCo}(\text{dmgH})_2\text{PPh}_3$ exhibits a shoulder at $\lambda 480$ nm ($\epsilon=240 \text{ M}^{-1} \text{ cm}^{-1}$) and a peak at $\lambda 318$ nm ($\epsilon=2240 \text{ M}^{-1} \text{ cm}^{-1}$). Addition of an excess of pyridine results in the loss of the shoulder at $\lambda 480$ nm. The effect of pyridine on the $\lambda 318$ nm maximum was not examined. Addition of an excess of 4-picoline produces a similar effect upon the $\text{ClCo}(\text{dmgH})_2\text{PPh}_3$ spectrum.

Spectral titrations were performed to determine the stoichiometry of the reactions. Loss of the shoulder at $\lambda 480$ nm was used to monitor the titration. For the pyridine reaction, two values obtained were 0.970 and 1.020, their average 0.995 ± 0.035 . The 4-picoline reaction gave three values, 1.000, 1.020, and 1.020, for an average value of 1.013 ± 0.012 . In all cases, a sharp break was not seen in the titration plots but rather a sweeping curve was noted about the region of the end-point, indicative of an equilibrium condition.

Kinetics

Conventional methods

Carbon tetrachloride reactions Stock solutions of reagents were prepared as follows.

Cobaloxime(II) reagents The desired amount of the cobaloxime(II) complex is measured out and added to a volumetric flask, usually 50 or 100 mL in size. The flask is fitted with a rubber septum and attached to an inert gas line. The flask is then purged 45 minutes with a strong flow of argon. The desired solvent, previously

deoxygenated 1.5 hours by passing argon through the neat liquid, is then added to the volumetric flask by use of a transfer needle. Thorough mixing of the cobaloxime(II) solution is achieved by briefly (20 seconds) passing a mild flow of argon through the solution. A positive pressure of argon is maintained above the solution by removing the exit needle from the flask and keeping the flask attached to the inert gas line. After one hour, a fresh stock solution is prepared in the manner just described.

Carbon tetrachloride solutions Two reagent solutions were employed in these experiments. Use of either type of solution gave identical results.

The first stock solution of carbon tetrachloride is the neat liquid itself. Approximately 40 ml of the neat reagent is transferred to a small amber tinted bottle. The bottle is fitted with a rubber septum and the liquid is deoxygenated by passing a mild argon flow through the liquid for one hour. When not in use, the bottle is left attached to the inert gas line. A value of 10.14 M is used as the concentration of the neat reagent. The concentration in the reaction cell is calculated by appropriate dilution expression $M_1V_1 = M_2V_2$ and knowing the volume of carbon tetrachloride injected and the final volume the cell contained.

The second stock solution is a dilute carbon tetrachloride solution in acetone. This stock solution was used only for the triphenylphosphinecobaloxime(II) reactions in acetone.

A Barnes dropping bottle is fitted with a rubber septum and weighed

accurately. Approximately 28 mL of acetone is added and the liquid is deoxygenated 30 minutes with a strong flow of argon. The bottle is reweighed and the difference in weight is the weight of acetone in the bottle. Using 0.7852 g/mL as the density of acetone, the volume of acetone is calculated. A known volume of deoxygenated carbon tetrachloride is added by syringe to the bottle. This volume is totalled with the volume of acetone already in the bottle to give the final volume. The bottle is weighed a third time to give the weight of carbon tetrachloride added. The concentration of carbon tetrachloride is then calculated. Concentration in the reaction cell is calculated in a manner identical to the case where neat carbon tetrachloride is used.

Kinetic measurements A Cary 219 spectrophotometer equipped with a constant temperature cell holder was employed to monitor the reaction between cobaloxime(II) and carbon tetrachloride. The decrease in absorbance due to the loss of cobaloxime(II) was followed either by single wavelength monitoring or by overlay spectra. The latter method was used only in the study of slower reactions, i.e., low concentrations of carbon tetrachloride.

The monitoring wavelength, in the case of a single wavelength followed with time, varied with the nature of the axial ligand on the cobaloxime(II) and the solvent and corresponded to the maximum exhibited by the cobaloxime(II) reagents. The following wavelengths were used in acetone: λ_{460} nm, triphenylphosphine complex; λ_{420} nm, pyridine complex; and λ_{420} nm, 4-picoline complex. In benzene, the monitoring wavelengths were λ_{460} nm, triphenylphosphine complex; λ_{430} nm pyridine complex; and

$\lambda 430$ nm 4-picoline complex. When overlay spectra monitoring was employed, the scans usually covered the range $\lambda 600$ nm to $\lambda 400$ nm or $\lambda 380$ nm.

Reaction cells were prepared in a variety of ways, the variation arising in the order of components added. Identical results were obtained regardless of the order of additions. The most common and preferred preparation is outlined below.

2.0 cm quartz cells were deoxygenated by passing argon vigorously through them for one hour. 5.4 mL of deoxygenated solvent is added by syringe to the quartz cell. The required microliter amount of carbon tetrachloride is added to the cell next. When dilute carbon tetrachloride solutions were employed, less pure solvent was added to the cell in lieu of that added when the dilute carbon tetrachloride was injected to the cell.

The quartz cell now with solvent and carbon tetrachloride is placed in the thermostatted cell holder in the Cary 219 spectrophotometer. For room temperature runs, the cell was allowed to sit in the cell holder for 25 minutes. Higher or lower temperature runs saw the quartz cell resting in the cell holder for 45 minutes.

After sufficient time thermostating, 0.6 mL of the cobaloxime(II) reagent is injected into the Cary cell and the cell is shaken two or three times to ensure thorough mixing. The decrease in absorbance at the appropriate wavelength is then monitored until the reaction has reached an apparent infinity value of absorbance. Due to a slow secondary reaction, the absorbance at infinity tends to drift slowly

downward.

Data analyses Several methods of analysis were used to interpret the pseudo-first-order rate data obtained.

Early runs were analyzed by first submitting the data to a Kedzy-Swinbourne analysis to obtain D_{∞} . A step size of 1.4-1.6 half lives was used in this analysis. Suitable $\ln(D_t - D_{\infty})$ vs. time plots were then made using this value of D_{∞} .

Later runs were analyzed by computer analysis, using either a D_{∞} obtained in the manner above, or by computer. The data were then analyzed by use of least squares fitting program.

Second order rate constants were obtained by making plots of k_{obs} vs. concentration of carbon tetrachloride. Refinement of the rate constant was achieved by least squares analysis. The final value of k_1 is found by dividing the value obtained from least squares analysis by two.

Pseudo-first-order rate plots were linear through three half lives or better. Plots of k_{obs} vs. $[RX]$ were also linear and passed through the origin.

Bromoform reactions These reactions were followed in a manner identical to the carbon tetrachloride reactions with the following exceptions:

- (1) Neat bromoform was used in all cases. A value of 11.44 M was used for the concentration of the neat liquid.
- (2) Data in some instances were collected directly into the computer used for analyses and stored on disk.

Scavenging in the carbon tetrachloride reactions The details for experiments of this nature are identical to the experiments done without any scavenging agents present with the following additions.

Scavenging agents were added after addition of carbon tetrachloride but prior to addition of cobaloxime(II) In the case of solid scavenging agents, highly concentrated stock solutions were prepared in the same manner used to prepare the cobaloxime(II) stock solutions. In the make-up of the reaction cells, less solvent was added to the cell to compensate for that solvent brought in by injection of the scavenging agent solution. This method was used for the scavenging agents α -phenyl-N-t-butyl nitroxide and 4-hydroxy-2,2,6,6-tetramethylpiperidinoxy.

For liquid reagents, such as 1-octene, di-N-t-butyl nitroxide, acrylonitrile, and 1,3-cyclohexadiene, the neat liquid or stock solution, after deoxygenation with argon, was injected into the reaction cell. Concentrations then were calculated as follows:

1. 1-Octene. A molarity of 6.37 M was calculated for the neat liquid and used in the dilution calculations.
2. Di-t-butyl nitroxide. A concentrated stock solution, 1.50 M in concentration was prepared by addition of 1.079 g of the liquid into a 5.0 mL volumetric flask followed by addition to mark with solvent.
3. Acrylonitrile. A molarity of 15.19 M was calculated for the neat reagent.
4. 1,4-Cyclohexadiene. A molarity of 10.57 M was calculated for the neat reagent.

In some runs with low concentrations ($<1.5 \times 10^{-4}$ M) of 4-hydroxy-2,2,6,6-tetramethylpiperidinoxy, the scavenging agent and cobaloxime(II) were prepared as a single stock solution, i.e., both solids were added to the same flask. The results obtained were identical to runs of same scavenging agent concentration where two separate stock solutions were prepared.

Flash photolysis initiated reactions

BrCCl₃ and CBr₄ reactions with cobaloxime(II) Stock solutions of isopropyl(pyridine)cobaloxime(III) were prepared by adding the desired amount of the complex to a volumetric flask (usually .02 g in a 250 mL flask). The flask with solid is thoroughly deoxygenated with argon followed by addition of deoxygenated benzene via transfer needle. Alternatively, benzene is added to the flask, deoxygenated for one hour, the cobaloxime(III) reagent then added, and deoxygenation for 20 additional minutes. In the event of any loss of benzene during deoxygenation, it is compensated for by addition of deoxygenated benzene by syringe to mark. The flask is wrapped in foil at all times the organocobaloxime(III) is in solution.

BrCCl₃ was deoxygenated as the neat liquid. CBr₄ stock solutions were prepared similarly to the organocobaloxime(III) stock solutions. Solutions of molarity approximately 1.5 M were prepared. 1-Octene was deoxygenated as the neat liquid.

Reaction cells were prepared by adding 6.0 mL of the organocobaloxime(III) solution to a thoroughly deoxygenated (one hour sweep

with argon) quartz cell. The polyhalogenomethane was then added by microsyringe, followed by 1-octene if desired. The quartz cell is then wrapped in foil until transported to a constant temperature water bath.

After 35 minutes of thermostating, the quartz cell is quickly moved to the cell holder of the flash photolysis unit. A 25.6 J flash (of unfiltered UV-visible radiation from fast extinguishing Xenon flash lamps in the Xenon Corporation's Model 710 system)⁶¹ is then applied and the increase in transmittance due to loss of cobaloxime(II) (formed in the flash) is recorded on the oscilloscope. Percent transmittance is converted to absorbance by application of appropriate formulas. First-order rate constants were obtained by least squares analysis. Second-order rate constants were also obtained by least squares analysis of a plot of k_{obsd} vs. concentration of polyhalogenomethane.

Test reactions employing carbon tetrachloride in place of the brominated analogs were performed in a similar manner, only the quartz cell was transferred to a Cary 219 spectrophotometer to follow the absorbance decrease. Results agreed well with the values obtained by conventional means.

The amount of cobaloxime(II) produced in the flash was determined by repeating the above experiments with no polyhalogenomethane present. The visible spectrum was recorded before and after the flash. Using the following epsilon values, $3554 \text{ M}^{-1} \text{ cm}^{-1}$ for (pyridine)cobaloxime(II) and $1450 \text{ M}^{-1} \text{ cm}^{-1}$ for isopropyl(pyridine)cobaloxime(III), the amount of (pyridine)cobaloxime(II) was calculated.

Activation parameters

Kinetic measurements were made following the details already presented at the desired temperatures. For low temperature runs on the Cary 219 spectrophotometer, dry nitrogen was swept through the cell holder area to prevent fogging of the quartz windows.

Data analyses were handled by submitting the results obtained to computer fitting, using the Eyring equation as fit.

Determination of molar absorptivities for absorbing species in (pyridine)cobaloxime(III) - carbon tetrachloride-4-hydroxy-2,2,6,6-tetramethylpiperidinoxy - benzene system

Kinetic measurements following the procedures outlined earlier were performed. The data collected were submitted to least squares analysis. Rate constants obtained agreed well with the expected values and D_{∞} also agreed well between calculated and experimental values.

Several sets of kinetic runs were done, a range of carbon tetrachloride concentrations being covered. The first set of data obtained involved only runs where no scavenger was employed. The critical value desired in these runs is ΔD , the overall change in absorbance for the kinetic run. A total of 18 runs were done, the value of ΔD falling in the range 1.1 to 1.2 absorbance, the average value being 1.148 ± 0.024 for the experimental trace and 1.157 ± 0.040 for the computer calculation.

The following expression (41) was then used to calculate the sum

$$\epsilon_{Cl(Co)py} + \epsilon_{CCl_3(Co)py} = 2 \cdot \epsilon_{(Co)py} - \frac{2\Delta D}{b \cdot [(Co)py]} \quad (41)$$

of the epsilons for chloro(pyridine)cobaloxime(III) and

trichloromethyl(pyridine)cobaloxime(III). b is the cell path length (2.0 cm in the actual experiment) and the epsilon for (pyridine)-cobaloxime(II) in benzene was measured independently at $3646 \pm 61 \text{ M}^{-1} \text{ cm}^{-1}$. The concentration of (pyridine)cobaloxime(II) was held constant at $1.980 \times 10^{-4} \text{ M}$ for all runs.

Using $\Delta D(\text{expt})$ gave a value $1493 \pm 120 \text{ M}^{-1} \text{ cm}^{-1}$ for the sum of the epsilons and $\Delta D(\text{calc})$ gave a value of $1449 \pm 201 \text{ M}^{-1} \text{ cm}^{-1}$. The average of these two values, $1471 \pm 161 \text{ M}^{-1} \text{ cm}^{-1}$, was used as the sum of the epsilons.

A second set of experiments employing very high concentration of 4-hydroxy-2,2,6,6-tetramethylpiperidinoxy so that it contributed a constant background was also done. These data were analyzed as above and gave the following ΔD values: $1.048 \pm .019$ for the experimental traces and $1.041 \pm .015$ for the calculated values.

Expression 2 was then used to calculate the epsilon for chloro-(pyridine)cobaloxime(III).

$$\epsilon_{Cl(Co)py} = \frac{D_{(Co)py} - \Delta D}{b \cdot [(Co)py]_0} \quad (42)$$

Again, all runs employed $[(Co)py]_0 = 1.981 \times 10^{-4} \text{ M}$ and a 2.0 cm cell.

Using expression 42 gave the following values for the epsilon of chloro(pyridine)cobaloxime(III) in benzene: $670 \pm 38 \text{ M}^{-1} \text{ cm}^{-1}$ (expt) and $693 \pm 48 \text{ M}^{-1} \text{ cm}^{-1}$ (calc). The average value is $682 \pm 43 \text{ M}^{-1} \text{ cm}^{-1}$.

The epsilon for trichloromethyl(pyridine)cobaloxime(III) was determined by subtracting the result from the second set of experiments

from the first set of experiments. A value of $789 \pm 167 \text{ M}^{-1} \text{ cm}^{-1}$ was found.

4-hydroxy-2,2,6,6-tetramethylpiperidinoxy was found to have an epsilon of $9.4 \pm 0.2 \text{ M}^{-1} \text{ cm}^{-1}$ by measuring the absorbance of solutions of known concentration.

Repeated measurements for (pyridine)cobaloxime(II) gave a final epsilon of $3554 \pm 72 \text{ M}^{-1} \text{ cm}^{-1}$ for the complex in benzene.

Mathematical modeling of the reaction sequence represented by equations 30-32

The data from experiments involving 4-HTMPO as a competitor/scavenger for the trichloromethyl radical intermediate were compared and contrasted with simulated data. The GEAR routine,^{46,47} a predictor-corrector forward integration system solver, was used to generate data based on the mechanism proposed in equations 30-32. All computations were performed on an IBM 3600 computer.

Two sets of computations were done. The first was designed to determine the k_3/k_2 ratio. The second was to compare actual and simulated absorbance curves.

For both sets of computations, the (pyridine)cobaloxime(II) reaction with carbon tetrachloride in benzene was selected as the system to be modeled. The necessary parameters were $k_1 = 0.558 \text{ M}^{-1} \text{ s}^{-1}$ (experimentally determined) and $k_2 = 8.0 \times 10^7 \text{ M}^{-1} \text{ s}^{-1}$ (arbitrarily selected). Several sets of data were then generated by varying the value of k_3 . Values used were 1.0, 1.2, 1.4, 1.5, and $1.6 \times 10^8 \text{ M}^{-1} \text{ s}^{-1}$. Concentrations of reactants were held fixed at one particular set of values

throughout these computations so that only the effect due to variation in k_3 could be observed.

The simulated data produced by these computer runs were then subjected to the same analyses as the experimental data. The analyzed computer data were then plotted on the same curve (Figure III-5) as the analyzed experimental data. Simple observation led to the best fit ratio of k_3/k_2 .

The second set of computations involved taking the ratio of k_3/k_2 as 1.8 and generating several data sets using actual experimental concentrations of reactants and then comparing the computer generated and experimental absorbance vs. time curves. Excellent agreement was observed in most cases further supporting the k_3/k_2 ratio as 1.8.

REFERENCES

1. Bury, A.; Cooksey, C. J.; Funabiki, T.; Gupta, B. D.; Johnson, M. D. *J. C. S. Perkin Trans. 2* 1979, 1050
2. Crease, A. E.; Gupta, B. D.; Johnson, M. D.; Bialkowska, E.; Duong, K. N. V.; Gaudemer, A. *J. C. S. Perkin Trans. 1* 1979, 2611
3. Veber, M.; Duong, K. N. V.; Gaudemer, A.; Johnson, M. D. *J. Organomet. Chem.* 1981, 209, 393
4. Schrauzer, G. N. *Acc. Chem. Res.* 1968, 1, 97
5. Pratt, J. M. "Inorganic Chemistry of Vitamin B₁₂"; Academic Press: London, 1972
6. Schrauzer, G. N. *Inorg. Synth.* 1968, 11, 61
7. Randaccio, L.; Bresciani-Pahor, N.; Toscano, P. S.; Marzilli, L. G. *Inorg. Chem.* 1981, 20, 2722
8. Halpern, J.; Maher, J. *J. Am. Chem. Soc.* 1964, 86, 2311
9. Kwiatek, J.; Seyler, J. *J. Organomet. Chem.* 1965, 3, 421
10. Kwiatek, J.; Seyler, J. *J. Organomet. Chem.* 1965, 3, 433
11. Goh, S. H.; Goh, L.-Y. *J. Organomet. Chem.* 1972, 43, 401
12. Goh, L.-Y. *J. Organomet. Chem.* 1975, 88, 249
13. Halpern, J.; Maher, J. P. *J. Am. Chem. Soc.* 1965, 87, 5361
14. Chock, P. B.; Halpern, J. *J. Am. Chem. Soc.* 1969, 91, 582
15. Schneider, P. W.; Phelan, P. F.; Halpern, J. *J. Am. Chem. Soc.* 1969, 91, 77
16. Halpern, J.; Phelan, P. F. *J. Am. Chem. Soc.* 1972, 94, 1881
17. Schrauzer, G. N.; Ribeiro, A.; Lee, L. P.; Ho, R. K. Y. *Angew. Chem. Internat. Edit.* 1971, 10, 807
18. Roussi, P. F.; Widdowson, D. A. *J. C. S. Chem. Comm.* 1979, 810
19. Pinault, F. S.; Crumbliss, A. L. *J. Organomet. Chem.* 1981, 215, 229
20. Blaser, H. V.; Halpern, J. *J. Am. Chem. Soc.* 1980, 102, 1684

21. Marzilli, L. G.; Marzilli, P. A.; Halpern, J. J. Am. Chem. Soc. 1970, 93, 1374
22. Espenson, J. H.; Tinner, U. J. Organomet. Chem. 1981, 212, C43
23. Anet, F. A. L.; LeBlanc, E. J. Am. Chem. Soc. 1957, 79, 2649
24. Kochi, J. K.; Davis, D. D. J. Am. Chem. Soc. 1964, 86, 5264
25. Coombes, R. G.; Johnson, M. D.; Winterton, N. J. Chem. Soc. 1965, 7029
26. Dodd, D.; Johnson, M. D. J. Chem. Soc. (A) 1968, 34
27. Sevcík, P.; Jakubcová, D. Collection Czechoslov. Chem. Commun. 1977, 42, 1767
28. Sevcík, P. Inorg. Chim. Acta 1979, 32, L16
29. Pohl, M. C.; Espenson, J. H. Inorg. Chem. 1980, 19, 235
30. Marty, W.; Espenson, J. M. Inorg. Chem. 1979, 18, 1246
31. Kochi, J. K.; Mocadlo, P. E. J. Am. Chem. Soc. 1966, 88, 4094
32. Kochi, J. K.; Powers, J. W. J. Am. Chem. Soc. 1970, 92, 137
33. Samuels, G. J.; Espenson, J. H. Inorg. Chem. 1979, 18, 2587
34. Samuels, G. J.; Espenson, J. H. Inorg. Chem. 1980, 19, 233
35. Lal, D.; Giller, D.; Husband, S.; Ingold, K. V. J. Am. Chem. Soc. 1974, 96, 6355
36. Kochi, J. K.; Krusic, P. J.; Eaton, D. R. J. Am. Chem. Soc. 1969, 91, 1877
37. Crease, A. E.; Gupta, B. D.; Johnson, M. D.; Moorhouse, S. J. C. S. Dalton 1978, 1821
38. Crease, A. E.; Johnson, M. D. J. Am. Chem. Soc. 1978, 100, 8013
39. Ashcroft, M. R.; Bury, A.; Cooksey, C. J.; Davies, A. G.; Gupta, B. D.; Johnson, M. D.; Morris, H. J. Organomet. Chem. 1980, 195, 89
40. Bougeard, P.; Gupta, B. D.; Johnson, M. D. J. Organomet. Chem. 1981, 206, 211
41. Bougeard, P.; Johnson, M. D. J. Organomet. Chem. 1981, 206, 221

42. Dodd, D.; Johnson, M. D.; Lockman, B. L. *J. Am. Chem. Soc.* 1977, 99, 3664
43. Halpern, J. *Pure Appl. Chem.* 1979, 51, 2171
44. Dodd, D.; Johnson, M. D. *Organometallic Chemistry Review*, 1973, 52, 1
45. Janzen, E. G.; Evans, C. A.; Davis, E. R. in "Organic Free Radicals", Pryor, W. A., Ed.; ACS Press: Washington, D.C., 1978; Chapter 26
46. Gear, C. W. "Numerical Initial Value Problems in Ordinary Differential Equations"; Prentice-Hall: Englewood Cliffs, N.J., 1971
47. Hindmarsh, A. C. "GEAR: Ordinary Differential Equation System Solver"; Lawrence Livermore Laboratory, Report UCID-300001(3), 1974
48. Huber, W. "Titrations in Non-Aqueous Solvents"; Academic Press: New York, 1967
49. Jaffe, H. H.; Doak, G. O. *J. Am. Chem. Soc.* 1955, 77, 4441
50. Mendenhall, G. D.; Golden, D. M.; Benson, S. W. *J. Phys. Chem.* 77, 2707 (1973)
51. Furuyama, S.; Golden, D. M.; Benson, S. W. *J. Am. Chem. Soc.* 91, 7564 (1969)
52. King, K. D.; Golden, D. M.; Benson, S. W. *J. Phys. Chem.* 75, 987 (1971)
53. Nigam, S.; Asmus, K.-D.; Willson, R. L. *J. Chem. Soc., Faraday Trans. 1* 1976, 2324
54. Roche, T. S.; Endicott, J. F. *Inorg. Chem.* 1974, 13, 1515
55. Tait, A. M.; Hoffman, M. L.; Hayon, E. *Int. J. Radiat. Phys. Chem.* 1976, 8, 691
56. Elroi, H.; Meyerstein, D. *J. Am. Chem. Soc.* 1978, 100, 5540
57. Thomas, J. K. *J. Phys. Chem.* 1967, 71, 1919
58. Yamazaki, N.; Hohokabe, Y. *Bull. Chem. Soc. Jpn.* 1971, 44, 63
59. Burkhardt, E. W.; Burmeister, J. L. *Inorg. Chim. Acta.* 1978, 27, 115
60. Randaccio, L.; Bresciani-Pahor, N.; Toscano, P. J.; Marzilli, L. G. *Inorg. Chem.* 1981, 20, 2722
61. Ryan, D. A. Ph.D. Thesis, Iowa State University, 1981

APPENDIX. SUPPLEMENTAL DATA

Table III-A-1. Kinetic data^a for the reaction of CCl_4 and $\text{Co}(\text{dmgH})_2\text{PPh}_3$ at 25.0°C in acetone

$10^3[\text{CCl}_4]/$ $\underline{\text{M}}$	$10^3k_{\text{obs}}/$ s^{-1}	$k_1^b/$ $\underline{\text{M}}^{-1} \text{s}^{-1}$	$10^3[\text{CCl}_4]/$ $\underline{\text{M}}$	$10^3k_{\text{obs}}/$ s^{-1}	$k_1^b/$ $\underline{\text{M}}^{-1} \text{s}^{-1}$
4.98	2.88	0.289	(35.0	23.3	0.333) ^c
5.08	3.20	0.315	35.3	21.6	0.306
5.10	3.30	0.324	42.7	26.8	0.314
(5.15	3.25	0.315) ^c	46.8	28.1	0.300
5.23	3.30	0.315	47.3	29.6	0.313
8.58	4.99	0.291	48.4	29.7	0.307
17.1	10.5	0.329) ^c	51.2	30.4	0.301
(17.5	11.5	0.329) ^c	51.2	30.4	0.297
18.6	11.5	0.309	(51.2	33.0	0.322) ^c
19.0	11.5	0.303	(52.5	36.0	0.343) ^c
19.3	12.0	0.311	53.7	32.6	0.304
29.0	17.8	0.307	55.1	33.1	0.300
(29.1	19.5	0.335) ^c	60.9	36.2	0.298
29.2	17.6	0.301	68.2	44.9	0.329
29.7	18.1	0.305	(68.2	45.7	0.335) ^c
(34.2	22.8	0.333) ^c	76.7	45.9	0.299
34.7	21.0	0.303	85.1	51.9	0.305
			(90.2	60.5	0.335) ^c

^a $T = 25.00\text{-}25.07^\circ\text{C}$; $[\text{Co}(\text{dmgH})_2(\text{PPh}_3)]_0 = (1.9\text{-}2.5) \times 10^{-4} \underline{\text{M}}$, added as $\text{Co}(\text{dmgH})_2 \cdot 2\text{PPh}_3$.

$$^b k_1 = k_{\text{obs}}/2[\text{CCl}_4].$$

^cLess reliable values are given in parentheses.

Table III-A-2. Kinetic data^a for the reaction of CCl_4 and $\text{Co}(\text{dmgH})_2\text{PPh}_3$ at $T \neq 25^\circ\text{C}$ in acetone

$T/^\circ\text{C}$	$10^3[\text{CCl}_4]/\text{M}$	$10^3k_{\text{obs}}/\text{s}^{-1}$	$k_1^b/\text{M}^{-1}\text{s}^{-1}$
15.74	8.58	2.76	0.161
	(17.1)	7.14	0.209) ^c
	42.4	14.1	0.166
	68.2	22.7	0.166
	85.1	27.1	0.159
34.61	(3.43)	6.84	0.997) ^c
	(6.86)	9.84	0.717) ^c
	8.58	11.9	0.693
	10.3	15.2	0.738
	12.9	17.7	0.686
	17.1	20.1	0.588
	(30.8)	43.8	0.711) ^c
	37.6	44.3	0.589
	42.7	47.8	0.560
	47.8	56.4	0.590
	54.6	62.8	0.575
	68.2	82.2	0.603

^a $T = 25.00\text{--}25.07^\circ\text{C}$; $[\text{Co}(\text{dmgH})_2(\text{PPh}_3)]_0 = (1.9\text{--}2.5) \times 10^{-4} \text{ M}$, added as $\text{Co}(\text{dmgH})_2 \cdot 2\text{PPh}_3$.

$$^b k_1 = k_{\text{obs}}/2[\text{CCl}_4].$$

^cLess reliable values are given in parentheses.

Table III-A-3. Kinetic data^a for the reaction of CCl_4 with $\text{Co}(\text{dmgH})_2\text{PPh}_3$ in benzene

$T/^\circ\text{C}$	$10^3[\text{CCl}_4]/\text{M}$	$10^3k_{\text{obs}}/\text{s}^{-1}$	$k_1^b/\text{M}^{-1}\text{s}^{-1}$
19.67	17.1	2.25	0.0658
	51.2	7.61	0.0743
	85.1	13.6	0.0799
	119	25.9	0.109
	169	27.5	0.0814
25.0	25.7	5.35	0.104
	52.1	11.9	0.114
	78.3	15.5	0.099
	82.3	18.9	0.115
	104	25.0	0.120
	167	34.5	0.103
34.44	8.58	3.08	0.179
	17.1	6.58	0.192
	59.7	23.9	0.200
	85.1	36.3	0.213

^a $T = 25.00\text{--}25.07^\circ\text{C}$; $[\text{Co}(\text{dmgH})_2(\text{PPh}_3)]_0 = (1.9\text{--}2.5) \times 10^{-4}\text{ M}$,
added as $\text{Co}(\text{dmgH})_2 \cdot 2\text{PPh}_3$.

$$^b k_1 = k_{\text{obs}}/2[\text{CCl}_4].$$

Table III-A-4. Kinetic data^a for the reaction of CCl₄ with Co(dmgh)₂py in benzene

T/°C	10 ³ [CCl ₄]/M	10 ³ k _{obs} /M	k ₁ ^b /M ⁻¹ s ⁻¹
10.88	8.58	2.93	0.171
	25.7	8.44	0.164
	34.2	13.9	0.203
	51.2	19.1	0.187
	85.1	33.8	0.198
24.96-25.00	5.15	5.82	0.565
	(6.38)	8.04	0.630) ^c
	(12.8)	16.1	0.629) ^c
	(13.5)	17.4	0.644) ^c
	17.1	19.4	0.567
	(20.4)	25.4	0.623) ^c
	27.4	32.6	0.595
	(33.8)	46.6	0.689) ^c
	39.3	40.6	0.601
	51.2	59.5	0.581
(54.1)	69.6	0.643) ^c	
34.77	5.15	10.5	1.02
	8.58	21.7	1.26
	17.1	41.4	1.21
	38.4	89.9	1.17

^a[Co(dmgh)₂py]₀ = (2.1-2.4) × 10⁻⁴ M, added as Co(dmgh)₂·2py.

^bk₁ = k_{obs}/2[CCl₄].

^cLess reliable value.

Table III-A-5. Kinetic data^a for the reaction of CCl_4 with $\text{Co}(\text{dmgH})_2\text{L}$ ($\text{L} \neq \text{PPh}_3$) at 25.0°C in acetone and benzene

Axial base L	Solvent	$10^3[\text{CCl}_4]/\underline{\text{M}}$	$10^3k_{\text{obs}}/\text{s}^{-1}$	$k_1^b/\underline{\text{M}}^{-1}\text{s}^{-1}$
pyridine	acetone	4.26	16.3	1.91
		4.39	19.0	2.16
		6.93	29.1	2.10
		13.4	50.8	1.90
		13.7	52.3	1.91
		18.1	71.1	1.97
		19.4	73.3	1.90
4-picoline	acetone	1.98	14.5	3.66
		4.24	29.2	3.44
		5.93	42.3	3.57
		7.91	56.5	3.57
		10.6	72.2	3.41
4-picoline	benzene	3.80	7.98	1.05
		6.65	13.8	1.04
		7.54	15.9	1.05
		12.1	26.5	1.10
		24.1	50.0	1.04

^a $[\text{Co}(\text{dmgH})_2\text{L}]_0 = (1.0-2.1) \times 10^{-4} \underline{\text{M}}$, added as $\text{Co}(\text{dmgH})_2 \cdot 2\text{L}$.

^b $k_1 = k_{\text{obs}}/2[\text{CCl}_4]$.

Table III-A-6. Kinetic data^a for the reaction of CHBr_3 with $\text{Co}(\text{dmgH})_2\text{py}$ in acetone and benzene

T/°C	Solvent	$10^2[\text{CHBr}_3]/\underline{\text{M}}$	$10^2k_{\text{obs}}/\text{s}^{-1}$	$k_1^b/\underline{\text{M}}^{-1}\text{s}^{-1}$
14.49	C_6H_6	0.762	0.356	0.233
		1.90	0.988	0.260
		5.69	2.80	0.246
		6.64	3.12	0.235
		18.75	10.3	0.275
24.96	$(\text{CH}_3)_2\text{CO}$	0.762	2.11	1.38
		0.952	2.37	1.24
		1.14	2.77	1.22
		3.80	8.67	1.14
25.00	C_6H_6	0.476	0.505	0.530
		0.952	0.904	0.475
		1.90	1.76	0.463
		8.52	8.75	0.513
34.78	C_6H_2	0.762	1.32	0.866
		0.953	1.55	0.813
		1.90	3.15	0.829
		3.33	5.37	0.806
		4.75	7.80	0.821

^a $[\text{Co}(\text{dmgH})_2\text{py}]_0 = (1.9-3.4) \times 10^{-4} \underline{\text{M}}$ added as $\text{Co}(\text{dmgH})_2 \cdot 2\text{py}$.

^b $k_1 = k_{\text{obs}}/2[\text{CHBr}_3]$.

Table III-A-7. Kinetic data^a for the reaction of CHBr_3 with $\text{Co}(\text{dmgH})_2\text{PPh}_3$ in acetone and benzene at 25.0°C

Solvent	$10^2[\text{CHBr}_3]/\text{M}$	$10^2k_{\text{obs}}/\text{s}^{-1}$	$k_1^b/\text{M}^{-1}\text{s}^{-1}$
Acetone	0.526	0.202	0.192
	0.842	0.367	0.218
	1.05	0.460	0.219
	2.10	0.934	0.222
	2.62	1.14	0.218
	3.14	1.40	0.223
	3.67	1.87	0.255
	4.19	1.90	0.227
	4.70	2.44	0.260
	5.22	2.89	0.277
Benzene	(4.75	0.449	0.047) ^c
	11.33	1.89	0.083
	23.33	3.40	0.073

^a $[\text{Co}(\text{dmgH})_2\text{PPh}_3]_0 = (1.9-2.1) \times 10^{-4} \text{ M}$.

^b $k_1 = k_{\text{obs}}/2[\text{CHBr}_3]$.

^cUnreliable data.

Table III-A-8. Kinetic data^a for the reaction of BrCCl_3 with $\text{Co}(\text{dmgH})_2\text{py}$ in benzene

$T/^\circ\text{C}$	$10^2[\text{BrCCl}_3]/\underline{\text{M}}$	$k_{\text{obs}}/\text{s}^{-1}$	$10^{-2}k_1^b/\underline{\text{M}}^{-1}\text{s}^{-1}$
14.89	(0.506	4.91	4.9) ^c
	1.69	24.5	7.2
	3.37	45.6	6.8
	5.88	93.6	8.0
	8.37	119	7.1
25.35	0.506	10.6	10.5
	1.69	29.7	8.8
	3.37	59.7	8.9
	4.21	87.8	10.4
	5.04	99.8	9.9
	5.88	111	9.5
	6.71	134	10.0
10.0	183	9.2	
35.45	0.506	16.0	15.8
	1.69	45.2	13.4
	5.04	142	14.1
	6.71	166	12.4

^aBy photolysis of $(\text{CH}_3)_2\text{CHCo}(\text{dmgH})_2\text{py}$ in benzene.

^b $k_1 = k_{\text{obs}}/2[\text{BrCCl}_3]$.

^cUnreliable data.

Table III-A-9. Kinetic data^a for the reaction of CBr_4 with $\text{Co}(\text{dmgH})_2\text{py}$ in benzene

$T/^\circ\text{C}$	$10^2[\text{CBr}_4]/\underline{\text{M}}$	$k_{\text{obs}}/\text{s}^{-1}$	$10^{-3}k_1^b/\underline{\text{M}}^{-1}\text{s}^{-1}$
5.91	0.542	27.1	2.50
	1.08	57.2	2.65
	2.15	87.5	2.04
	5.26	212	2.02
	6.52	250	1.92
14.21	0.525	26.1	2.49
	1.31	73.7	2.81
	2.59	157	3.03
	3.85	194	2.52
	5.09	266	2.61
25.02	0.521	52.6	5.05
	1.30	117	4.50
	2.57	239	4.65
	5.06	464	4.58

^a $\text{Co}(\text{dmgH})_2\text{py}$ generated by photolysis of $(\text{CH}_3)_2\text{CHCo}(\text{dmgH})_2\text{py}$.

^b $k_1 = k_{\text{obs}}/2[\text{CBr}_4]$.

Table III-A-10. Kinetic data for the reactions of BrCCl_3 and CCl_4 with $\text{Co}(\text{dmgH})_2\text{py}$ in benzene at 25.0°C in the presence of 4-HTMPO

	$10^4 [4\text{-HTMPO}]/\text{M}$	$10^2 [\text{RX}]/\text{M}$	$k_{\text{obs}}/\text{s}^{-1}$	$m = \frac{k_{\text{obs}}}{[\text{RX}]k_1}$
Part 1. BrCCl_3 ($k_1 = 938 \text{ M}^{-1} \text{ s}^{-1}$)				
	0.28	5.05	75.4	1.59
	1.10	5.87	71.7	1.30
	2.20	5.85	60.6	1.10
	54	5.88	47.4	(0.86)
	54	10.9	102.9	1.01
	60	1.31	12.9	1.05
	60	2.81	18.5	(0.70)
Part 2. CCl_4 ($k_1 = 0.586 \text{ M}^{-1} \text{ s}^{-1}$)				
	1.00	1.71	1.54×10^{-2}	1.54
	1.00	4.27	3.60×10^{-2}	1.44
	5.00	1.71	1.11×10^{-2}	1.11
	5.00	4.27	2.85×10^{-2}	1.14
	10.1	1.71	9.4×10^{-2}	0.94
	10.1	4.27	2.44×10^{-2}	0.98
	18-66	0.51-6.8	--	1.0

GENERAL SUMMARY

A convenient, clean, and efficient method for the production of superoxide ion in aqueous solution has been developed. The utility of this method has been demonstrated by employing it as the source of O_2^- in the study of the reactions of superoxide ion with several Co(III) complexes and ferricinium ion. These reactions obey a second order rate law and proceed through an outer sphere electron transfer mechanism. Some conclusions about the $O_2(aq)/O_2^-$ electron self-exchange rate constant were made.

The reaction of various polyhalomethanes and cobaloxime(II) also obeys a second-order rate law and proceeds by a halogen atom abstraction as the initial step in the mechanism. The free radical nature of the mechanism was demonstrated through the use of radical trapping agents. Mathematical simulations support the proposed mechanism.

ACKNOWLEDGMENTS

I would like to thank Professor James H. Espenson for his support and encouragement throughout my graduate studies. Dr. Andreja Bakač has been most generous in her time given for suggestion, criticism, and discussion.

I am grateful to Dr. Robert Lambert for assistance in implementing the numerical integration routine using Gear's method.

Special thanks are due for my parents, Warner and Kathe, for the unwavering support and love. Without them, I could not have succeeded in my studies.

Finally, a very special thanks is given to Gudrun Lukat, a very close and dear friend, who was always there in a most difficult time in my life. Without her, a successful completion to my studies would not have come to pass.